CR-147

CLASSIFICATION CHANGED
TO *Unclassified* *[signature]*
BY DD294 *[signature]*
DATE *16 August 1966*
[signature] Q. Patterson
7-14-67

AN ENGINE OUT CONTROLLABILITY
STUDY OF THE S-IB STAGE OF THE
SATURN IB VEHICLE MODEL DSV-4B

(u)

APRIL 1964
DOUGLAS REPORT SM-46569

MISSILE & SPACE SYSTEMS DIVISION
DOUGLAS AIRCRAFT COMPANY, INC.
SANTA MONICA/CALIFORNIA

DOUGLAS

AN ENGINE OUT CONTROLLABILITY
STUDY OF THE S-IB STAGE OF THE
SATURN IB VEHICLE MODEL DSV-4B

(u)

DOUGLAS MISSILE & SPACE SYSTEMS DIVISION

ABSTRACT

The effect of a single engine failure during first stage
flight of the Saturn IB vehicle was investigated as
authorized by Scope Change 1128. The prime considerations
were vehicle controllability, aerodynamic loading, and
mission completion. The range of allowable time of engine
failure for each of these considerations was established.
The more critical trajectories were used to study the
effects of dispersions in selected vehicle parameters on
the vehicle performance and controllability.

TABLE OF CONTENTS

LIST OF TABLES

LIST OF ILLUSTRATIONS (Continued)

LIST OF SYMBOLS

a_o — Pitch and yaw attitude gain; engine deflection/attitude error (deg/deg)

a_1 — Pitch and yaw attitude error rate gain; engine deflection/ attitude error rate, (deg/deg/sec)

a_{x_m} — Longitudinal acceleration as sensed by an accelerometer at the cg (ft/sec^2)

a_{y_m} — Pitch normal acceleration as sensed by an accelerometer at the cg (ft/sec^2)

a_{z_m} — Yaw normal acceleration as sensed by the accelerometer at the cg (ft/sec^2)

b_o — Pitch and yaw angle of attack gain; engine deflection/angle of attack (deg/deg)

C_{z_α} — Normal force gradient (1/rad)

C_D — Drag coefficient (nondimensional)

cg — Center of gravity (inches forward of gimbal point)

cp — Center of pressure (inches forward of gimbal point)

D — Reference diameter (inches)

FPR — Flight Performance Reserve (lb)

h — Altitude (ft)

h_o — Altitude of circular orbit (n mi)

h_p — Altitude of orbit perigee (n mi)

IECO — Inboard Engine Cutoff Time (sec)

OECO — Outboard Engine Cutoff Time (sec)

M — Mach number (nondimensional)

M_x — Total moment about vehicle x-axis (ft-lbs)

M_y — Total moment about vehicle y-axis (ft-lbs)

M_z — Total moment about vehicle z-axis (ft-lbs)

m — Bending moment (in-lbs)

N'_c — Equivalent compressive load (lbs/in)

P — Vehicle roll rate (deg/sec)

$\dot{P}$ — Vehicle roll acceleration (deg/sec^2)

p — Axial load (lbs)

q — Dynamic pressure (lb/ft^2)

Q — Vehicle pitch rate (deg/sec)

$\dot{Q}$ — Vehicle pitch acceleration (deg/sec^2)

R — Vehicle yaw rate (deg/sec)

$\dot{R}$ — Vehicle yaw acceleration (deg/sec^2)

r — Stage radius (inches)

S — Range (n mi)

S_{ref} — Reference vehicle cross-section area (ft^2)

T — Thrust (lb)

T_u — Thrust unbalance of control engines (expressed in percent deviation from nominal)

t — Time of flight measured from initial liftoff (sec)

t_{eo} — Time of engine-out (sec of flight time)

V_I — Inertial velocity (ft/sec)

V_W — Wind velocity (ft/sec)

X_e, Y_e, Z_e — Displacement in an orthogonal coordinate system fixed to the earth at the launch point. The X_e axis is oriented along the aiming azimuth, Y_e is vertical, and Z_e is cross-range. X_e is positive down-range, Y_e is positive up, and Z_e is positive to the right (ft)

α_P — Pitch angle of attack (deg)

α_Y — Yaw angle of attack (deg)

α — Total angle of attack (deg)

β_{P_A} — Average pitch engine deflection angle (deg)

β_{Y_A} — Average yaw engine deflection angle (deg)

β_{R_A} — Average roll engine deflection angle (deg)

γ_1 — Elevation flight path angle (deg)

γ_{1_I} — Inertial elevation flight path angle (deg)

∂_{D_j} — Vehicle parameter dispersion

∂_{P_i} — Average trajectory parameter variance

ΔD_j — Variance (3 sigma)

θ — Vehicle pitch attitude (deg)

$\Delta\theta$ — Pitch attitude error (deg)

ϕ — Vehicle roll attitude (deg)

$\Delta\phi$ — Roll attitude error (deg)

ψ — Vehicle yaw attitude (deg)

$\Delta\psi$ — Yaw attitude error (deg)

1.0 INTRODUCTION

This report presents the results of a study to determine the effects of a first stage engine failure on the performance of the Saturn IB vehicle. The criteria used to evaluate the vehicle performance included the ability to maintain control, to maintain the vehicle structural loads at a safe level, and to achieve the desired orbit. Wind disturbances and dispersions in selected vehicle parameters were considered in addition to engine failures. Engine failures were simulated from liftoff to outboard engine cutoff (OECO).

The vehicle dynamic response to a wind gust was determined for either engine 1 or engine 3 out at various times. Outboard engine failures were selected because of the resulting loss of control moment and the more severe, when compared to a fixed inboard engine, disturbing moment. The results for engine 2 or engine 4 failures are not presented since the effects of 1 or 4 and 2 or 3 in the pitch plane and 1 or 2 and 3 or 4 in the yaw plane are equivalent.

For each engine-out time, a wind profile was constructed such that the peak wind velocity was applied at the altitude of maximum dynamic pressure. This combination was found to be the most critical with respect to aerodynamic loading. Wind velocity was assumed parallel to the plane of the local horizontal. The results of the loads analysis, which was made for the most critical (maximum load) engine-out trajectories, are presented as the equivalent compressive load at the two most critical vehicle stations as a function of time of engine failure.

The vehicle dynamic response for various engine-out conditions is presented in the form of profiles of angle of attack, dynamic pressure, normal acceleration, angular acceleration, and engine deflection.

Variation in angle of attack, dynamic pressure, angular acceleration, normal acceleration and engine deflection were determined as functions of dispersions in center of pressure, center of gravity, attitude error and angle of attack gains, individual engine thrust, and total thrust. These variations were determined for the most critical engine-out trajectories.

Results indicate that controllability*, from either a tumbling or structural loading point of view, is critical for engine failures prior to 83 seconds (the time of peak dynamic pressure in the 8 engine trajectory) when wind disturbances and three sigma parameter variations are included. This is based on the most critical engine-out trajectories with respect to the maximum angle of attack-dynamic pressure product.

Actual loss of control or tumbling occurs for engine number 1 failures prior to about 20 seconds after liftoff and engine number 3 failures prior to about 10 seconds after liftoff. However, this tumbling doesn't occur until the vehicle reaches the region of maximum dynamic pressure which is between 115 and 125 seconds after liftoff for an engine failure

---

* For the purpose of the study, the vehicle was considered to be "controllable" if it did not tumble and if the structural integrity was maintained.

early in flight. These unstable conditions exist without the effects of disturbances due to winds and dispersions in vehicle parameters.

When disturbances due to winds are included, the time prior to which an engine failure results in unsatisfactory control is extended to 59 seconds due to excessive equivalent compressive loads at vehicle station 962.304. Winds also result in excessive loads at the above station for engine failures in the time interval from 72 to 83 seconds. The equivalent compressive loads were considered to be excessive if the loads, described in reference 5, were exceeded. These loads were not exceeded for engine failures in the time interval from 59 to 72 seconds with wind disturbances, but when variations in the compressive load due to dispersions in vehicle parameters were included, the loads at station 962.304 became excessive for engine failures in this interval.

Studies made to determine the effects of an engine failure on the resultant orbit indicate engine failures prior to 139 seconds yield resultant earth orbits whose perigee altitudes are deemed unacceptable. An unacceptable orbit was assumed to be an orbit having a perigee altitude less than 60 nautical miles. Engine failure after 139 seconds leads to orbits whose perigees are greater than 60 nautical miles but less than the nominal 105 nautical miles.

2.0 SIMULATION PROGRAM

2.1 Program Characteristics

The digital computer program used for simulating boost stage flight characteristics simulates 6-degree-of-freedom flight over a rotating, oblate spheroidal earth. The program includes the engine and actuator geometry of the S-IB stage. The force and moment contribution of each of the eight engines is treated separately so that an engine failure may be easily simulated. Each of the eight valve-actuator loops is simulated by an integrator with position feedback. In this way, both rate and position limits may be imposed on the actuator, and various servo malfunctions such as gain changes or open loops may be easily simulated if desired.

The available autopilot feedback signals include attitude error, attitude error rate, body rate, angle of attack, rate of change of angle of attack, normal acceleration, and integral of attitude error. Any or all of these signals may be used to simulate the autopilot.

2.2 Upper Stage Simulation

Two other digital programs were utilized for second stage and orbital flight. Second stage flight simulation was defined with a 2-dimensional trajectory optimization program which simulates the path adaptive guidance of this stage. An orbit determination program was used for flight evaluation after second stage burnout.

3.0 VEHICLE CONFIGURATION

3.1 Vehicle Characteristics

The Saturn IB vehicle outboard profile is shown in figure 1. The vehicle coordinate system and engine sign convention used for this study are presented in figure 2.

3.1.1 Weight and Propulsion Data

The mass characteristics given in references 1 and 2 were modified to reflect changes due to the redesigned fins and a subsequent 300 pound payload increase. A weight summary is presented in table I and the modified weight, center of gravity, and moments of inertia, as a function of propellant consumed, are given in table II. Table III lists the pertinent propulsive characteristics. The time of inboard engine cutoff (IECO) and OECO as a function of the time of an outboard engine failure are presented in figure 3.

3.1.2 Aerodynamic Data

The center of pressure, slope of the normal force coefficient, and the nominal drag coefficient were taken from reference 3 and are presented as a function of Mach number in figures 4 and 5. The 7-engine-burning drag coefficient (also presented in figure 4) is different from the 8-engine-burning drag coefficient due to the fact that the base pressure drag coefficient, which is a function of the exit pressure area, is reduced approximately 12 percent with the occurrence of an engine failure. The aerodynamic parameters given include the effects of the redesigned fins.

3.2 Trajectory

The reference trajectory is a direct ascent from AMR, with an aiming azimuth of 72 degrees measured east of north, to a 105 nautical mile circular orbit. The S-IB stage pitch command history is characterized by vertical ascent for 25 seconds followed by a commanded gravity tilt turning rate program, until OECO. The pitch command history was simulated by fitting the program with a fifth degree polynomial. The S-IVB stage trajectory is determined utilizing a simulated path adaptive guidance system to achieve orbit injection. Pertinent trajectory parameters are presented in tables IV and V. In each engine out trajectory constant missile attitude was commanded following the time of nominal OECO until actual S-IVB ignition.

3.3 Control System Data

The control equation for both the pitch and yaw autopilots of the S-IB stage included attitude error, rate of change of attitude error, and angle of attack feedback. The gains on these feedback signals were determined through the use of the drift minimum control principle (zero steady state normal acceleration in the presence of winds) and the

SATURN IB
OUTBOARD PROFILE

◭ SEPARATION

◈ FIELD SPLICE

APOLLO
SPACECRAFT

33°

8 °37'

INSTRUMENT UNIT

◈ STATION 1698.859
◈ STATION 1662.859

S-IVB STAGE

← 260 IN. DIA.

◭ STATION 1186.804

1086 (GIMBAL)

◈ STATION 962.304

LAUNCH
VEHICLE

← 257 IN. DIA

S-IB STAGE

STATION 100 (GIMBAL)

STATION −1.0
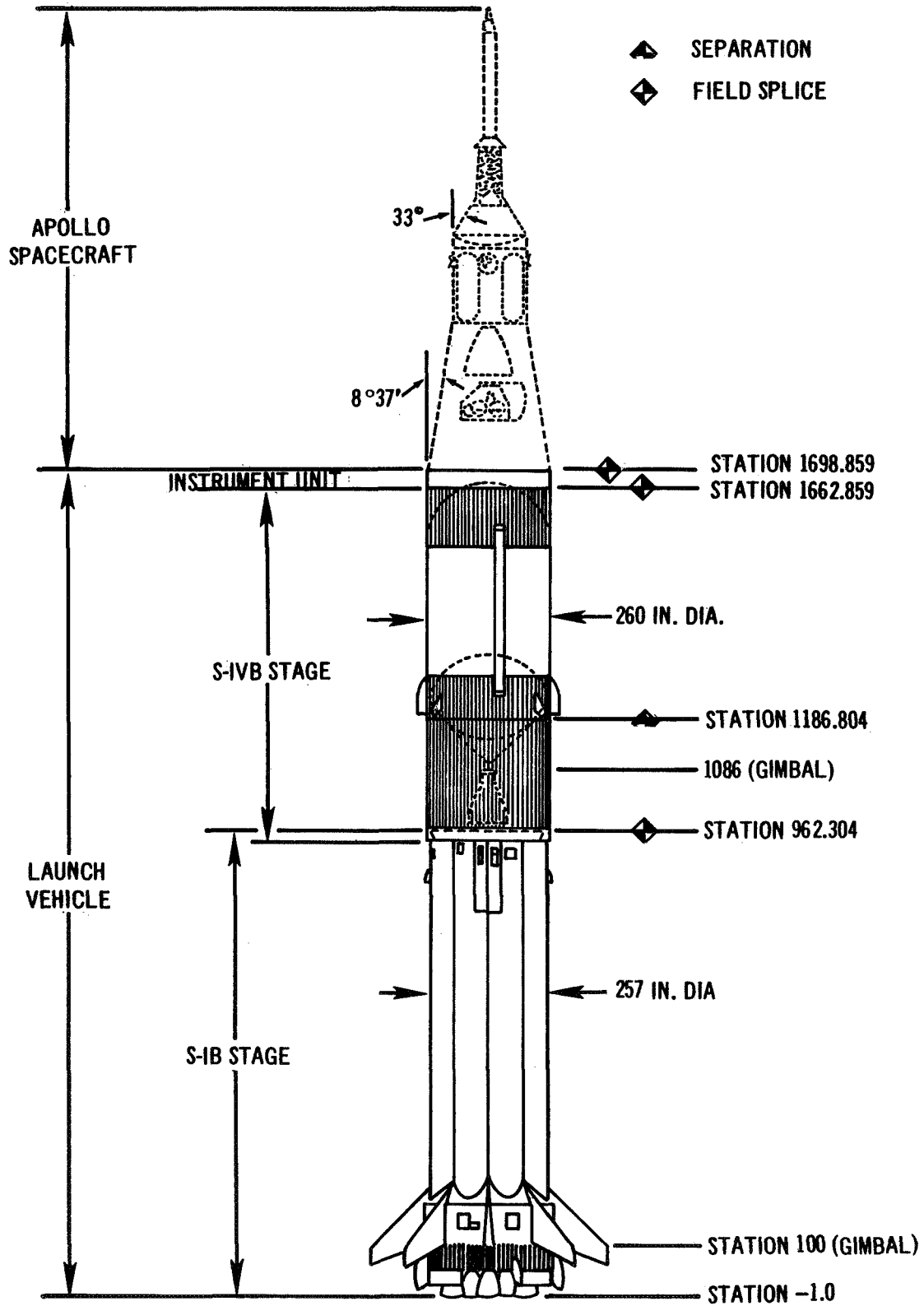
FIGURE 1

VEHICLE COORDINATE SYSTEM AND ENGINE SIGN CONVENTION

VIEW LOOKING FORWARD
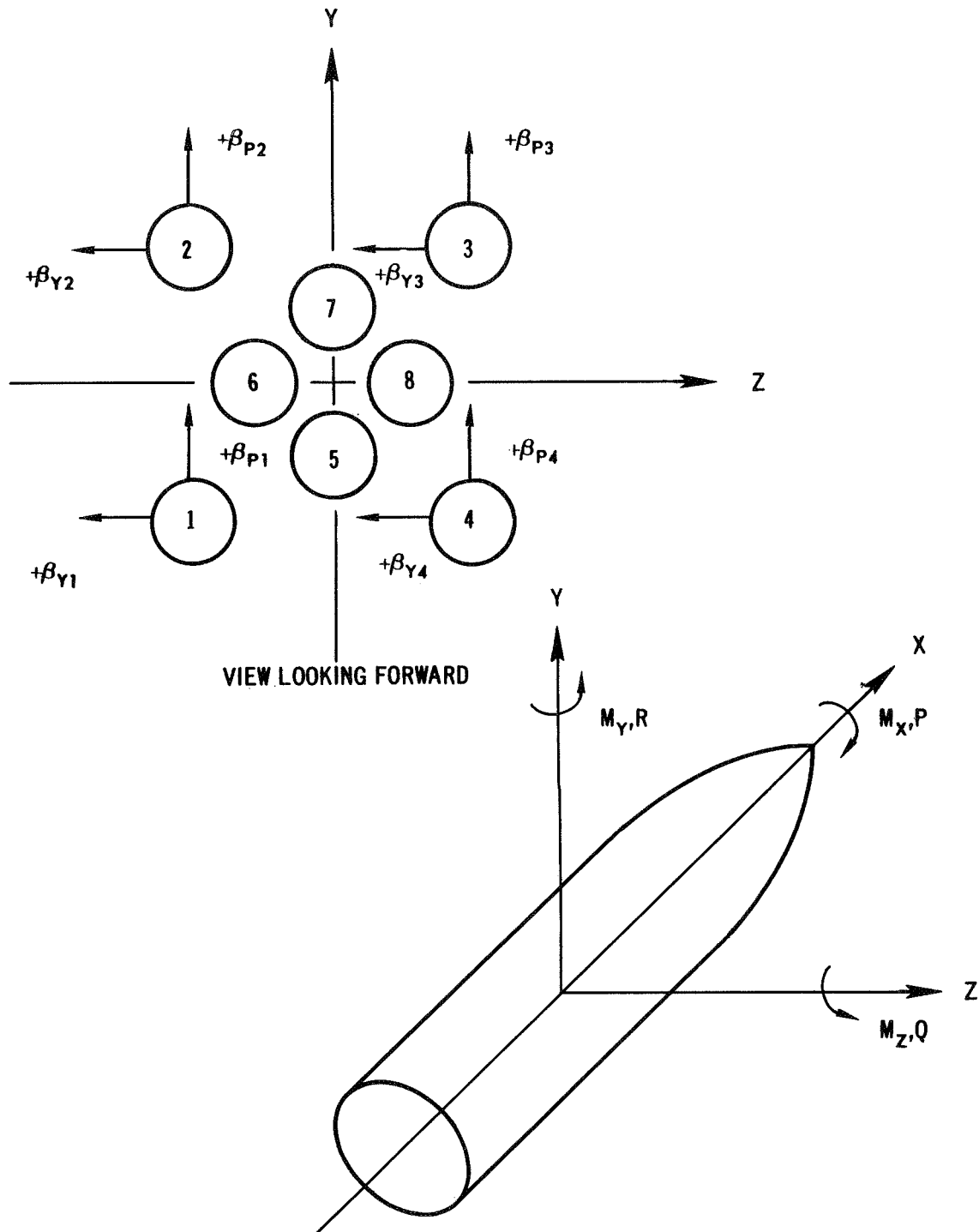
FIGURE 2

TABLE I

SATURN IB WEIGHT SUMMARY
ONE ENGINE OUT ANALYSIS

Event	Weight (lb)	Weight (lb)	Time (sec)
Vehicle at Lift-off		1,277,278	0.0
Propellant	864,447		
Frost, Fuel Additive, & Lube Oils	481		
IECO - Prior		412,350	147.1
Thrust Decay Propellant	1,448		
IECO - After		410,902	147.1
Propellant	16,019		
Frost, Fuel Additive, & Lube Oils	20		
OECO and Separation - Prior		394,863	153.1
Thrust Decay Propellant --- 10% Level	1,275		
S-IVB Ullage Propellant	182		
Interstage	-5,600		
S-IB Stage	100,585		
Frost, Fuel Additive, & Lube Oils	1,128		
OECO and Separation - After		286,093	153.1
S-IVB Ignition - Prior		286,093	158.6
Thrust Buildup Propellant	485		
S-IVB Ignition - After		285,608	158.6
S-IVB Propellant	4,695		
LES Jettison - Prior		280,913	168.6
LES	6,600		
Ullage Rockets	213		
LES Jettison - After		274,100	168.6
S-IVB Propellant	214,166		
S-IVB Cut-off		59,934	624.8

TABLE II

SATURN IB/S-IB STAGE MASS CHARACTERISTICS

WEIGHT OF S-IB PROPELLANT CONSUMED (LBS)	TIME (SEC.)	VEHICLE WEIGHT (LBS)	C.G.[1] POSITION (IN)	PITCH INERTIA (SLUG FT^2)	ROLL INERTIA (SLUG FT^2)
0	0	1,277,278	627.06	49,657,834	1,566,099.0
57,895	10	1,219,349	620.55	49,408,592	1,478,962.5
116,519	20	1,160,691	615.95	49,344,302	1,392,843.5
175,419	30	1,101,755	613.16	49,161,607	1,306,935.6
234,379	40	1,042,761	612.43	49,104,456	1,223,351.3
293,415	50	983,692	614.02	49,042,801	1,138,366.0
352,473	60	924,600	618.19	48,925,656	1,054,898.0
412,478	70	865,562	626.24	48,694,784	972,835.1
471,632	80	806,376	638.17	48,261,811	888,809.2
530,842	90	747,131	655.75	47,540,959	807,241.8
590,097	100	687,843	679.81	46,389,148	723,935.8
648,980	110	628,927	711.92	44,716,970	643,149.1
707,674	120	570,201	754.89	42,204,821	560,530.9
766,162	130	511,680	812.38	38,474,547	476,937.0
824,352	140	453,458	889.60	33,426,786	397,503.7
864,447	147.1	412,350	960.70	28,491,619	341,975.9
865,895	147.1	410,902	963.60	28,212,737	339,610.3
881,914	153.1	394,863	996.73	25,805,612	319,727.1
883,189	153.1	393,588	999.96	25,619,404	318,168.2

(1) Measured in inches
     forward of gimbal
     plane.

TABLE III

SATURN IB
ENGINE PROPULSION CHARACTERISTICS

S-IB FIRST STAGE   (8 H-1 Engines)

    Thrust Per Engine   188,000 lb Sea Level

    Specific Impulse   256 sec Sea Level

S-IVB SECOND STAGE   (1 J-2 Engine)

    Thrust   200,000 lb Vacuum

    Specific Impulse   426 sec Vacuum

INBOARD AND OUTBOARD ENGINE CUTOFF TIME ASSOCIATED WITH
TIME OF OUTBOARD ENGINE FAILURE
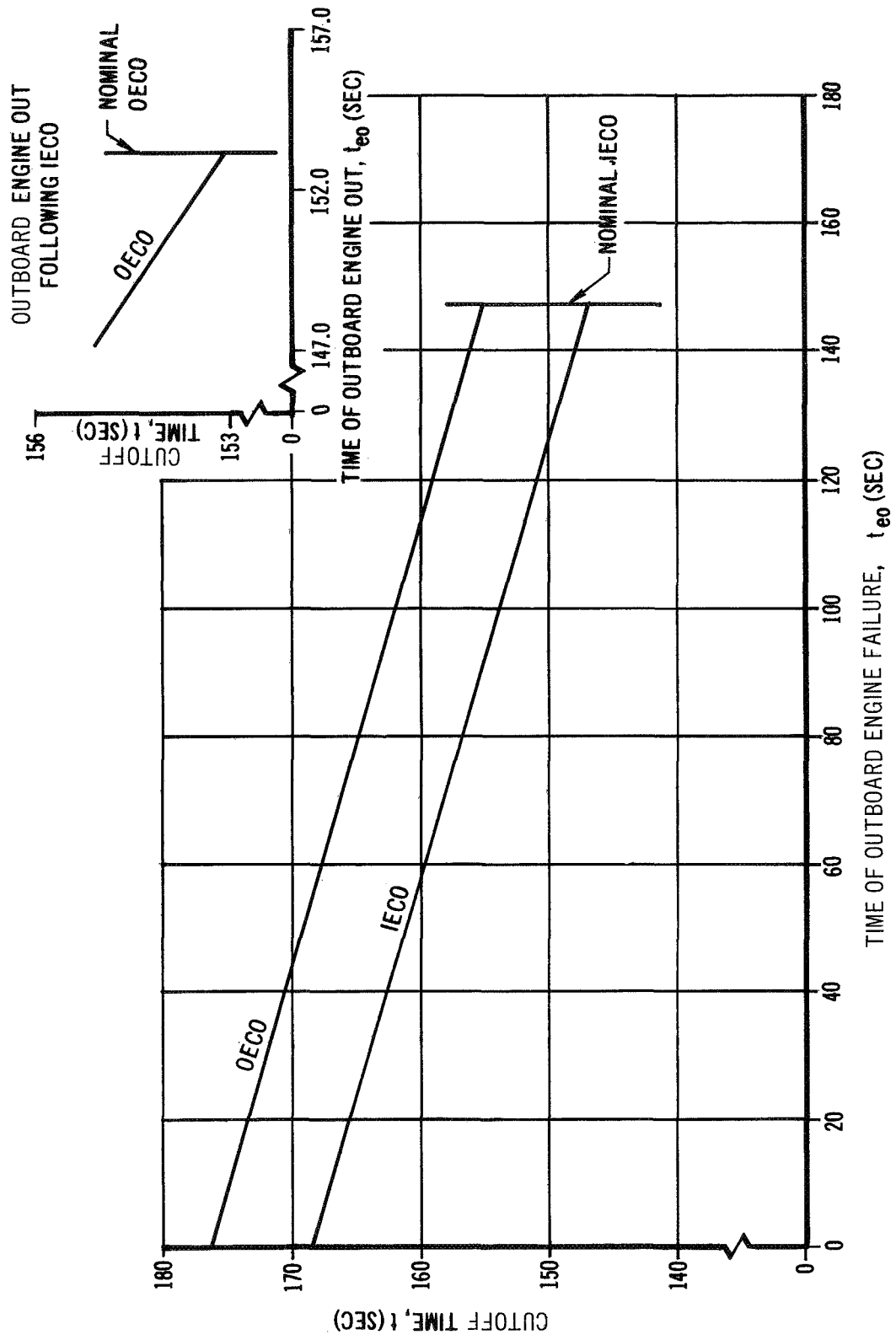
FIGURE 3

DRAG COEFFICIENT FOR BOTH 7 AND 8
ENGINE OPERATION
POWER ON
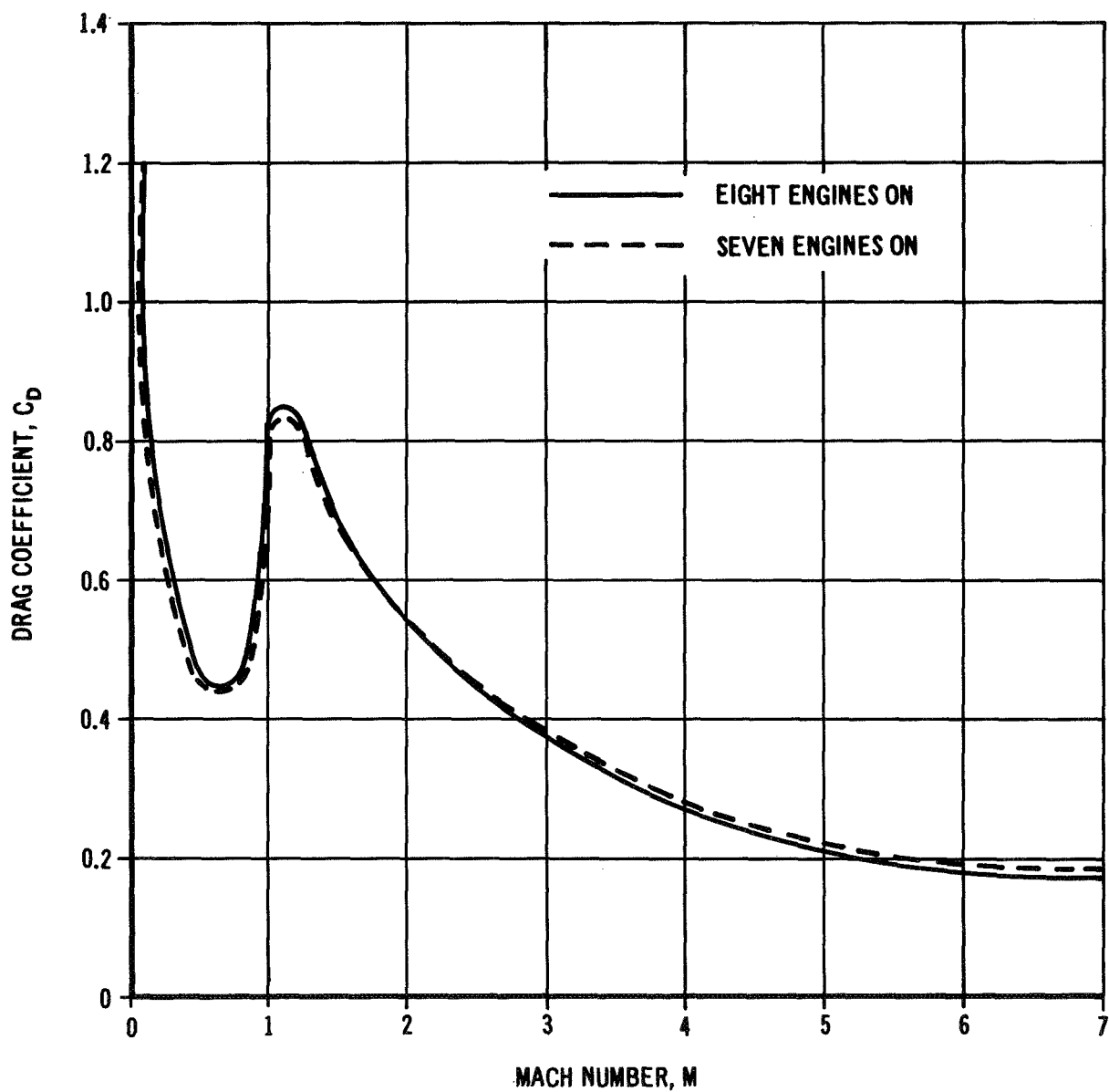
FIGURE 4

NORMAL FORCE GRADIENT & CENTER
OF PRESSURE

REF DIAMETER = 257"
ANGLE OF ATTACK = 0°
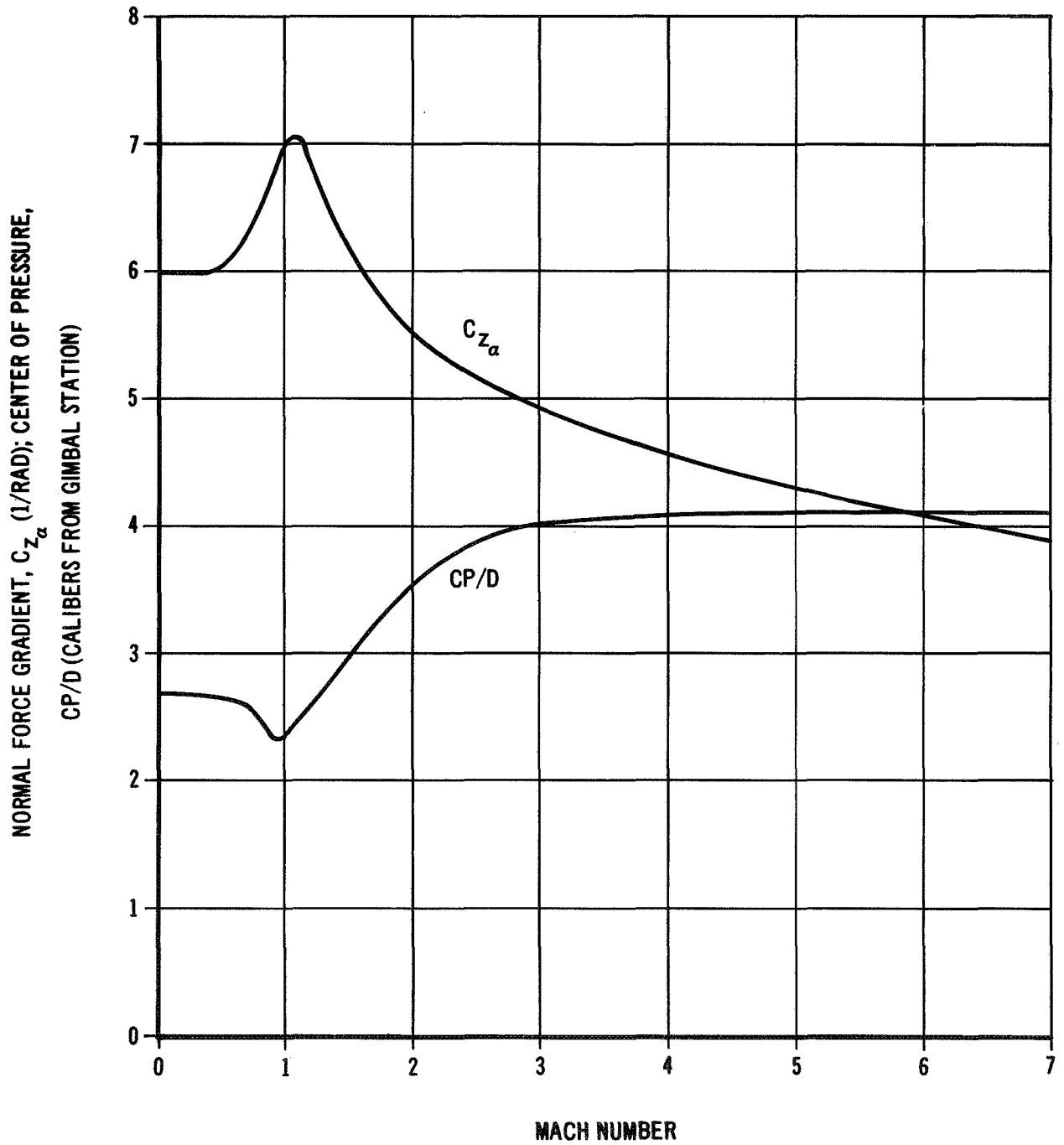
FIGURE 5

TABLE IV

SATURN IB

ONE ENGINE OUT ANALYSIS

S-IB STAGE PERTINENT TRAJECTORY PARAMETERS

(NOTE: NO ENGINE FAILURE)

TIME (SEC)	ALTITUDE (N. MI.)	INERTIAL VELOCITY (FPS)	INERTIAL ELEVATION FLIGHT PATH ANGLE (DEG)	MISSILE PITCH ATTITUDE ANGLE (DEG)	DYNAMIC PRESSURE (PSF)	MACH NUMBER
0	0	1342	0.0	90.0	0.0	0.0
10	0.1	1343	2.5	90.0	3.9	0.0
20	0.2	1349	6.0	90.0	21.9	0.1
30	0.5	1365	10.4	88.9	63.5	0.2
40	1.0	1412	15.5	86.1	136.0	0.3
50	1.8	1507	20.8	81.8	242.4	0.5
60	2.8	1665	25.6	76.5	373.9	0.7
70	4.2	1891	29.3	70.6	504.2	0.9
80	5.9	2173	31.3	64.4	576.3	1.3
90	7.9	2540	32.3	58.3	565.4	1.7
100	10.3	3009	32.6	52.6	430.5	2.1
110	13.3	3586	32.3	47.6	279.2	2.6
120	16.7	4274	31.6	43.2	162.4	3.2
130	20.6	5079	30.6	39.5	81.4	3.8
140	25.2	6016	29.6	36.4	38.2	4.5
147.1	28.8	6776	28.9	34.5	22.4	5.1
153.1	32.1	7079	28.0	33.1	12.9	5.7

TABLE V

SATURN IB

ONE ENGINE OUT ANALYSIS

S-IVB STAGE PERTINENT TRAJECTORY PARAMETERS

TIME (SEC)	ALTITUDE (N. MI.)	INERTIAL VELOCITY (FPS)	INERTIAL ELEVATION FLIGHT PATH ANGLE (DEG)	LONGITUDAL ACCELERATION (FT/SEC^2)
158.6	35.1	6,999	26.9	0.0
168.6	40.1	7,079	25.3	22.9
208.6	58.3	7,527	19.3	25.2
248.6	73.0	8,145	14.3	27.2
288.6	84.8	8,930	10.1	29.5
328.6	93.6	9,884	6.7	32.3
368.6	100.0	11,015	4.1	35.7
408.6	104.2	12,344	2.2	39.9
448.6	106.5	13,902	0.9	45.1
488.6	107.1	15,736	0.1	52.0
528.6	106.9	17,922	-0.4	61.2
568.6	106.0	20,581	-0.4	74.6
608.6	105.1	23,927	-0.2	95.3
624.8	105.0	25,559	0.0	107.4

specification of a control loop natural frequency of 0.15 cps and a damping ratio of 0.75. The resulting gain program for the 8-engine reference trajectory is presented in figure 6. This gain program was used for all trajectories studied.

The roll autopilot control equation utilized attitude error and rate of change of attitude error feedback. These gains, constant throughout first stage flight, were established by specifying an average roll natural frequency of 0.15 cps and an average damping ratio of 0.75.

Each engine servo loop was simulated by an integrator with position feedback. Each engine in both pitch and yaw had a position limit of $\pm$ 8 degrees and a rate limit of $\pm$ 15 degrees per second.

4.0 ORBIT CAPABILITY

An analysis was conducted to determine the orbit capability of the Saturn IB vehicle under the conditions of a first stage engine failure. The analysis did not include the effects of winds or dispersions in vehicle parameters.

The variations in the S-IB stage burnout conditions resulting from wind disturbances and vehicle parameter dispersions are small and have negligible effects on the resulting orbits.

The engine-out trajectories generated during this portion of the study were also used to determine the altitude of maximum dynamic pressure for use in the controllability analysis (section 5.0).

4.1 Boost Trajectory Characteristics

The primary parameter affected by an engine failure is angle of attack, which becomes intolerably high in the maximum dynamic pressure region (especially in the pitch plane) with an early engine failure. Following an engine failure, angle of attack buildup occurs in both the pitch and yaw plane because, 1) the pitch command program, which was designed to minimize the effects of gravity, is no longer compatible due to the reduced thrust level, and 2) a combination of attitude error and angle of attack feedback is necessary to command the trim engine deflection required to counteract the unbalanced moments about the pitch and yaw axes.

Since the nominal flight scheme strives to attain a minimum angle of attack history, the engine-out conditions are almost always more critical than the nominal trajectory with respect to controllability.

Other significant vehicle parameters which are affected by an engine failure are illustrated in the following figures. Ground track histories for both number 1 and 3 engine failures are presented in figures 7, 8, and 9. From figure 7 it can be seen that early failures of engine number 3 result in considerable dispersion uprange in the vicinity of the launch site.

PITCH AND YAW
DRIFT MINIMUM GAINS
REF: NOMINAL 8 ENGINE TRAJECTORY

$f = 0.15$ CPS
$\zeta = 0.75$
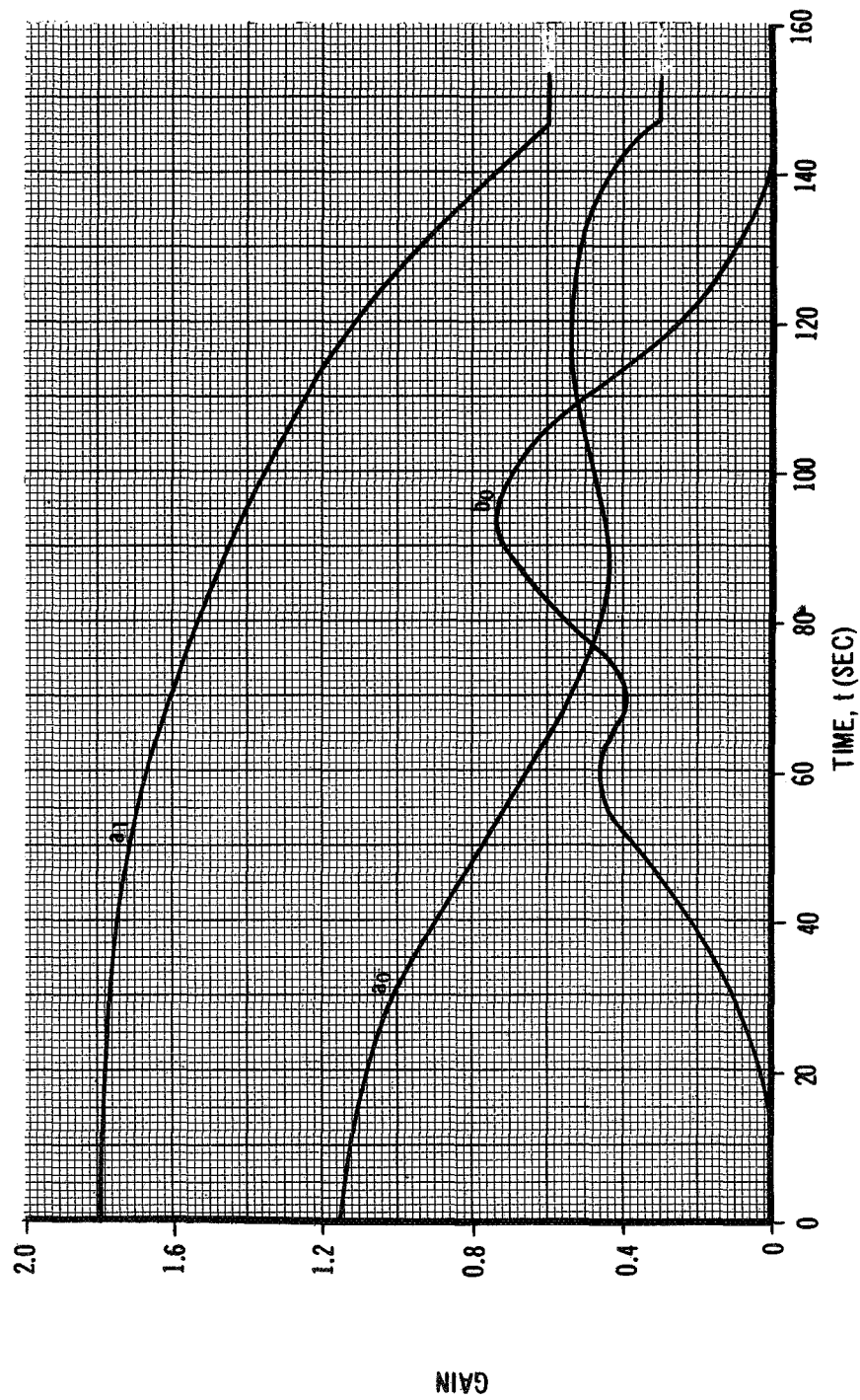
FIGURE 6

GROUND TRACK HISTORIES FOR VARIOUS ENGINE OUT TIMES

NUMBER 1 ENGINE OUT | NUMBER 3 ENGINE OUT
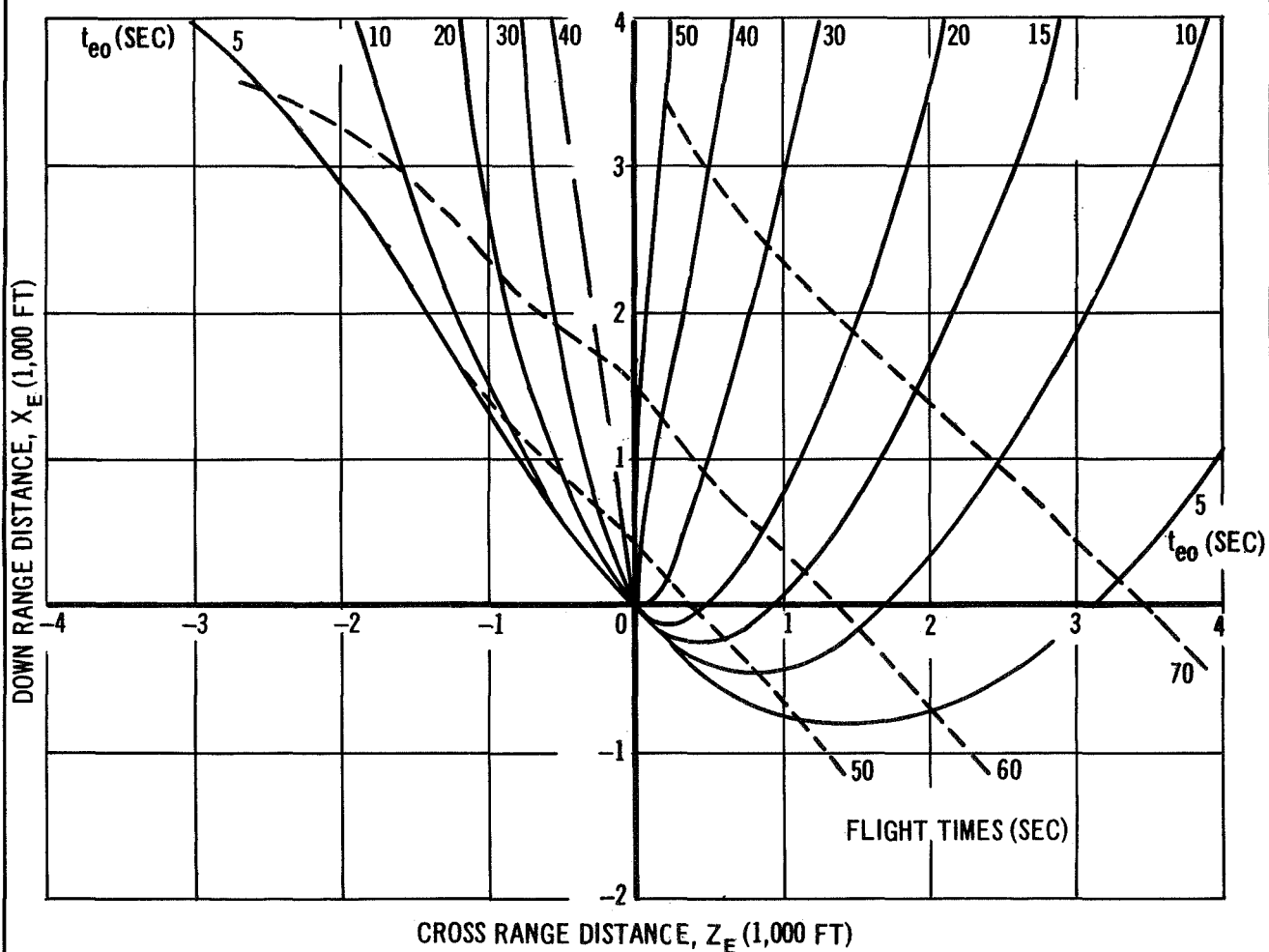
NOTE: THE X_E AXIS IS ORIENTED ALONG THE 72° AIMING AZIMUTH, POSITIVE DOWN RANGE Z_E IS POSITIVE TO THE RIGHT. THE X_E, Z_E PLANE IS FIXED TO THE EARTH AT THE LAUNCH POINT.

FIGURE 7

GROUND TRACK HISTORIES FOR NUMBER 3 ENGINE FAILURES
AT 5, 10, 15, 20, 30, 40, 50, 60, 70, 80, 100, AND 120 SECONDS
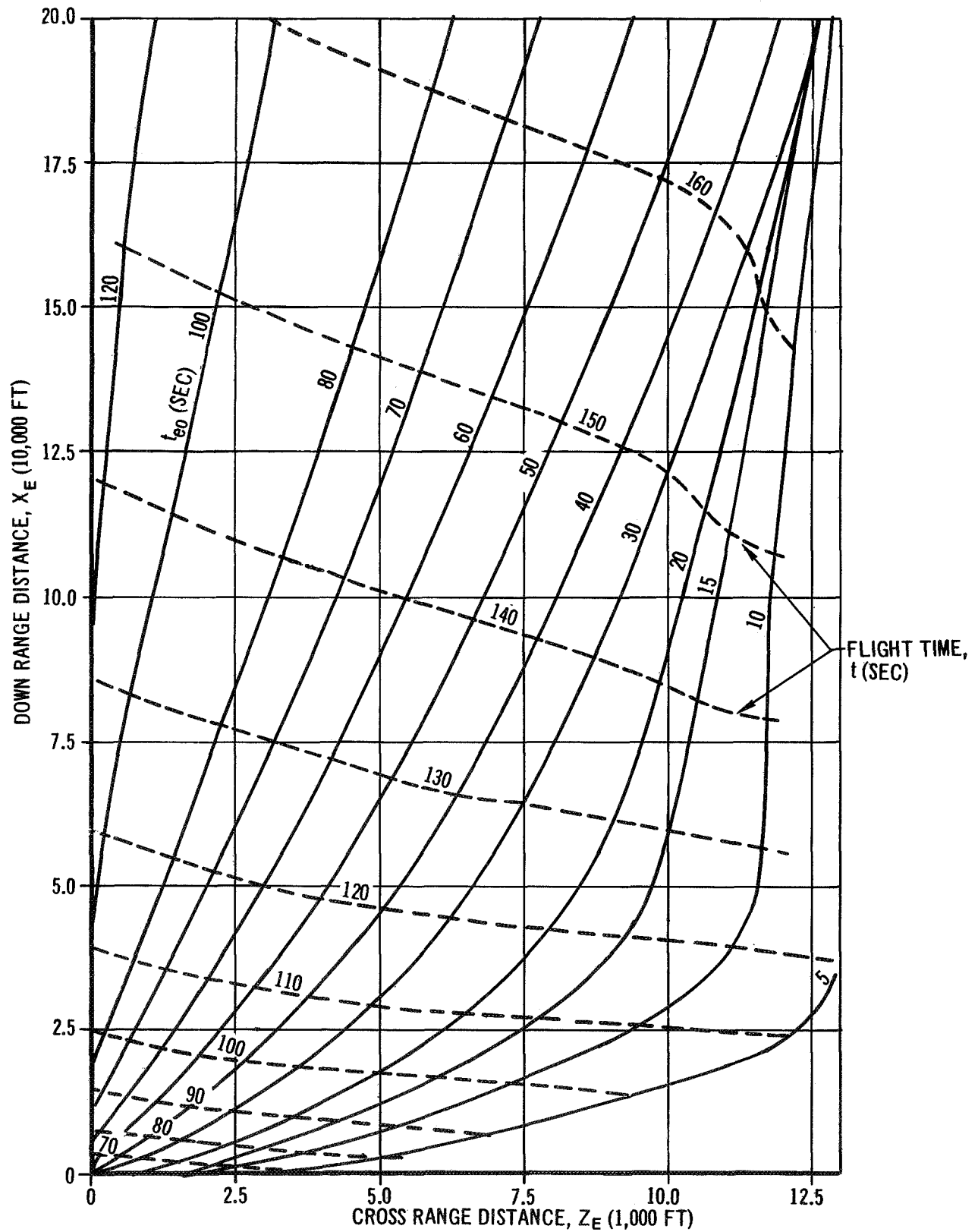
FIGURE 8

GROUND TRACK HISTORY FOR NUMBER 1 ENGINE OUT AT 5, 10, 15, 20, 30, 40, 50, 60, 70, 80, 100, 120, AND 140 SECONDS
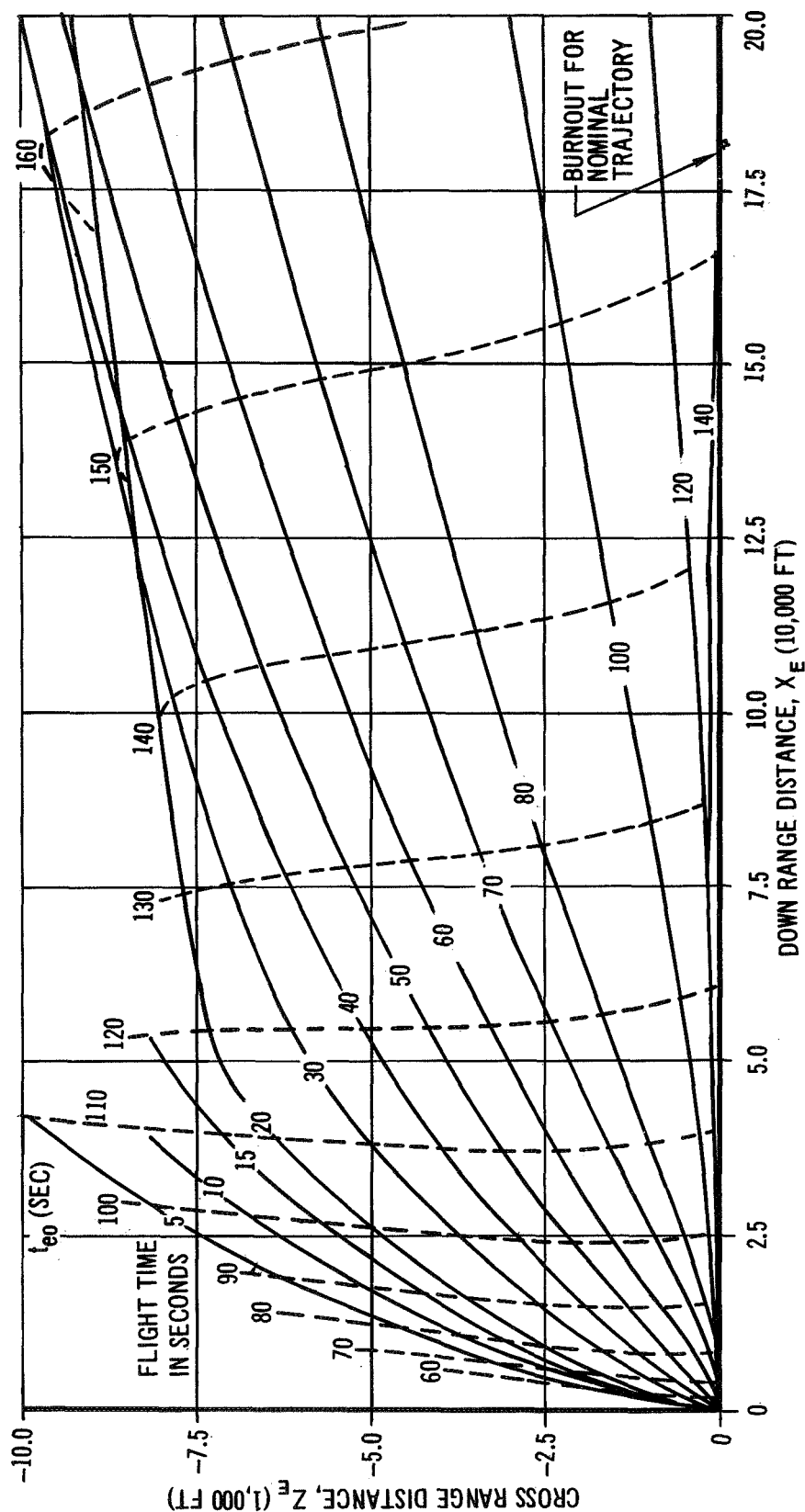
FIGURE 9

Inertial elevation flight path angle histories and range versus altitude
profiles, for several engine number 1 failure times, are compared with
the nominal 8-engine case in figures 10 and 11 respectively.

The conditions existing at the time of S-IB/S-IVB stage separation are
presented in figures 12 through 15. Engine failures prior to about 20
seconds after liftoff resulted in uncontrolled vehicle tumbling, thus,
separation will not be possible. Several of the more severe combinations
of angle of attack and dynamic pressure existing at the time of separa-
tion were investigated and it was determined that S-IVB attitude devi-
ations during the separation transient were less than 15 degrees.
Therefore, S-IVB stage control following separation is not critical
for those cases of engine failure for which S-IB stage controllability
is satisfactory.

4.2 Resultant Orbit

Achievement of the primary mission for the Saturn IB configuration is
jeopardized by the occurrence of a boost stage engine failure. Of
particular concern is the orbit resulting from a given engine-out con-
dition. The flight conditions existing at S-IVB propellant depletion
were used to establish the orbit ephemeris and the perigee altitude was
selected as the element used to judge the acceptability of the orbit.
Figures 10 and 11 indicate that the S-IVB stage burnout conditions for
flight path angle and altitude are near nominal, and therefore, burnout
velocity is the prime element in shaping the perigee altitude trend.
It was assumed that dispersions from the nominal flight history were
not sufficient to render the S-IVB guidance polynomial inapplicable.
Figure 16 shows that engine number 1 failures prior to 139 seconds yield
resultant earth orbits whose perigee altitude is deemed unacceptable,
i.e., less than 60 nautical miles, while failures after 139 seconds lead
to orbits whose perigees are greater than 60 nautical miles but less
than 105 nautical miles. By utilizing the S-IVB stage flight performance
reserve (FPR) propellants, the portion of flight time which can withstand
the loss of one engine and still maintain a minimum perigee altitude of
60 nautical miles is increased by approximately 39 seconds, such that
failures after 100 seconds result in an "acceptable" orbit. In addition,
by use of the S-IVB stage FPR, engine failure times after 109 seconds
result in the nominal 105 mile orbital condition. However, it should
be stressed that the eventual availability of the FPR is always question-
able until well into S-IVB flight due to the possible flux in the per-
formance characteristics.

Figure 17 presents perigee altitude versus time of engine-out for engine
3. A comparison with figure 16 indicates that engine 1 is slightly the
more critical.

Figure 18 shows the amount of FPR required for an acceptable perigee
orbit as a function of time of engine-out for both number 1 and 3 engine
failures. Engine failure times occurring on the horizontal segment of
the curve need all the available FPR, and if they receive all that is
loaded their resultant orbit perigee is that presented in figures 16

INERTIAL ELEVATION FLIGHT PATH ANGLE HISTORY COMPARISON BETWEEN NOMINAL
AND NUMBER 1 ENGINE OUT TRAJECTORIES AT 20, 40, 60, AND 120 SECONDS
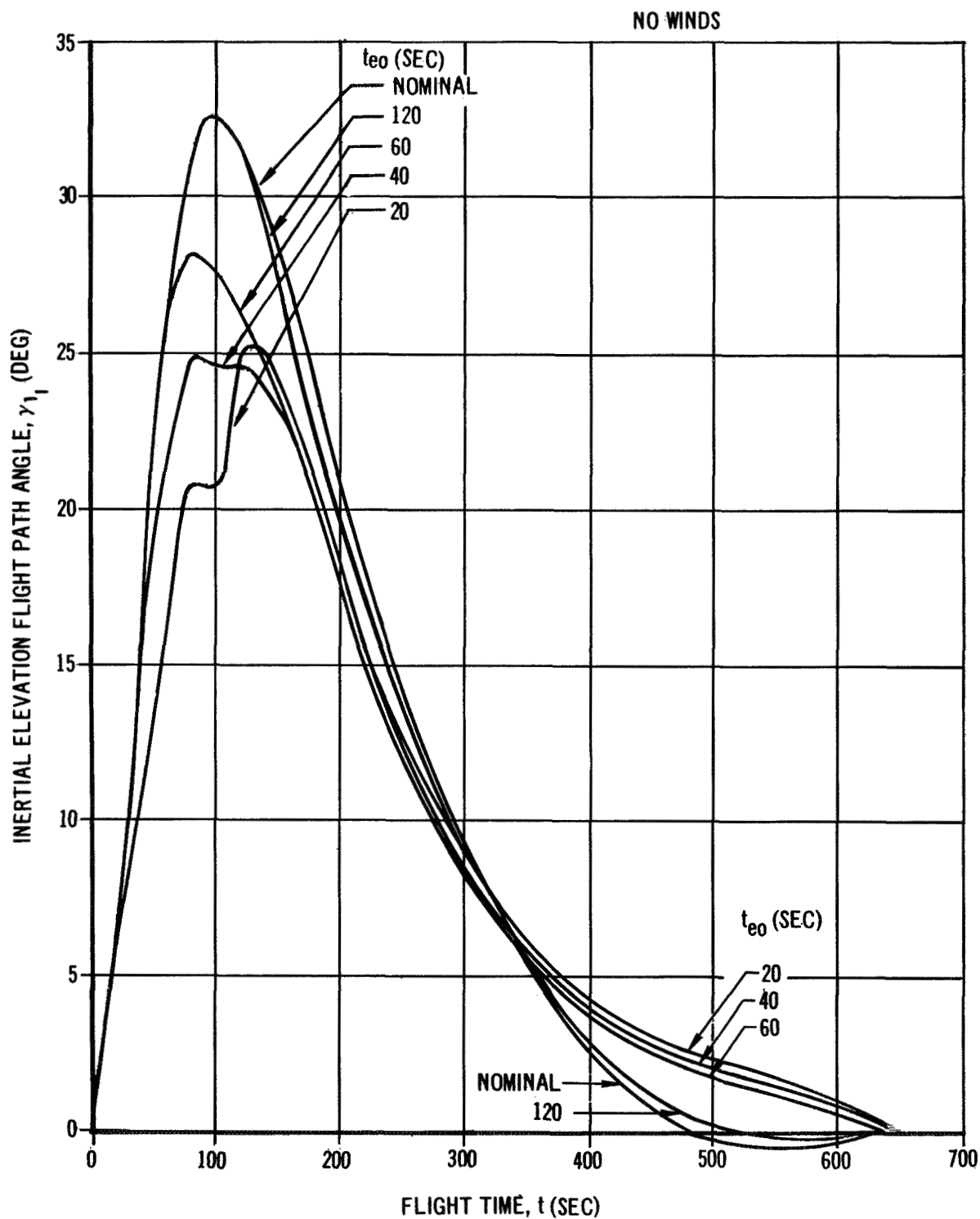
FIGURE 10

ALTITUDE AND RANGE HISTORY COMPARISON BETWEEN NOMINAL AND NUMBER 1 ENGINE OUT TRAJECTORIES AT 20, 60, 80, 100, AND 120 SECONDS
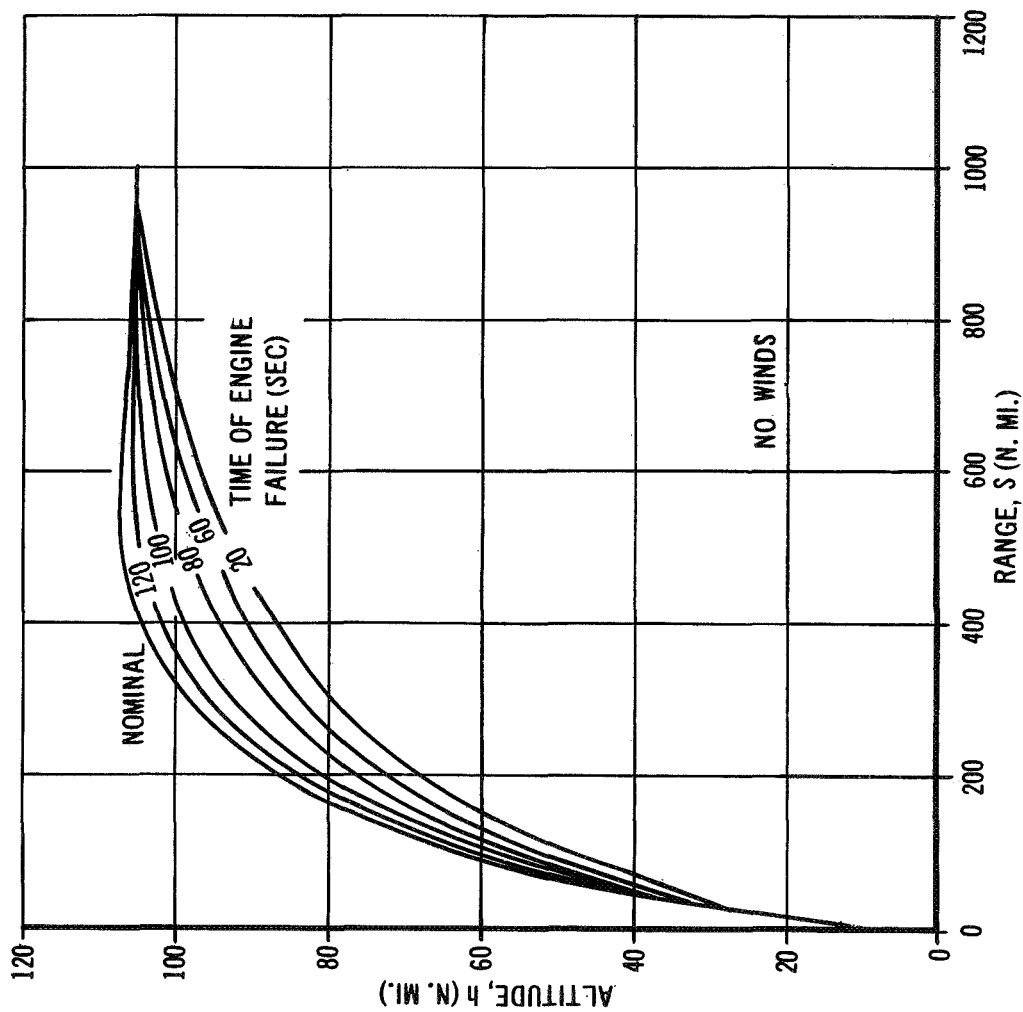
FIGURE 11

SEPARATION CONDITIONS FOR NUMBER 1 ENGINE FAILURES

(FLIGHT PATH ANGLE, VELOCITY, AND ALTITUDE)
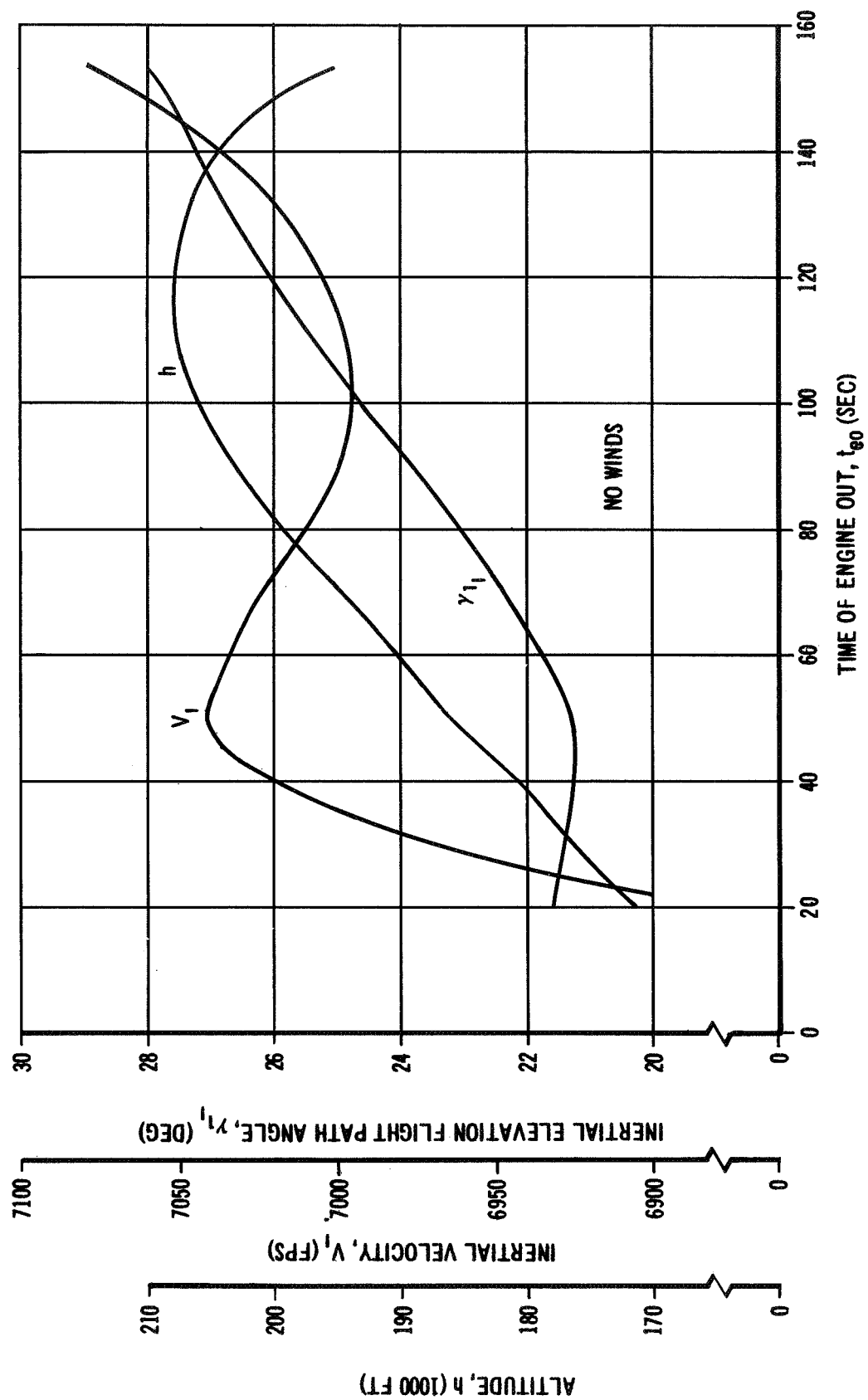
FIGURE 12

SEPARATION CONDITIONS FOR NUMBER 1 ENGINE FAILURES
(ATTITUDE, ANGLE OF ATTACK, AND DYNAMIC PRESSURE)
NO WINDS
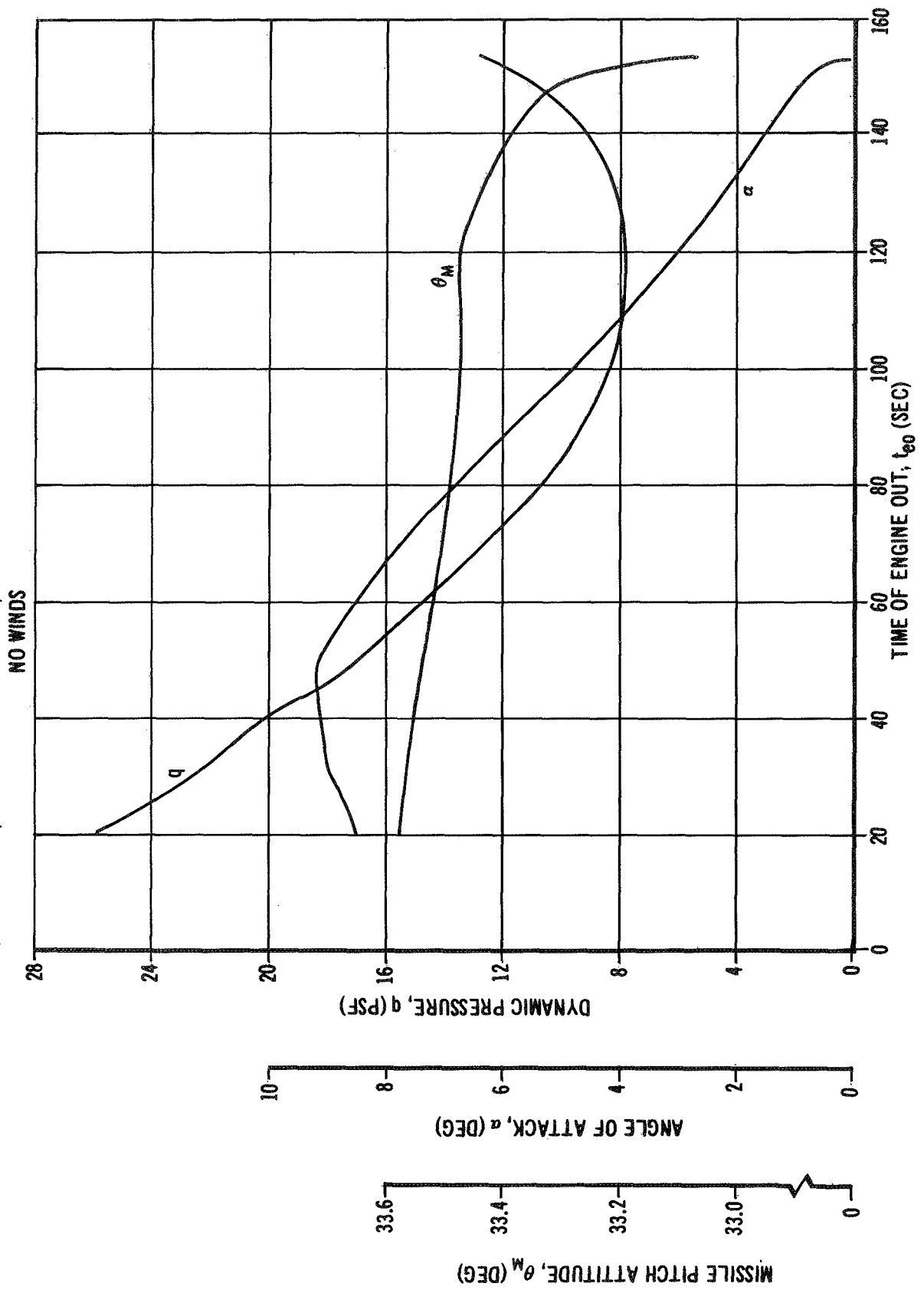
FIGURE 13

SEPARATION CONDITIONS FOR NUMBER 3 ENGINE FAILURES
(FLIGHT PATH ANGLE, VELOCITY, AND ALTITUDE)
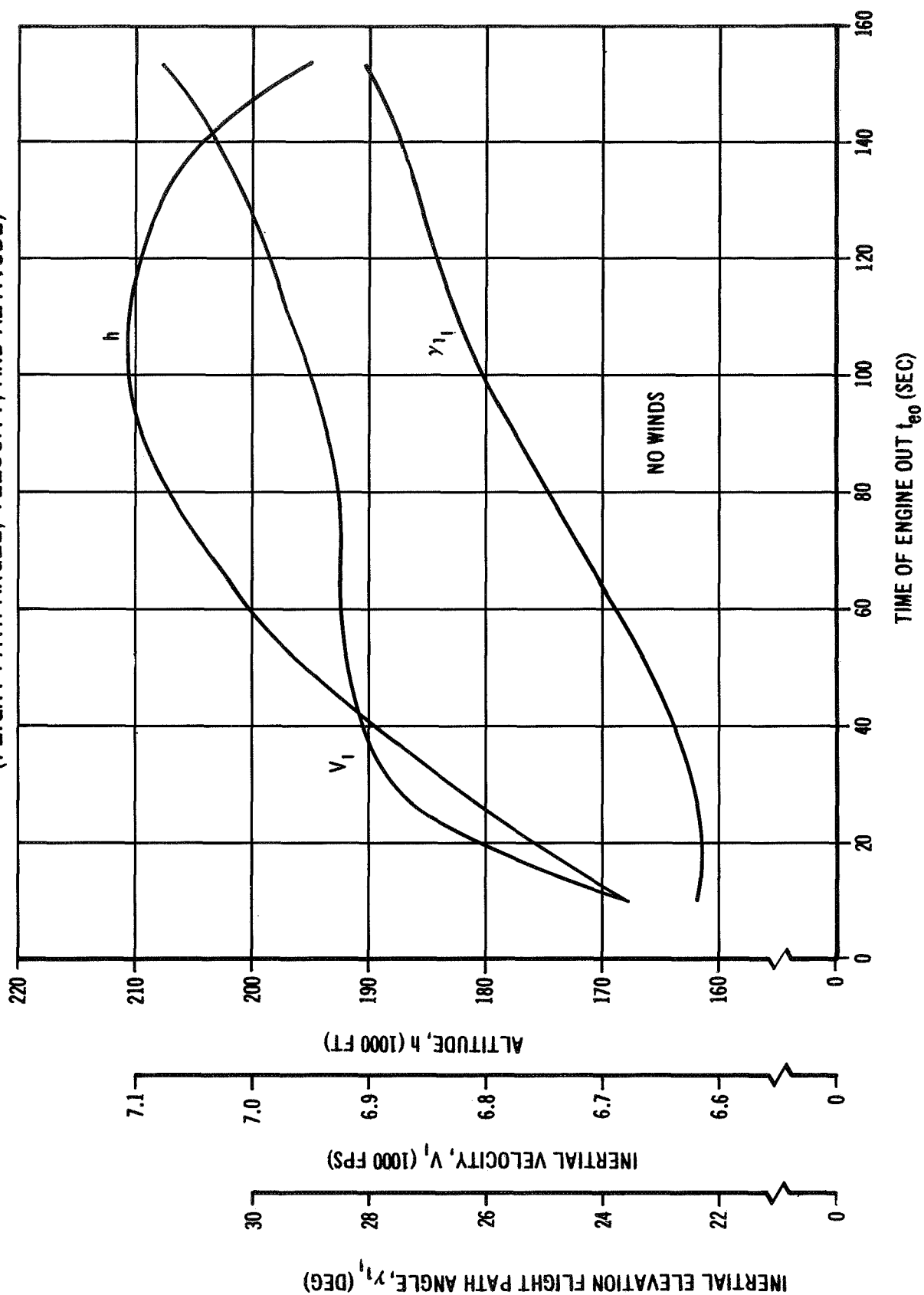
FIGURE 14

24

SEPARATION CONDITIONS FOR NUMBER 3
ENGINE FAILURES
(ATTITUDE, ANGLE OF ATTACK, AND DYNAMIC PRESSURE)
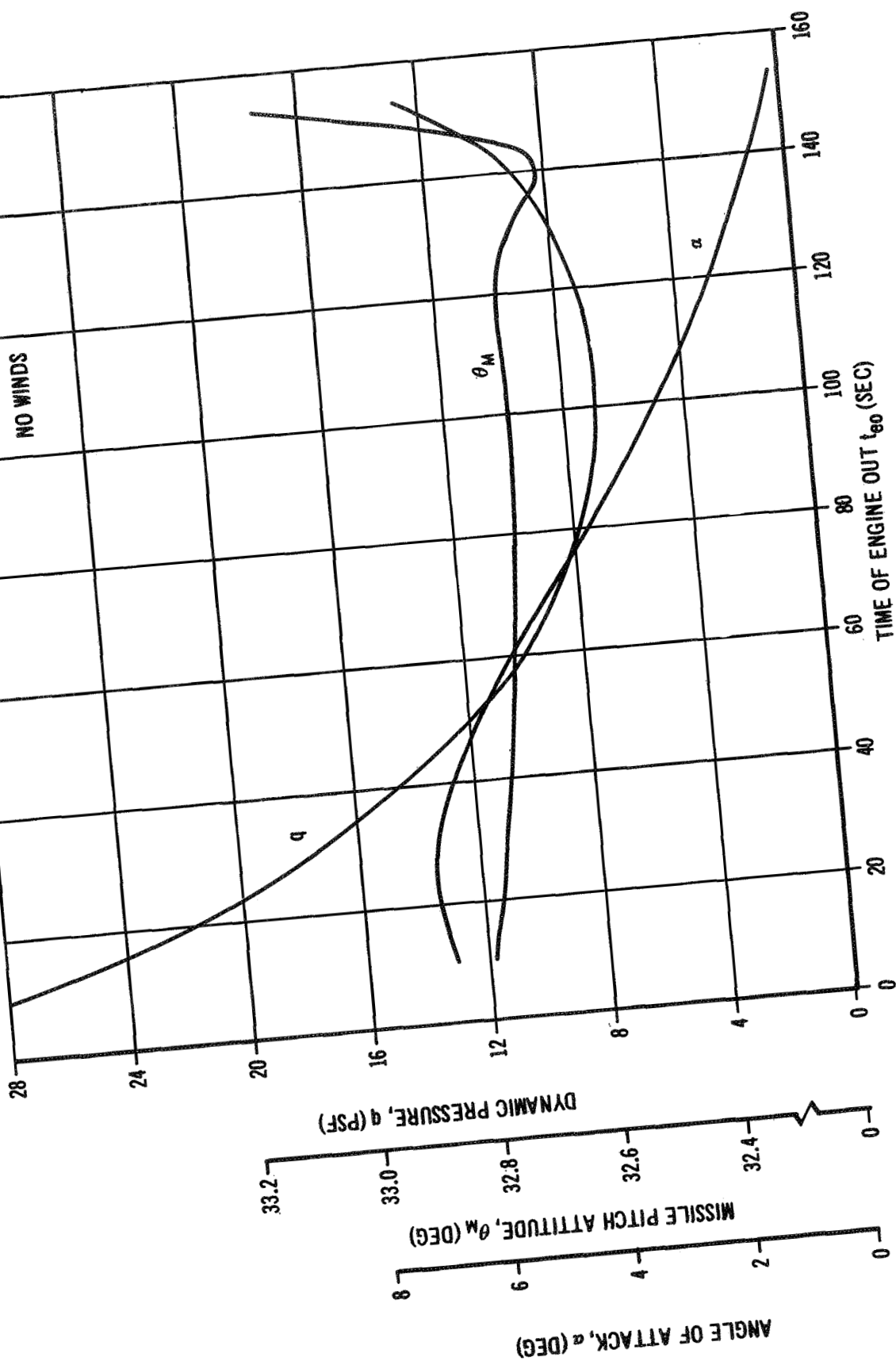
FIGURE 15

RESULTANT ORBIT PERIGEE ALTITUDE FOR NUMBER 1 ENGINE FAILURES
NO WINDS

FIGURE 16

RESULTANT ORBIT PERIGEE ALTITUDE FOR NUMBER 3 ENGINE FAILURES
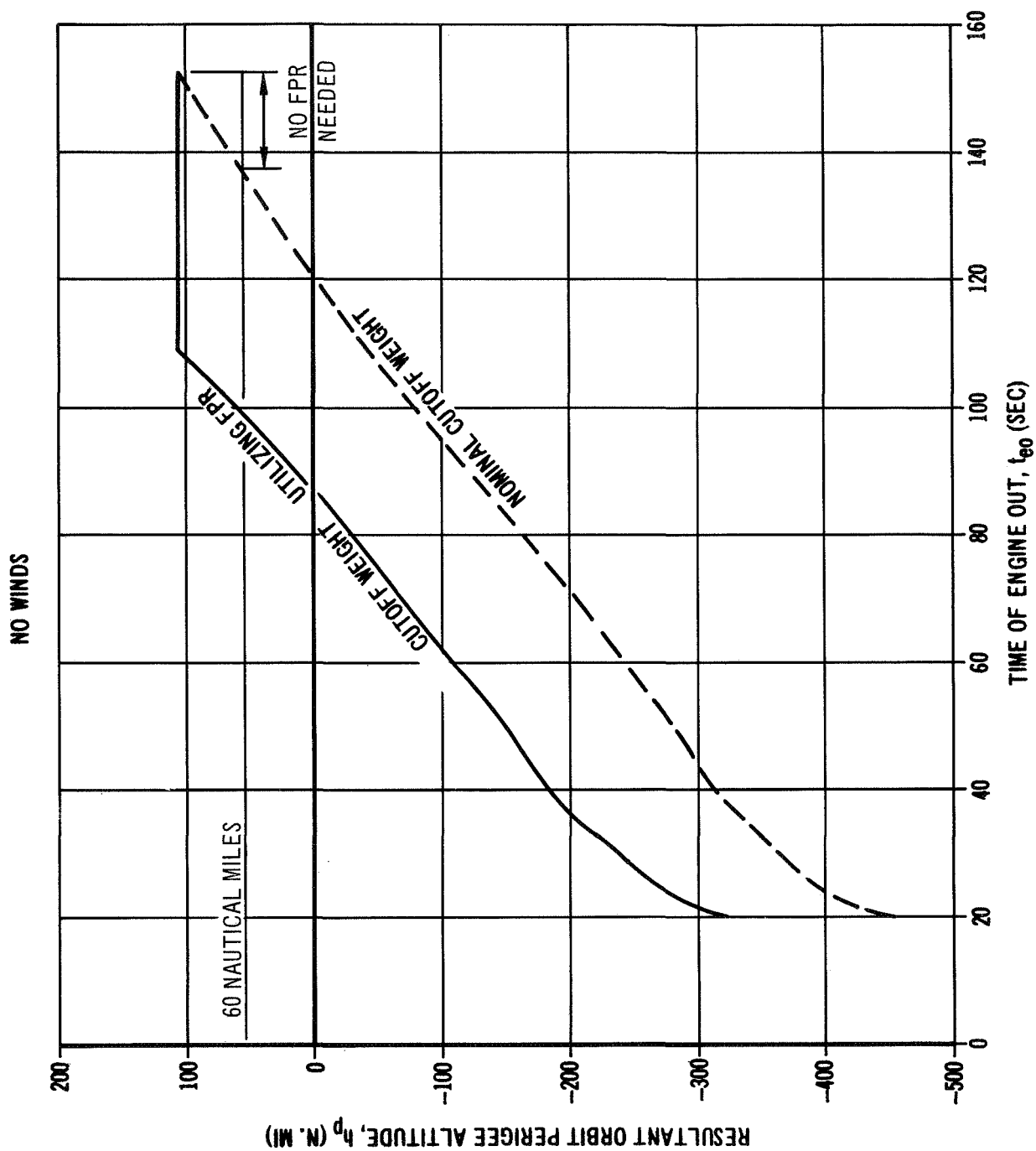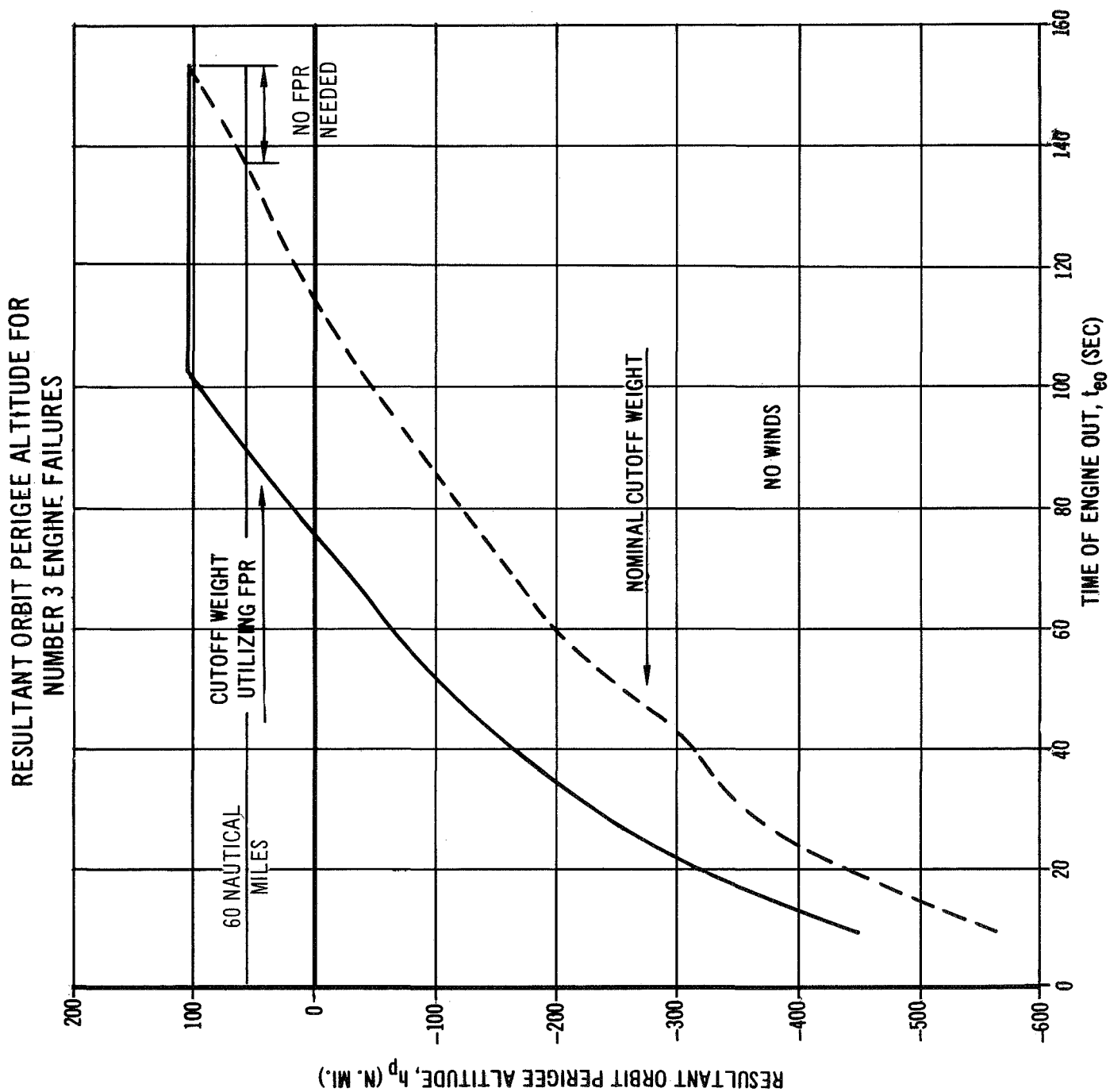
FIGURE 17

AMOUNT OF FLIGHT PERFORMANCE RESERVES REQUIRED TO ATTAIN NOMINAL ORBIT
ALTITUDE FOR BOTH NUMBER 1 AND 3 ENGINE FAILURES

FIGURE 18

and 17. For engine failure times on the sloped segment of the curve, the primary mission (105 nautical mile circular orbit) can be achieved if the indicated FPR propellant is available.

5.0 CONTROLLABILITY

The controllability of the vehicle was investigated for an engine number 1 failure and an engine number 3 failure for each of the following conditions:

a. No winds

b. Ninety-nine percent probability of occurrence wind shear with a gust at the altitude of maximum dynamic pressure

c. Dispersions of vehicle characteristics with the winds mentioned in b above.

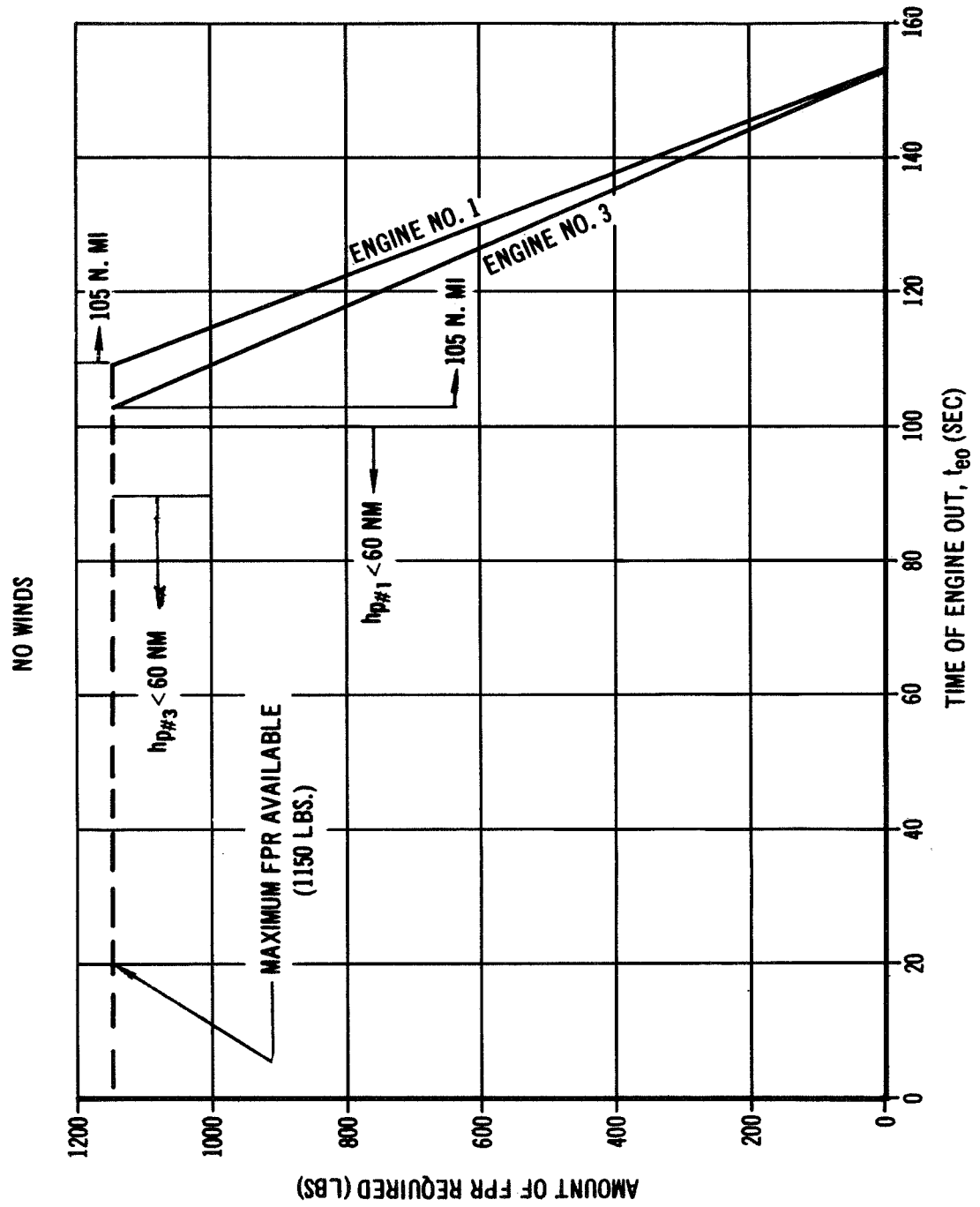Engine number 1 and engine number 3 failures were selected for the investigation because of their diametrically opposing influence on vehicle response. The antisymmetric effects of failures of engine 1 and 3 are evident in figures 19, 20 and 21, which represent typical parameter transients following an engine failure in the high dynamic pressure region. The results obtained through the simulation of engines 1 and 3 failures are the same as results that would be obtained by simulating engine 2 and 4 failures, except for negligible effects due to such asymmetries as the roll program and the nonspherical earth. Inboard engine failures were not considered because of the less severe disturbing moment, as compared to the disturbance due to an outboard engine failure. Also, since the inboard engines are not gimballed, no decrease in available control moment results under the condition of an inboard engine-out. For these reasons, the investigation of engine 1 and engine 3 failures was felt to be sufficient to yield those conditions of greatest interest, i.e., the "worst case" envelope is defined by engine 1 and 3 failures.

For the purposes of the study, the vehicle was considered to be "controllable" if it did not tumble and if the structural integrity was maintained. This definition of controllability requires a knowledge of the structural loads experienced by the vehicle. Therefore, a loads analysis was performed for several of the more critical engine-out trajectories.

5.1 "No Wind" Control Characteristics

The no wind trajectories, obtained for the orbit capability analysis, showed that the flight time before which an engine failure would result in tumbling was 20 seconds for engine 1 failures and 10 seconds for engine 3 failures. Attitude error histories for the borderline cases are presented in figures 22 through 25. From these figures it can be seen that the attitude errors begin to diverge in intervals of about 115 to 125 seconds. This time interval corresponds to the area of maximum dynamic pressure and angle of attack for the early time of engine-out

VEHICLE ANGULAR RATES FOR ENGINE NUMBER 1 AND 3 OUT AT 80 SECONDS
NO WINDS

FIGURE 19

30
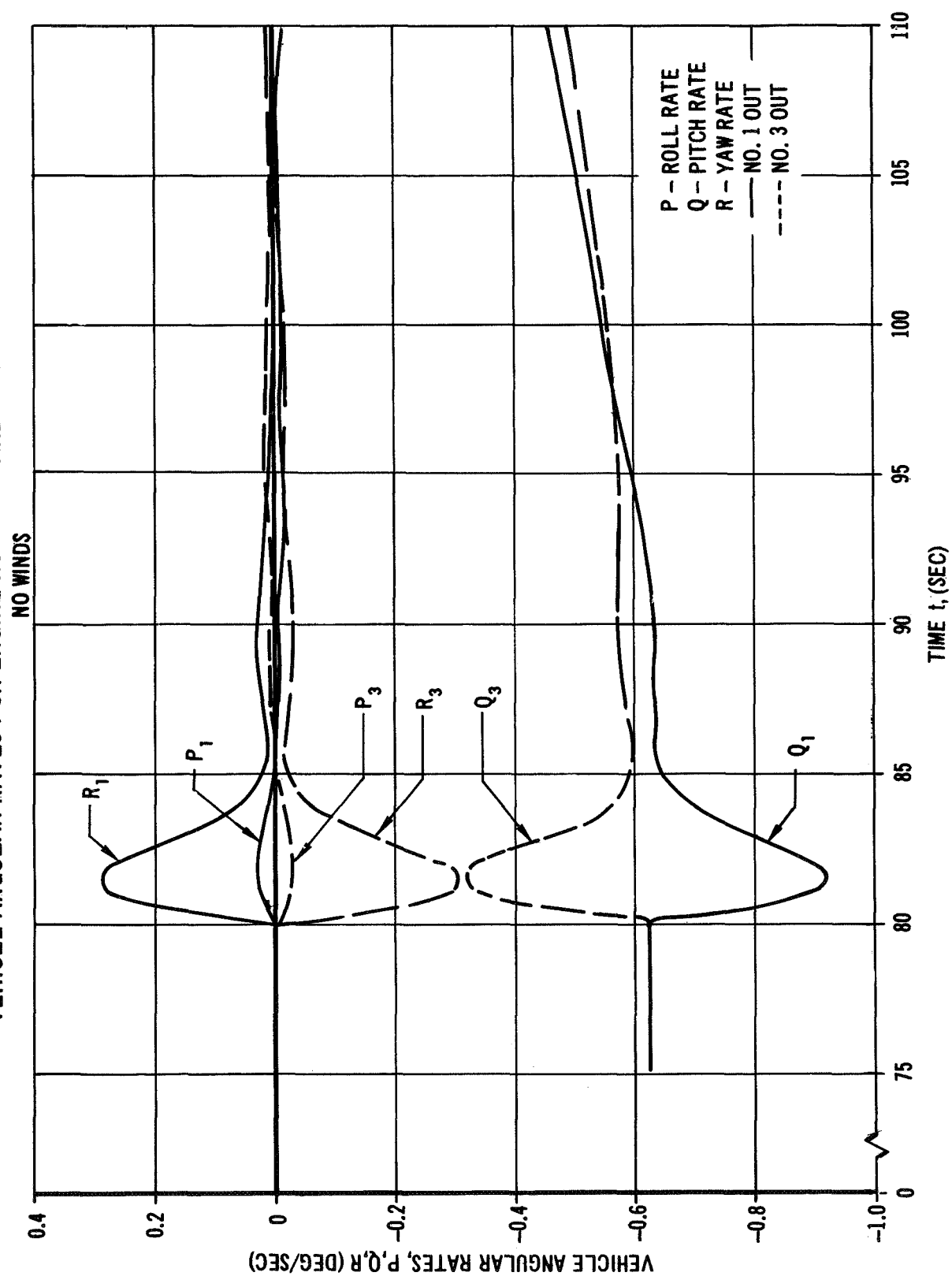
VEHICLE ATTITUDE ERROR HISTORIES FOR BOTH NUMBER 1 AND
NUMBER 3 ENGINE FAILURES AT 80 SECONDS
NO WIND
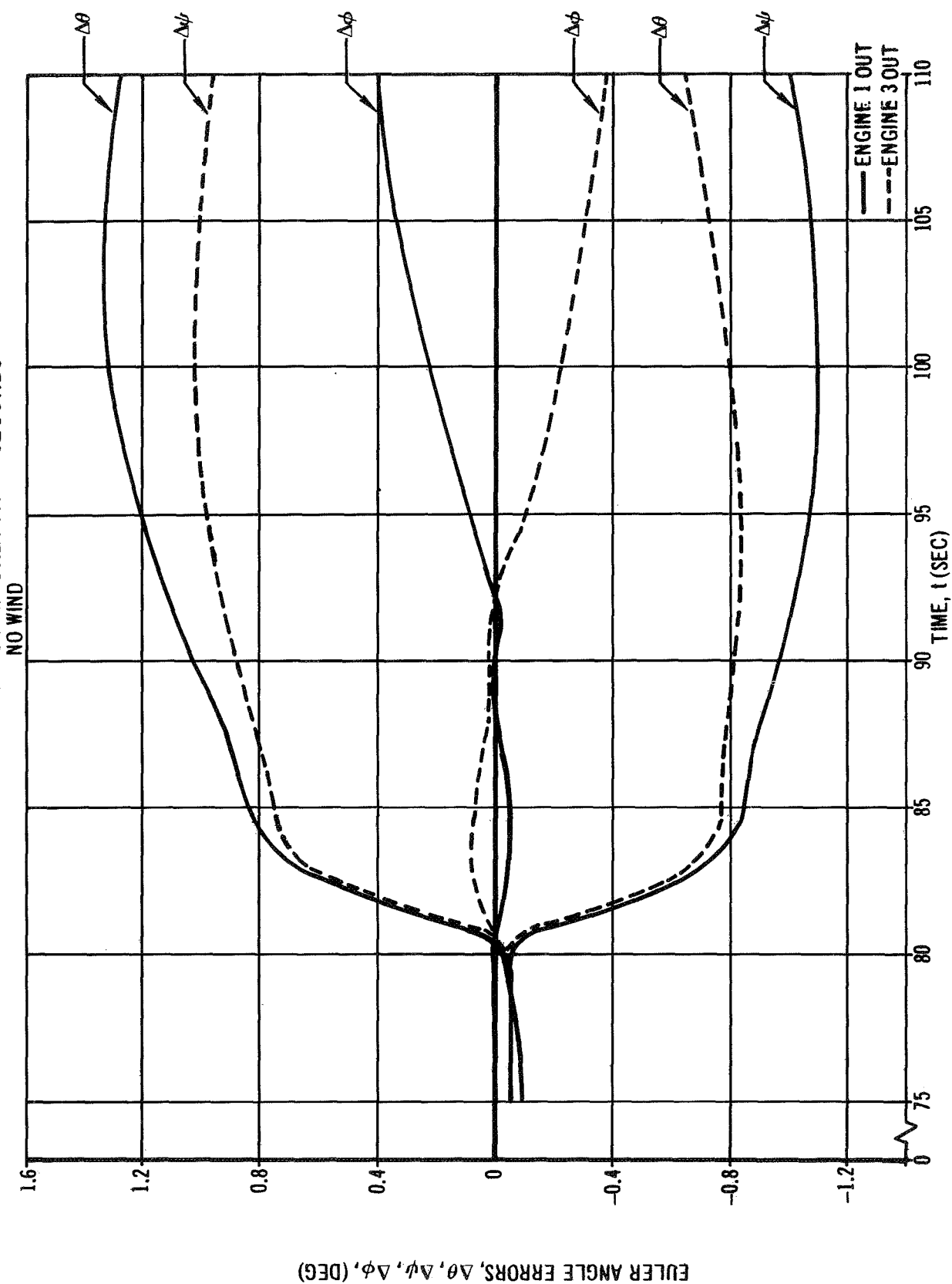
FIGURE 20

AVERAGE ENGINE DEFLECTION ANGLE HISTORIES FOR BOTH NUMBER 1
AND NUMBER 3 ENGINE FAILURES AT 80 SECONDS
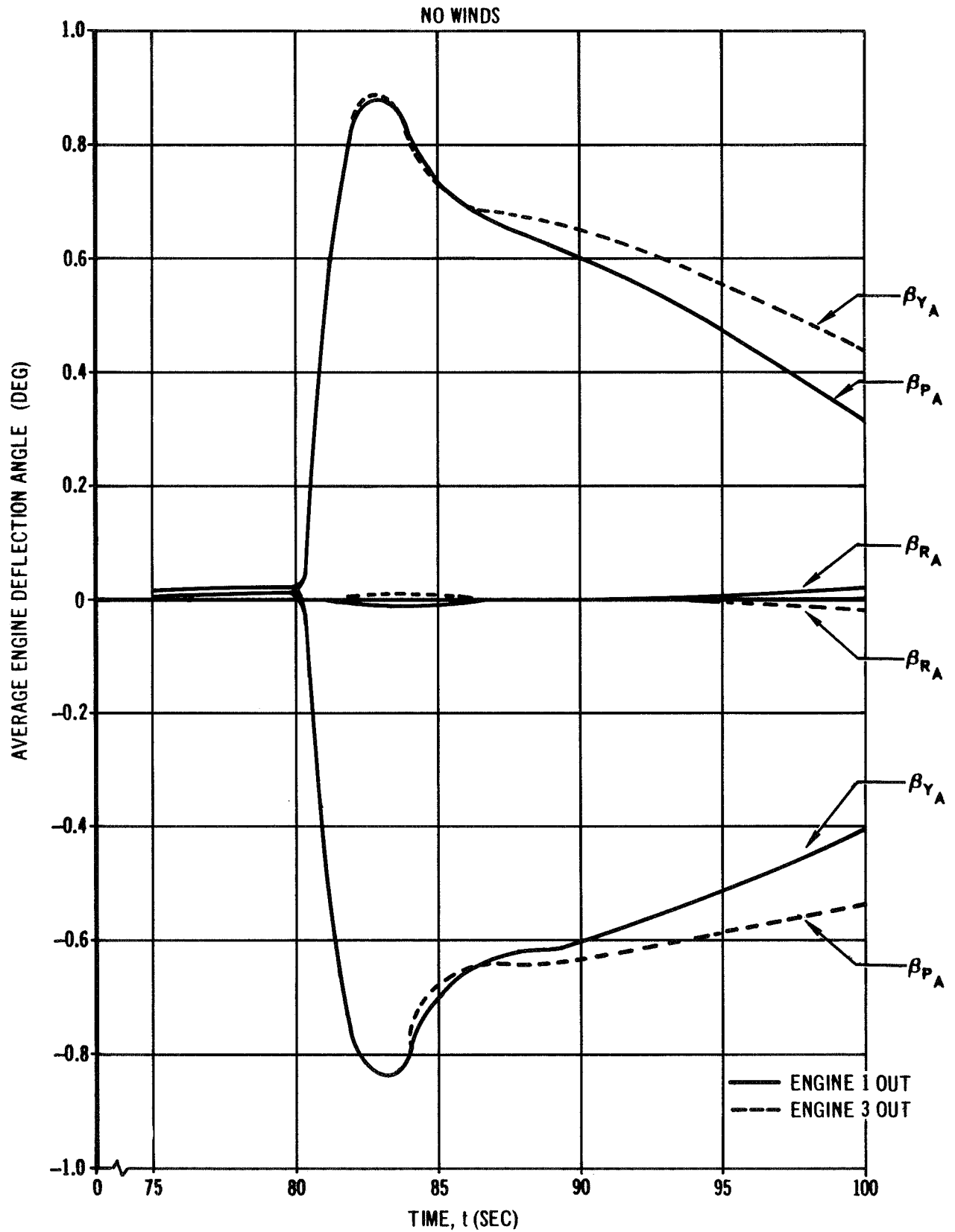
FIGURE 21

YAW ATTITUDE ERROR HISTORIES FOR NUMBER 1 ENGINE
FAILURES AT 15 AND 20 SECONDS
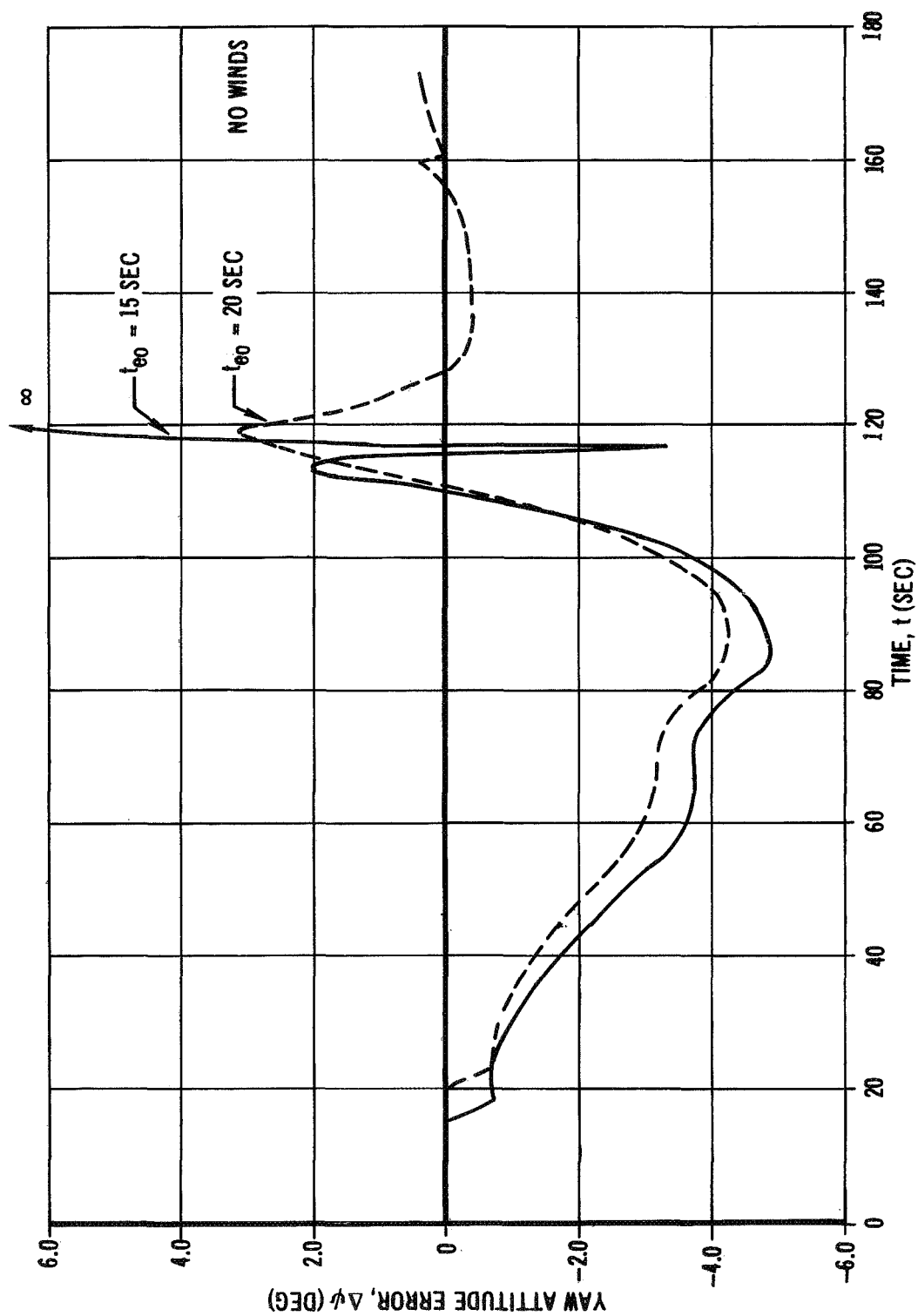
FIGURE 22

YAW ATTITUDE ERROR HISTORIES FOR NUMBER 3 ENGINE
FAILURES AT 5 AND 10 SECONDS

FIGURE 23

34
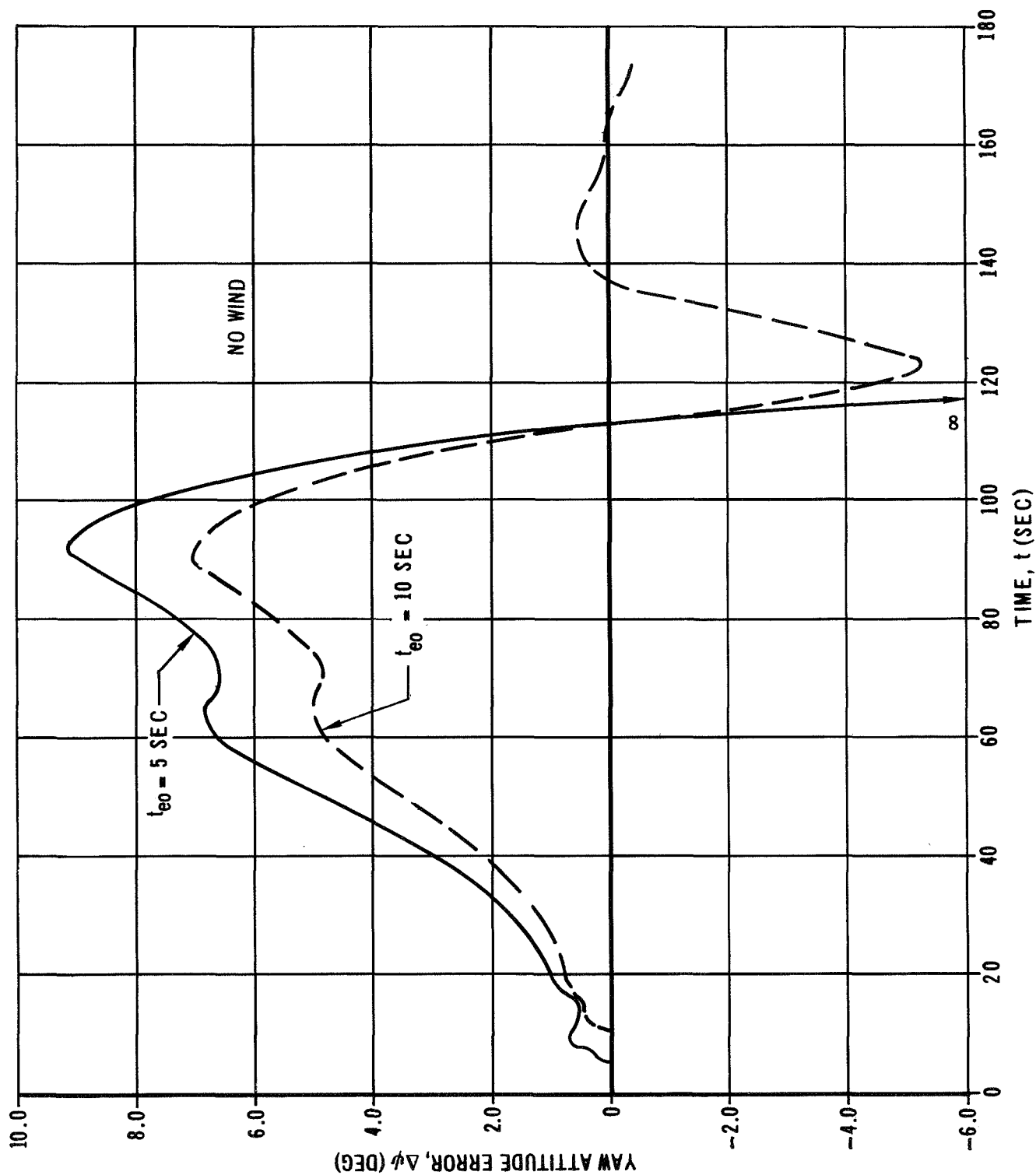
PITCH ATTITUDE ERROR HISTORIES FOR NUMBER 1 ENGINE
FAILURES AT 15 AND 20 SECONDS

NO WINDS
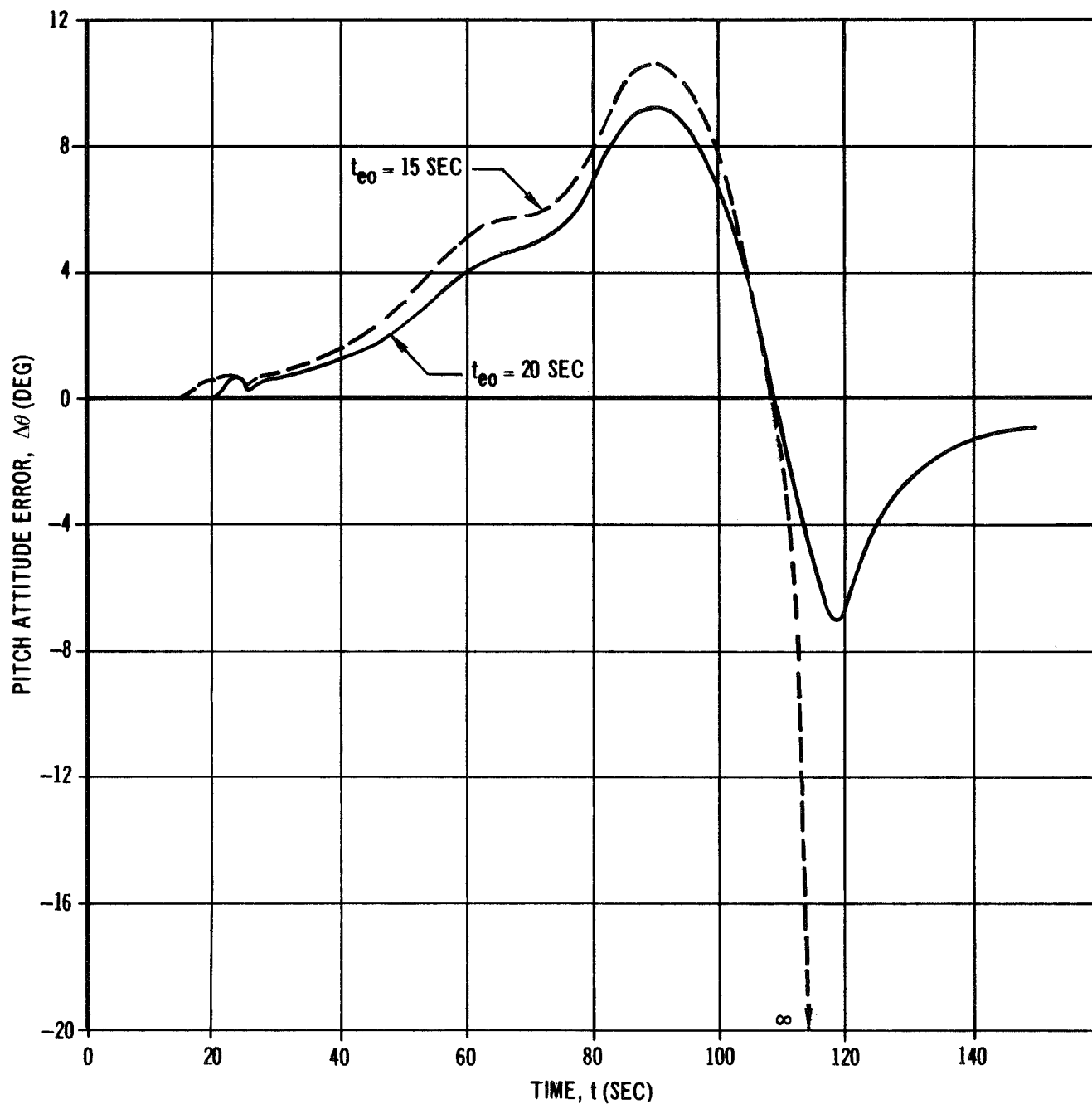
FIGURE 24

PITCH ATTITUDE ERROR HISTORIES FOR NUMBER 3 ENGINE
FAILURES AT 5 AND 10 SECONDS

NO WIND
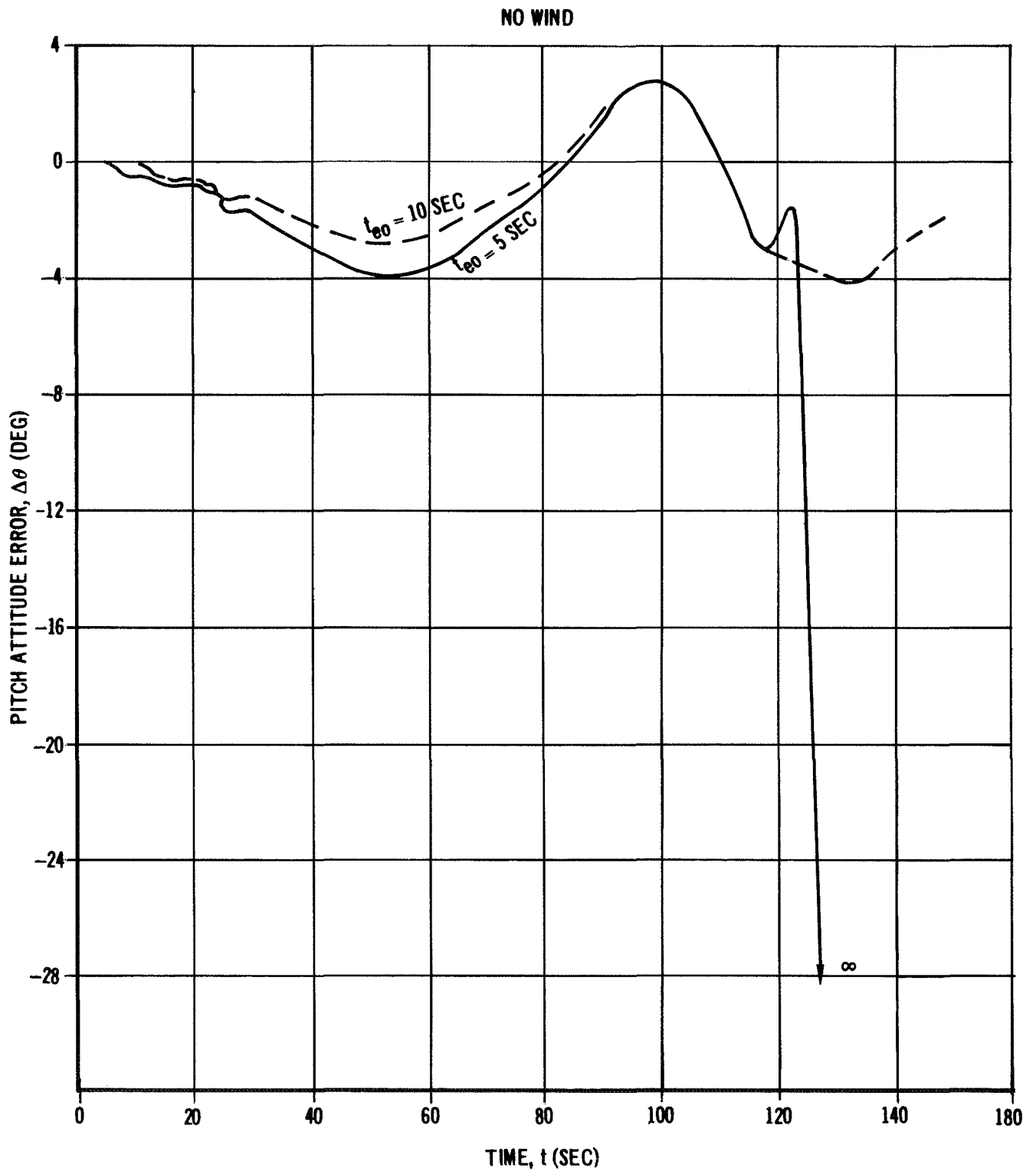
FIGURE 25

trajectories. The divergence or tumbling is due to the fact that the aerodynamic moment at the maximum pressure condition is greater than the maximum available control moment.

Bending moments were not calculated for these trajectories, but the aerodynamic loads were sufficiently high for all the cases in which tumbling occurred that it safely can be said that structural failure will occur; possibly before actual control is lost.

5.2 Dynamic Response to Winds

5.2.1 Winds Description

The winds employed in this study were developed using data obtained from reference 4. These data, which include the wind speed profile envelope, the vertical wind shear spectrum envelopes and the wind gust are presented in figures 26, 27 and 28. These winds were applied as a means of perturbing the vehicle from the "nominal" atmospheric conditions during first stage flight. The winds functioned as tests of the launch vehicle's ability to maintain control and/or structural integrity during specific phases of the S-IB boost stage trajectory.

5.2.1.1 Construction

In the development of the wind profiles, two basic assumptions were made. First, it was assumed that the flow always acted perpendicular to a radius vector drawn from the center of the earth to the vehicle. Second, in the construction of the final wind profiles, it was assumed that the wind profile "decay" phase would be a mirror image of the "build-up" phase.

The altitude of maximum dynamic pressure, and the associated dynamic pressure, angle of attack, and time of occurrence as a function of time of engine failure are presented in figures 29 and 30 for the no wind number 1 engine-out trajectories. The same parameters are given in figures 31 and 32 for the no wind number 3 engine-out trajectories. The dynamic pressure histories of each of the no wind trajectories were investigated to determine the altitude of maximum dynamic pressure for each engine-out condition. The wind profiles were then constructed, in the manner described in reference 4, so that the altitude of maximum wind velocity was equal to the altitude of maximum dynamic pressure.

Quasi-square wave shaped gusts (embedded jets) were also developed as set forth in reference 4. These gusts were composed of a wind velocity increase of 29.52 feet/second over a "build-up" altitude increase of 82 feet, a "life" of gust for 164 feet increase of altitude, and a velocity decrease of 29.52 feet/second over the "decay" altitude increase of 82 feet, as shown on figure 28. These gusts were imposed such that they were an extension of the build-up phase of the wind profiles, and occurred at the altitude of maximum wind velocity.

WIND SPEED PROFILE ENVELOPE FOR 95.0%
PROBABILITY OF OCCURRENCE
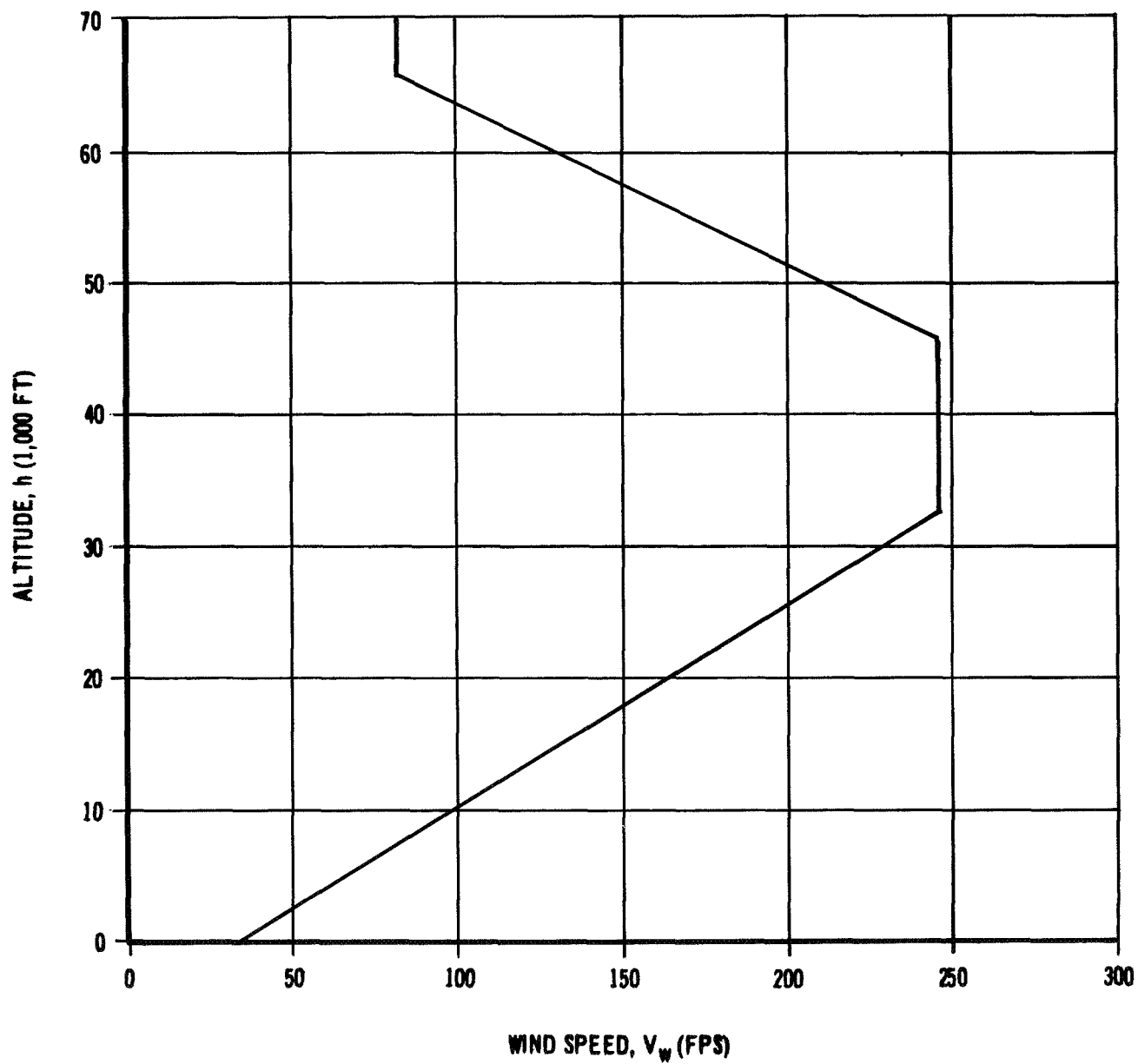
FIGURE 26

NINETY-NINE PERCENT PROBABILITY-OF-OCCURRENCE
VERTICAL WIND SHEAR SPECTRUM ENVELOPES

ID NO	SCALE-OF-DISTANCE (FT)
1	16,404.0
2	13,123.2
3	9,842.4
4	6,561.6
5	3,280.8
6	2,624.6
7	1,968.5
8	1,312.3
9	656.2
10	328.1
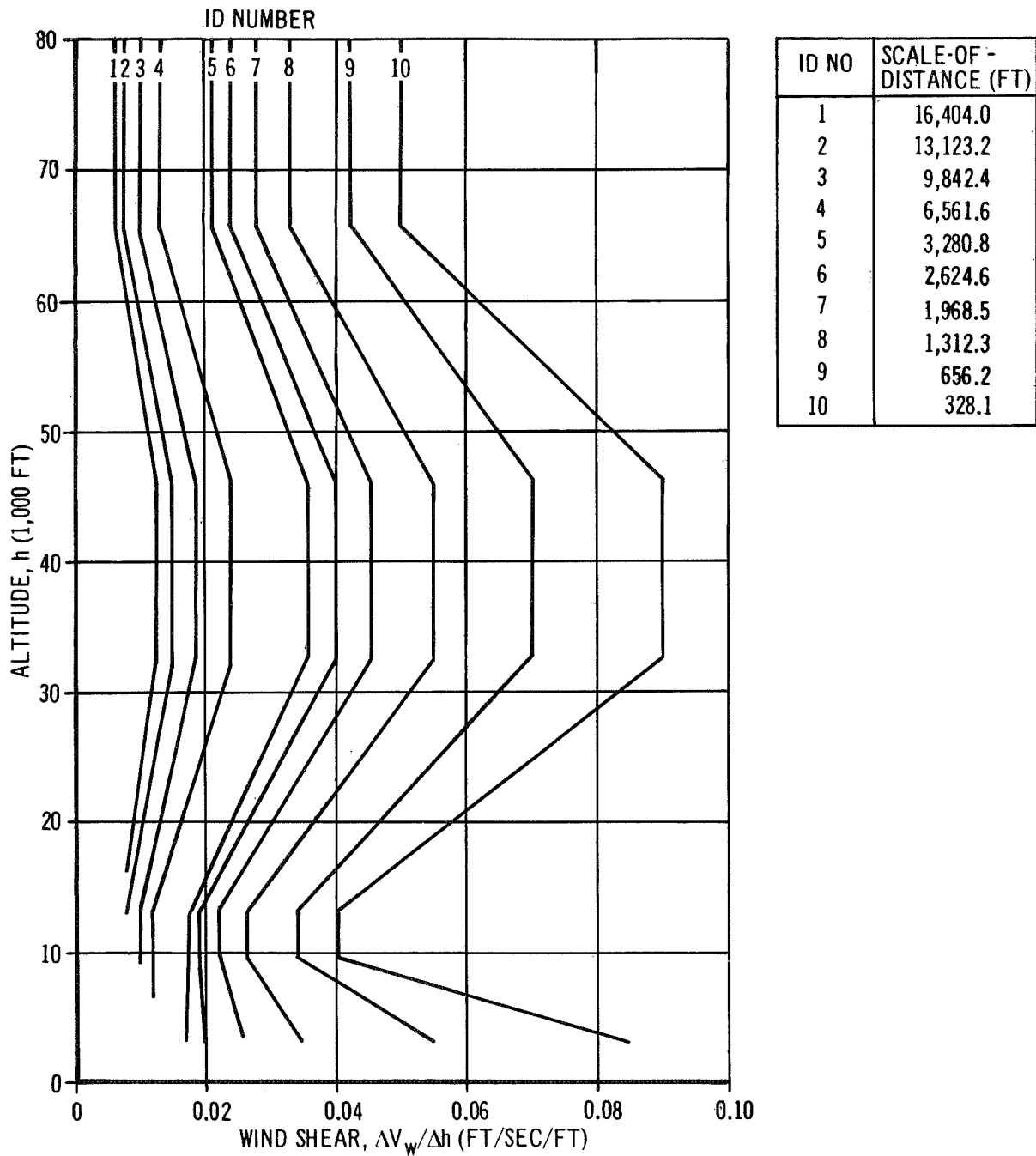
FIGURE 27

RELATIONSHIP BETWEEN ESTABLISHED GUSTS
AND/OR EMBEDDED JET CHARACTERISTICS
(QUASI SQUARE WAVE SHAPE) AND THE
IDEALIZED WIND SPEED (QUASI
STEADY STATE) PROFILE
ENVELOPE

29.52 FPS

29.52 FPS PER 82 FT Δh
(0.36 SEC⁻¹ GRADIENT)

164   FEET

WIND BUILD-UP
ENVELOPE

IDEALIZED WIND
SPEED ENVELOPE

IDEALIZED WIND
SPEED ENVELOPE
PLUS 29.52 FPS

FIGURE 28

MAXIMUM DYNAMIC PRESSURE AND THE ASSOCIATED ANGLE OF ATTACK DEPENDABILITY ON THE TIME OF NUMBER 1 ENGINE FAILURE
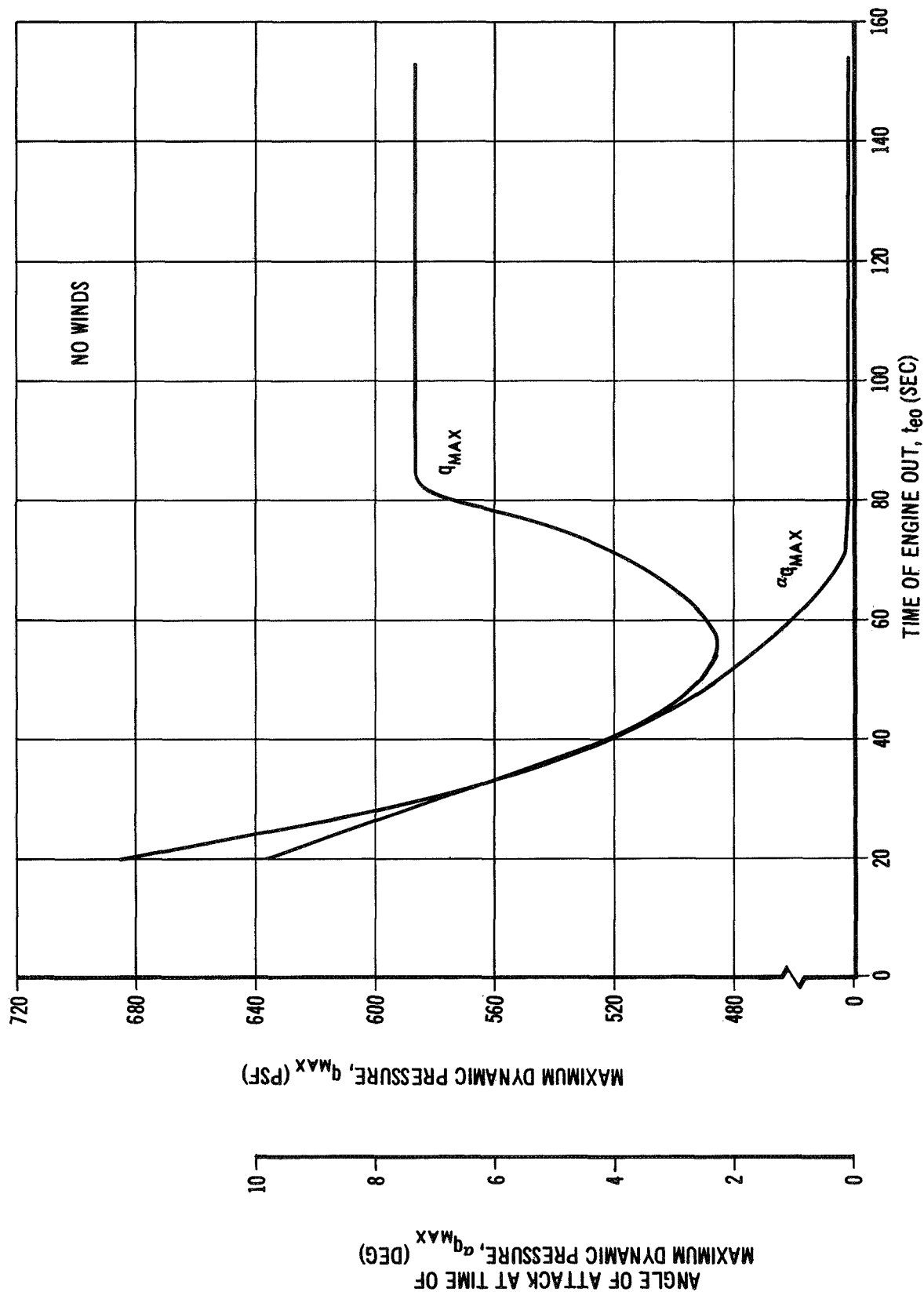
FIGURE 29

ALTITUDE AND TIME OF MAXIMUM DYNAMIC PRESSURE DEPENDABILITY ON TIME OF ENGINE NUMBER 1 FAILURE
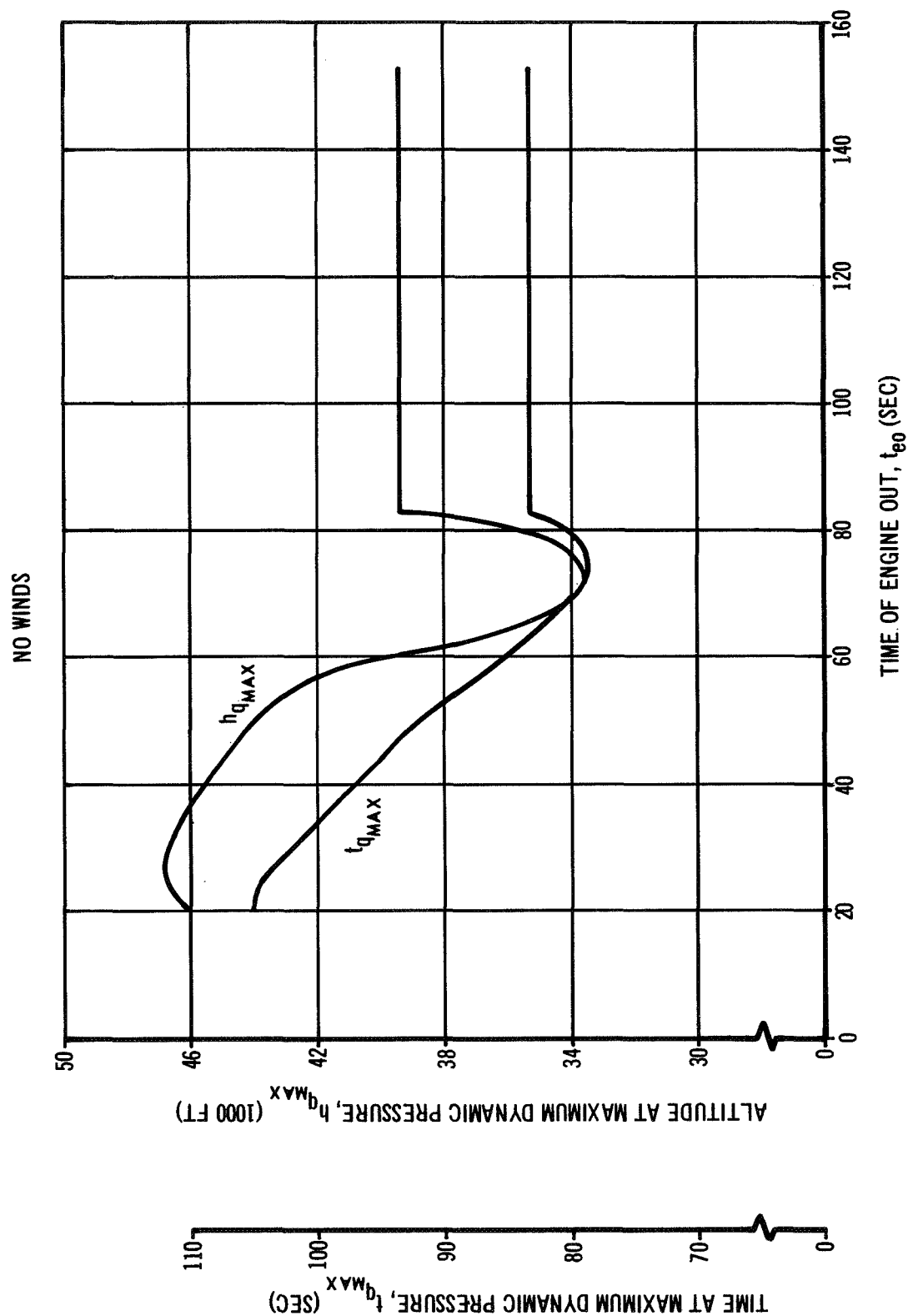
FIGURE 30

MAXIMUM DYNAMIC PRESSURE AND THE ASSOCIATED ANGLE OF ATTACK DEPENDABILITY
ON THE TIME OF NUMBER 3 ENGINE FAILURE
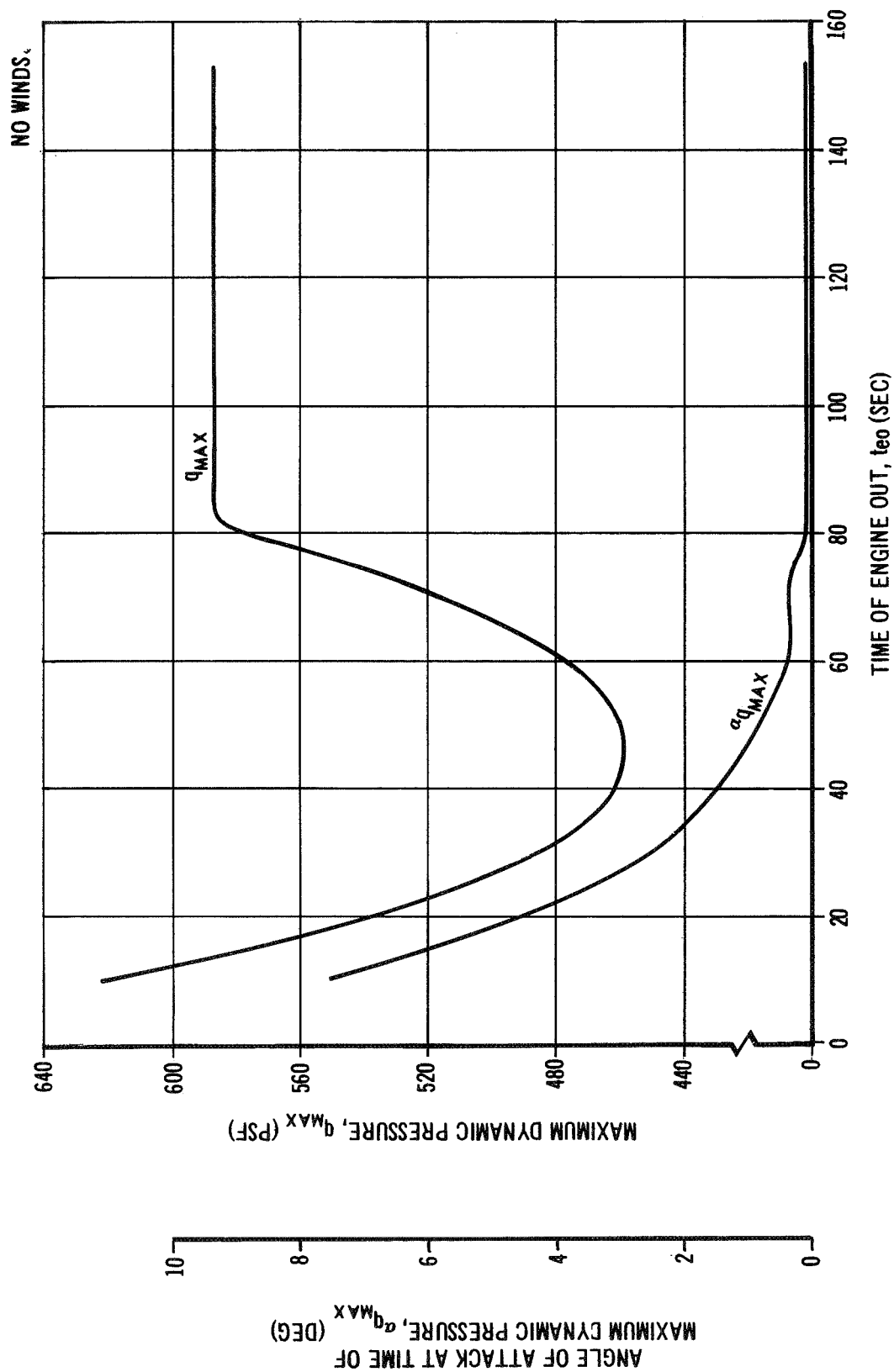
FIGURE 31

ALTITUDE AND TIME OF MAXIMUM DYNAMIC PRESSURE DEPENDABILITY ON THE TIME OF NUMBER 3 ENGINE FAILURE
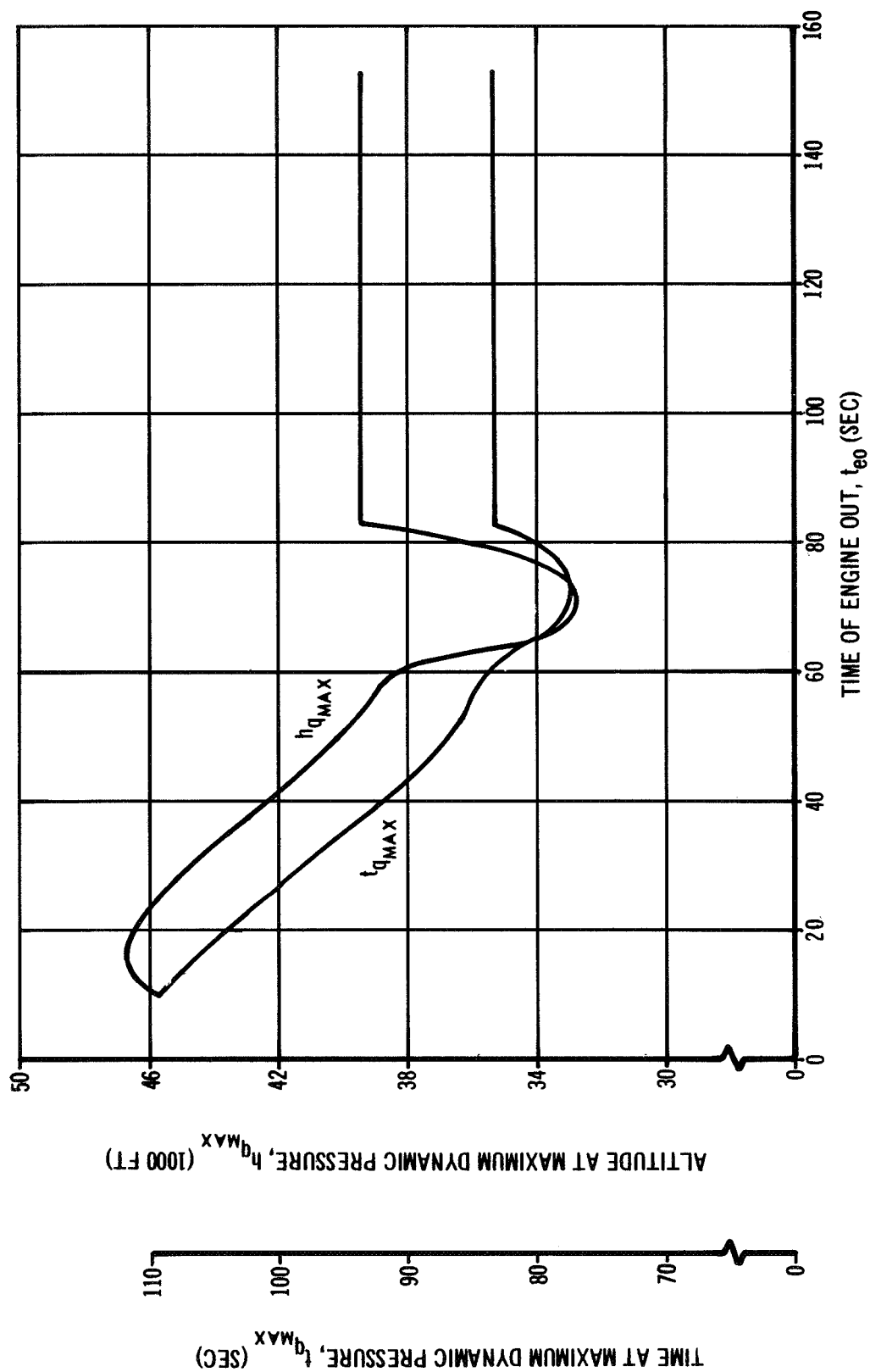
FIGURE 32

A separate wind profile was constructed for each engine-out trajectory. The profiles, with gust included, are shown in figures 33 and 34. The specific engine-out trajectory for which each profile was used is indicated on the figures.

5.2.1.2 Application

The vehicle dynamic response was determined for each engine-out condition using both head winds and side winds. Head winds were contained in the pitch plane, at a heading of 180 degrees to the flight azimuth. Side winds were contained in the yaw plane, at a heading of 90 degrees to the flight azimuth. Left side winds were used in t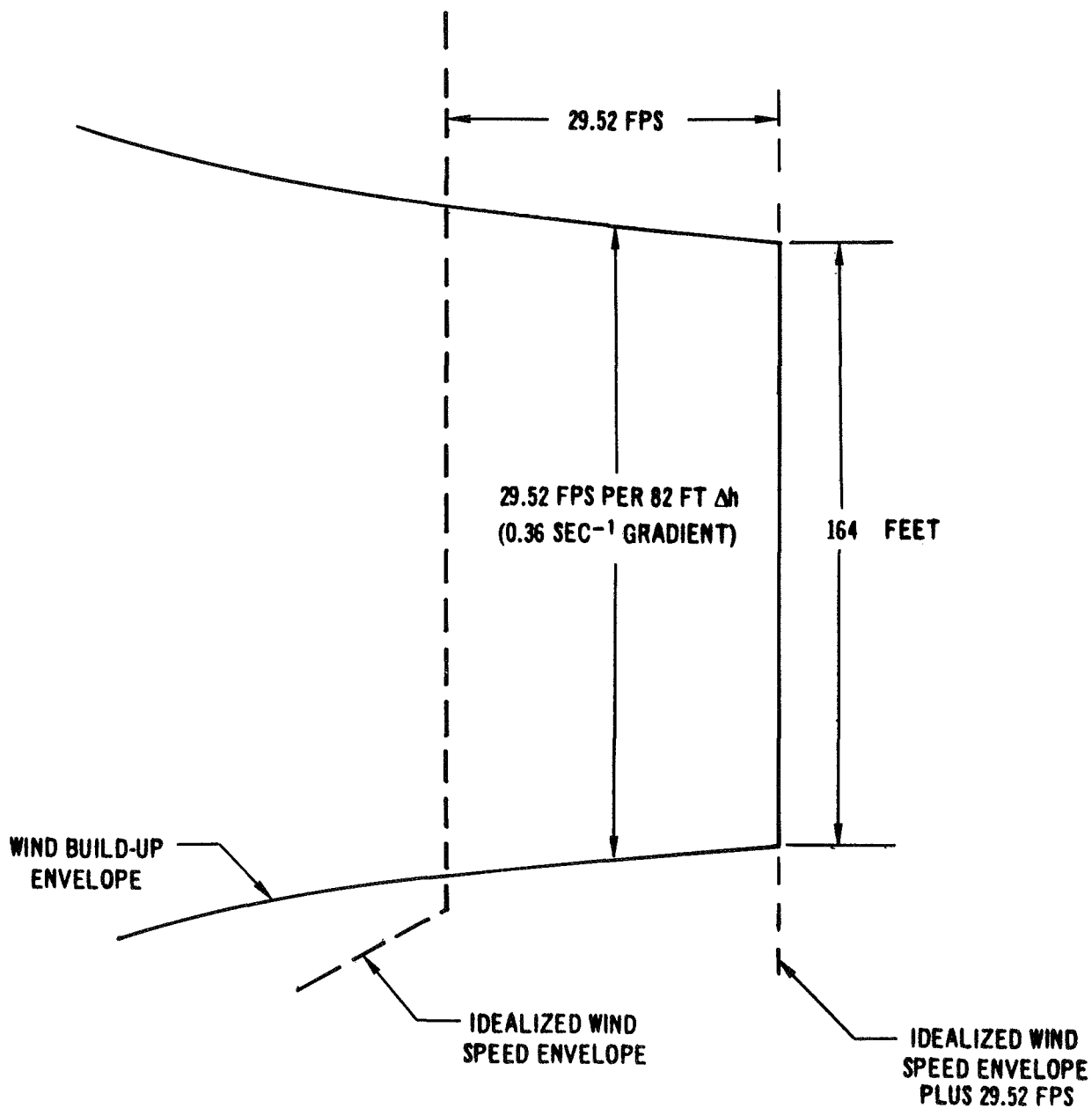he number 1 engine-out trajectories and right side winds were used in the number 3 engine-out trajectories. These side winds were applied in the directions described above so that the disturbing moment resulting from the wind angle of attack would add to, rather than subtract from, the disturbing moment due to the engine-out. Tail winds were not considered because of the resulting reduction in relative velocity and, therefore, reduction in dynamic pressure.

5.2.2 Controllability

Four sets of engine-out trajectories with wind have been defined and are listed below:

   a. Engine 1 out - head winds

   b. Engine 1 out - left side winds

   c. Engine 3 out - head winds

   d. Engine 3 out - right side winds

Engine-out times of 30, 40, 50, 60, 70 and 80 seconds were simulated for each of the above sets of trajectories.

The maximum product of dynamic pressure and angle of attack was calculated for each trajectory and the results used to develop a "worst case" envelope.

This worst case envelope is presented in figure 35. It must be understood that while this envelope presents the most critical conditions, there are, in some cases, other combinations of number and time of engine failure and prevailing wind mode which will result in a dynamic pressure-angle of attack product which is almost equally critical.

5.2.2.1 Control Profiles

The vehicle angle of attack, dynamic pressure, normal acceleration, angular acceleration, and average thrust vector deflection response is presented in figures 36 through 55. Figures 36 through 40, and 41 through 45 present number 1 engine out for head and left side winds, respectively. Number 3 engine failures, head and right side winds are

95% PROBABILITY-OF-OCCURRENCE WINDS
ENGINE NUMBER 1 FAILURE
GUSTS APPLIED AT ALTITUDE OF
MAXIMUM DYNAMIC PRESSURE
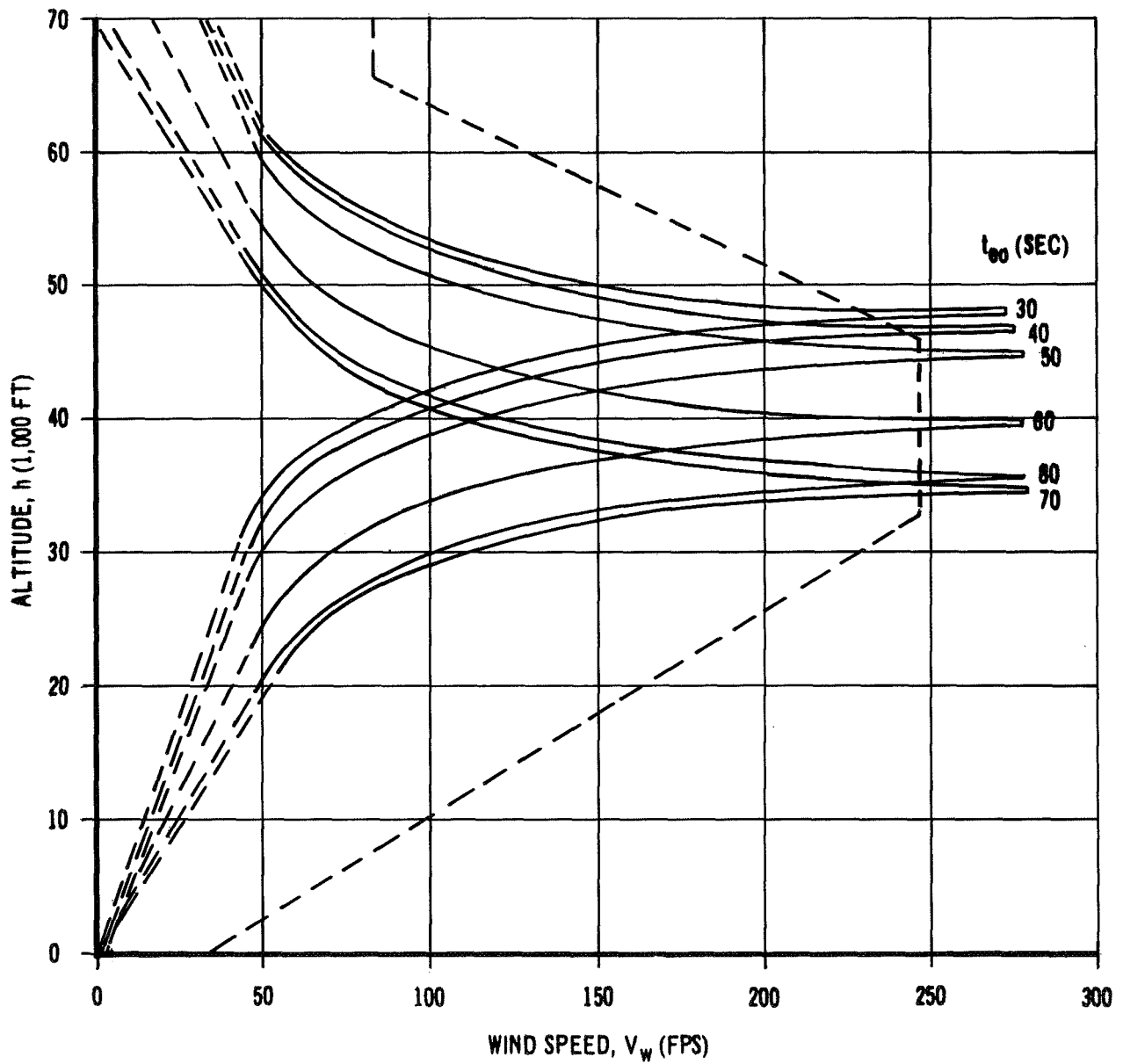
FIGURE 33

95% PROBABILITY-OF-OCCURRENCE WINDS
NUMBER 3 ENGINE FAILURE
GUSTS APPLIED AT ALTITUDE OF
MAXIMUM DYNAMIC PRESSURE
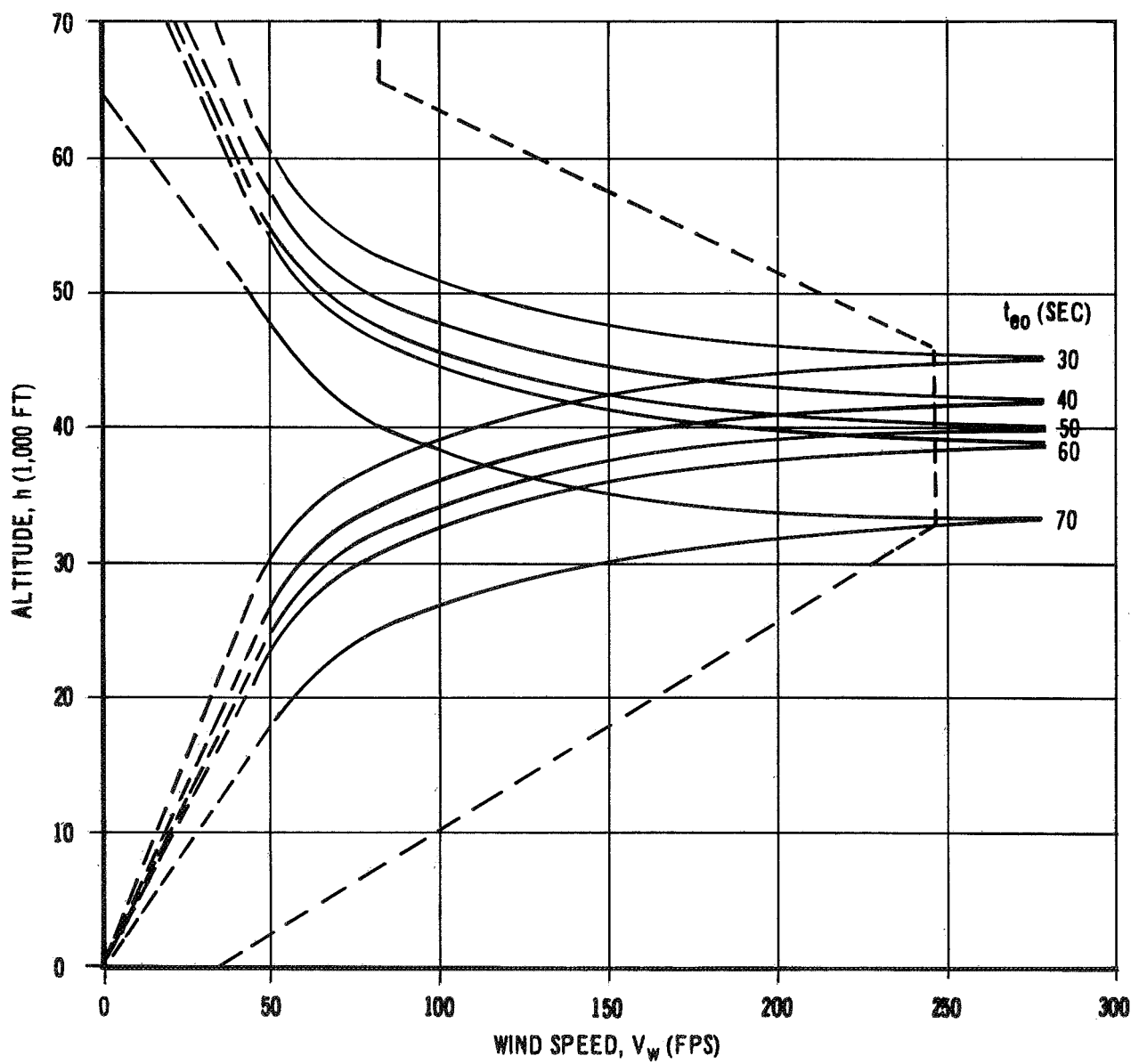
FIGURE 34

MAXIMUM ANGLE OF ATTACK AND DYNAMIC PRESSURE PRODUCT
ENGINE NUMBER 1 AND 3 FAILURE
HEAD WINDS OR SIDE WINDS WITH GUST
AT MAXIMUM DYNAMIC PRESSURE

FIGURE 35

PITCH ANGLE OF ATTACK RESPONSE TO A HEAD
WIND GUST
NUMBER 1 ENGINE FAILURE AT 30, 40, 50, 60, 70,
AND 80 SECONDS

FIGURE 36

DYNAMIC PRESSURE RESPONSE TO A HEAD WIND GUST
NUMBER 1 ENGINE FAILURE AT 30, 40, 50, 60, 70, AND 80 SECONDS

FIGURE 37

PITCH NORMAL ACCELERATION RESPONSE TO A HEAD
WIND GUST
NUMBER 1 ENGINE FAILURE AT 30, 40, 50, 60, 70,
AND 80 SECONDS

FIGURE 38

PITCH ANGULAR ACCELERATION RESPONSE
TO A HEAD WIND GUST

NUMBER 1 ENGINE FAILURE AT 30, 40, 50, 60, 70,
AND 80 SECONDS

FIGURE 39

AVERAGE PITCH ENGINE DEFLECTION ANGLE RESPONSE
TO A HEAD WIND GUST
NUMBER 1 ENGINE FAILURE AT 30, 40, 50, 60, 70,
AND 80 SECONDS

FIGURE 40

FIGURE 41

54

DYNAMIC PRESSURE RESPONSE TO A LEFT SIDE
WIND GUST

NUMBER 1 ENGINE FAILURE AT 30, 40, 50, 60, 70,
AND 80 SECONDS

FIGURE 42

YAW NORMAL ACCELERATION RESPONSE TO A
SIDE WIND GUST

NUMBER 1 ENGINE FAILURE AT 30, 40, 50, 60, 70,
AND 80 SECONDS

FIGURE 43

YAW ANGULAR ACCELERATION RESPONSE TO
A LEFT SIDE WIND GUST
NUMBER 1 ENGINE FAILURE AT 30, 40, 50, 60, 70,
AND 80 SECONDS
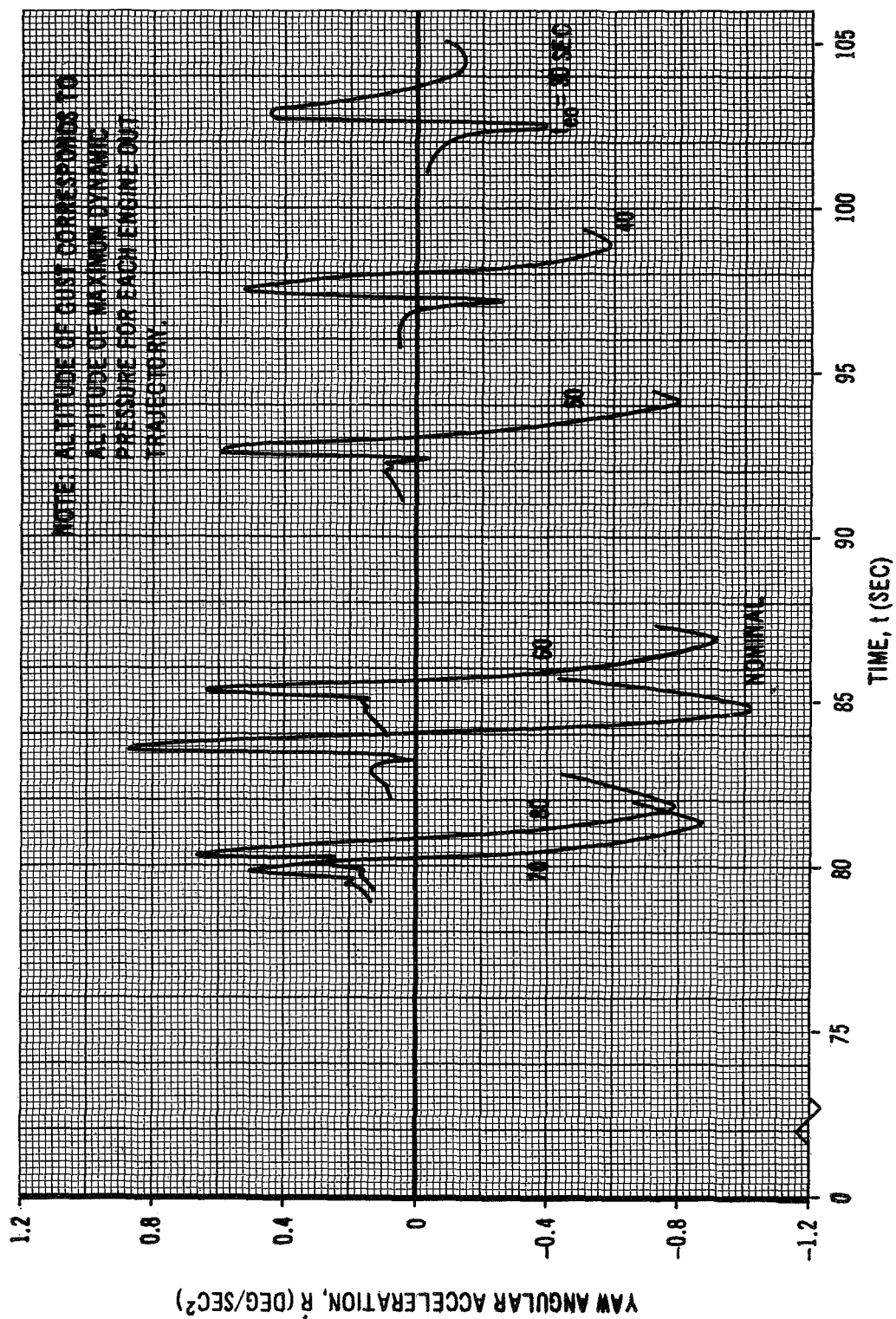
FIGURE 44

AVERAGE YAW ENGINE DEFLECTION ANGLE
RESPONSE TO A SIDE WIND GUST

NUMBER 1 ENGINE FAILURE AT 30, 40, 50, 60, 70,
AND 80 SECONDS

NOTE: ALTITUDE OF GUST CORRESPONDS TO
ALTITUDE OF MAXIMUM DYNAMIC
PRESSURE FOR EACH ENGINE OUT
TRAJECTORY.
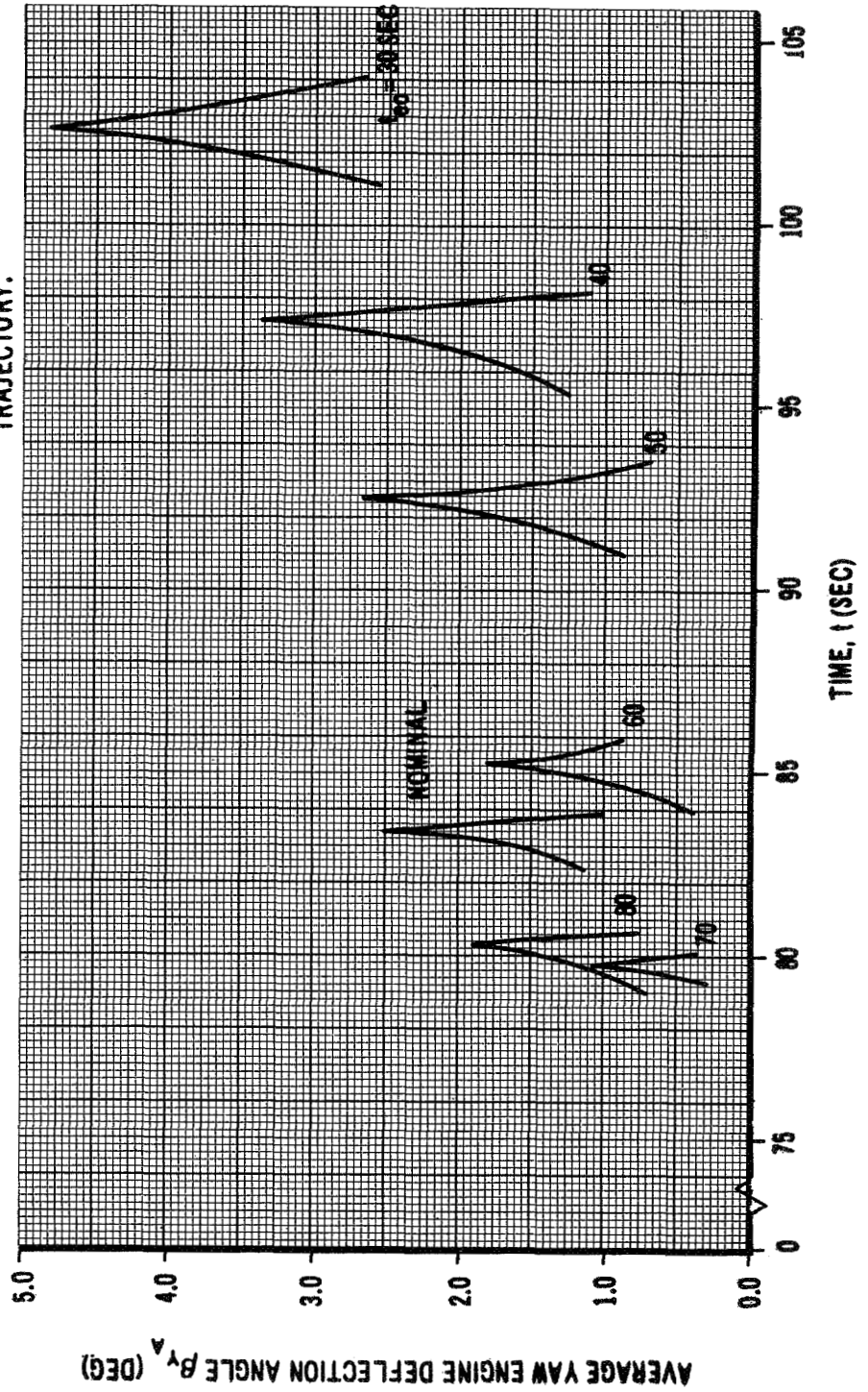
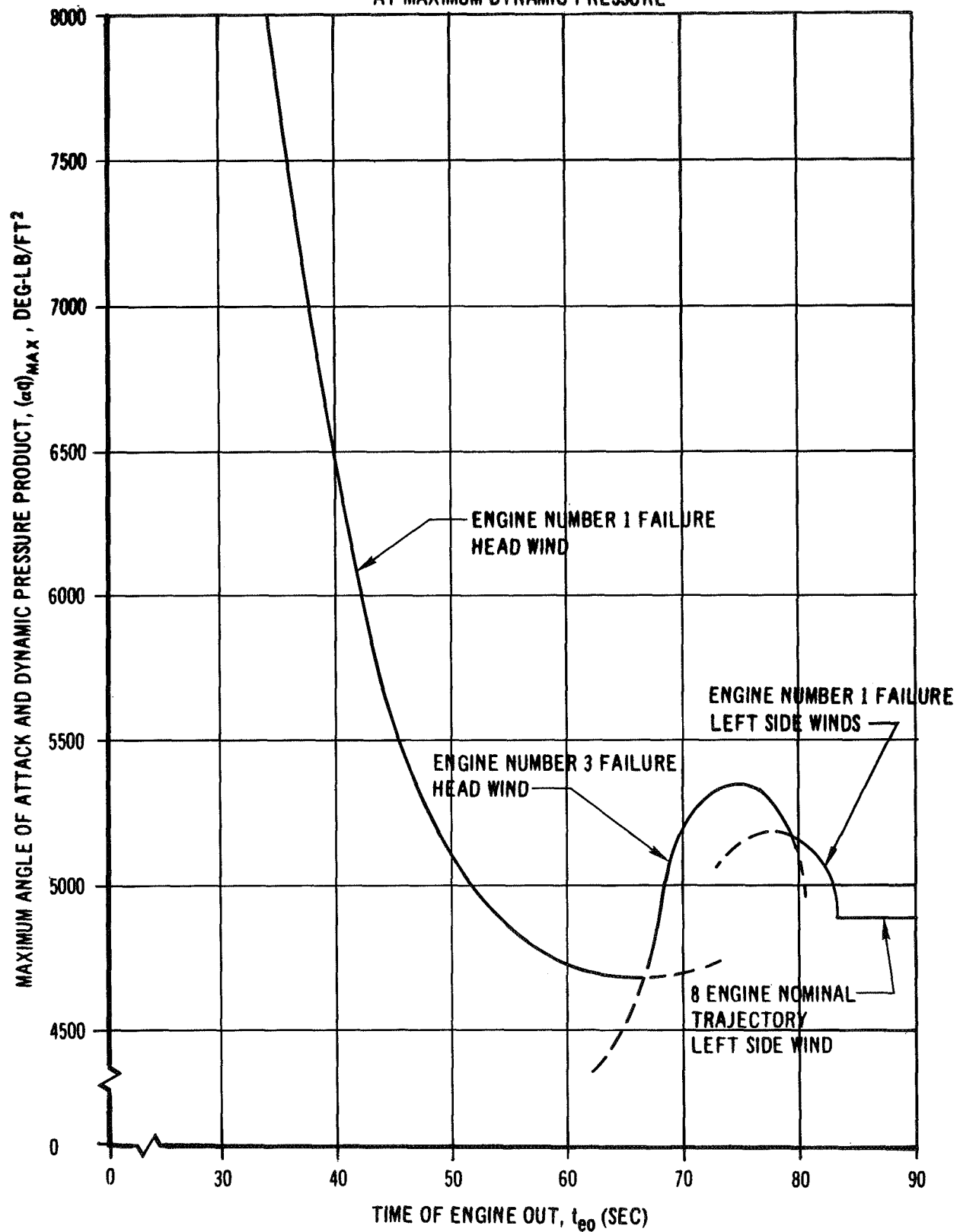**FIGURE 45**

ANGLE OF ATTACK RESPONSE TO A HEAD
WIND GUST
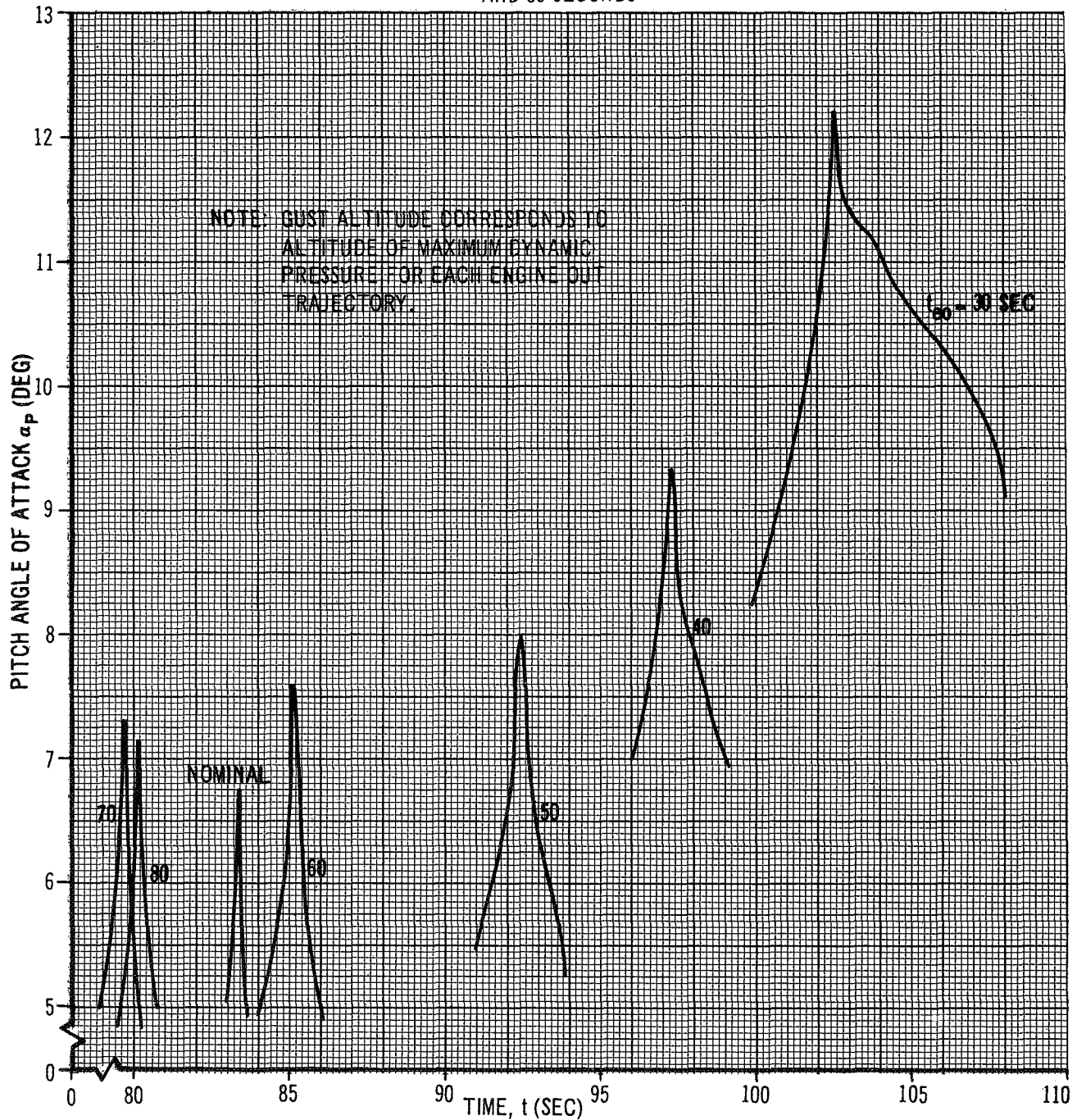NUMBER 3 ENGINE FAILURE AT 30, 40, 50, 60, 70,
AND 80 SECONDS

FIGURE 46

DYNAMIC PRESSURE RESPONSE TO A HEAD
WIND GUST
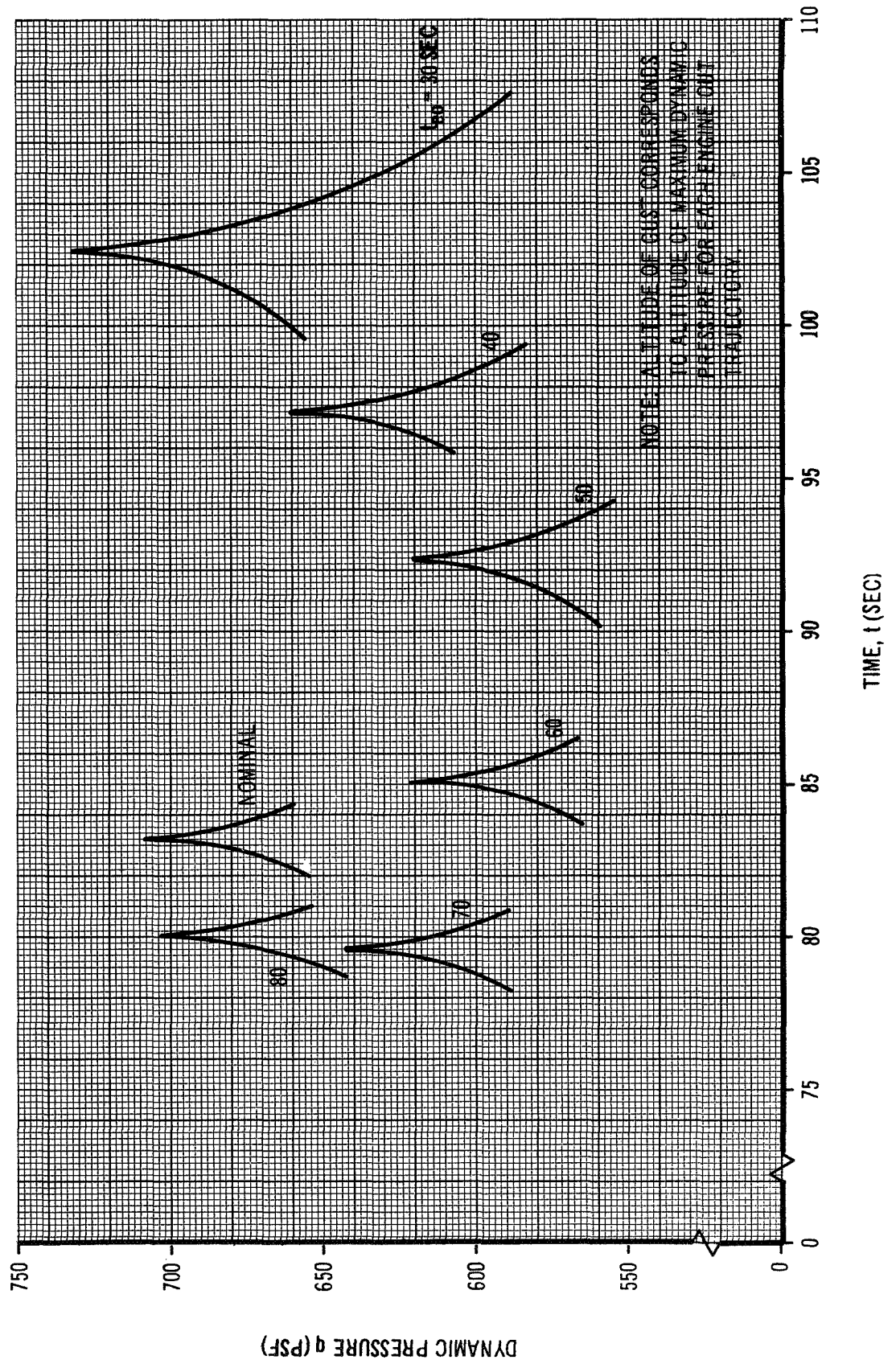## NUMBER 3 ENGINE FAILURE AT 30, 40, 50, 60, 70,
AND 80 SECONDS

NOTE: ALTITUDE OF GUST CORRESPONDS TO
ALTITUDE OF MAXIMUM DYNAMIC
PRESSURE FOR EACH ENGINE OUT
TRAJECTORY..

FIGURE 47

PITCH NORMAL ACCELERATION RESPONSE
TO A HEAD WIND GUST
NUMBER 3 ENGINE FAILURE AT 30, 40, 50, 60, 70, AND 80 SECONDS

NOTE: ALTITUDE OF GUST CORRESPONDS TO ALTITUDE OF MAXIMUM DYNAMIC PRESSURE FOR EACH ENGINE OUT TRAJECTORY.
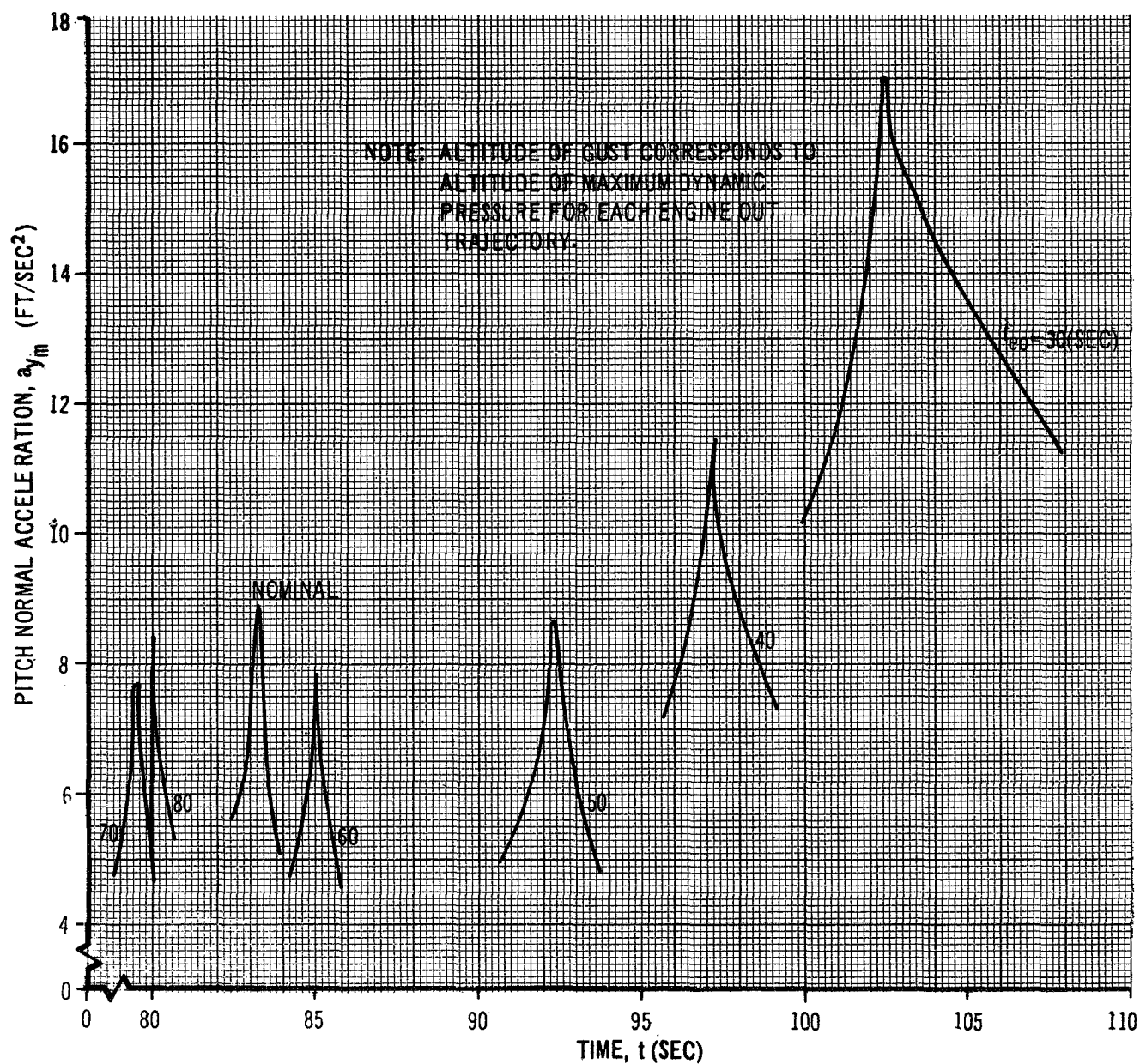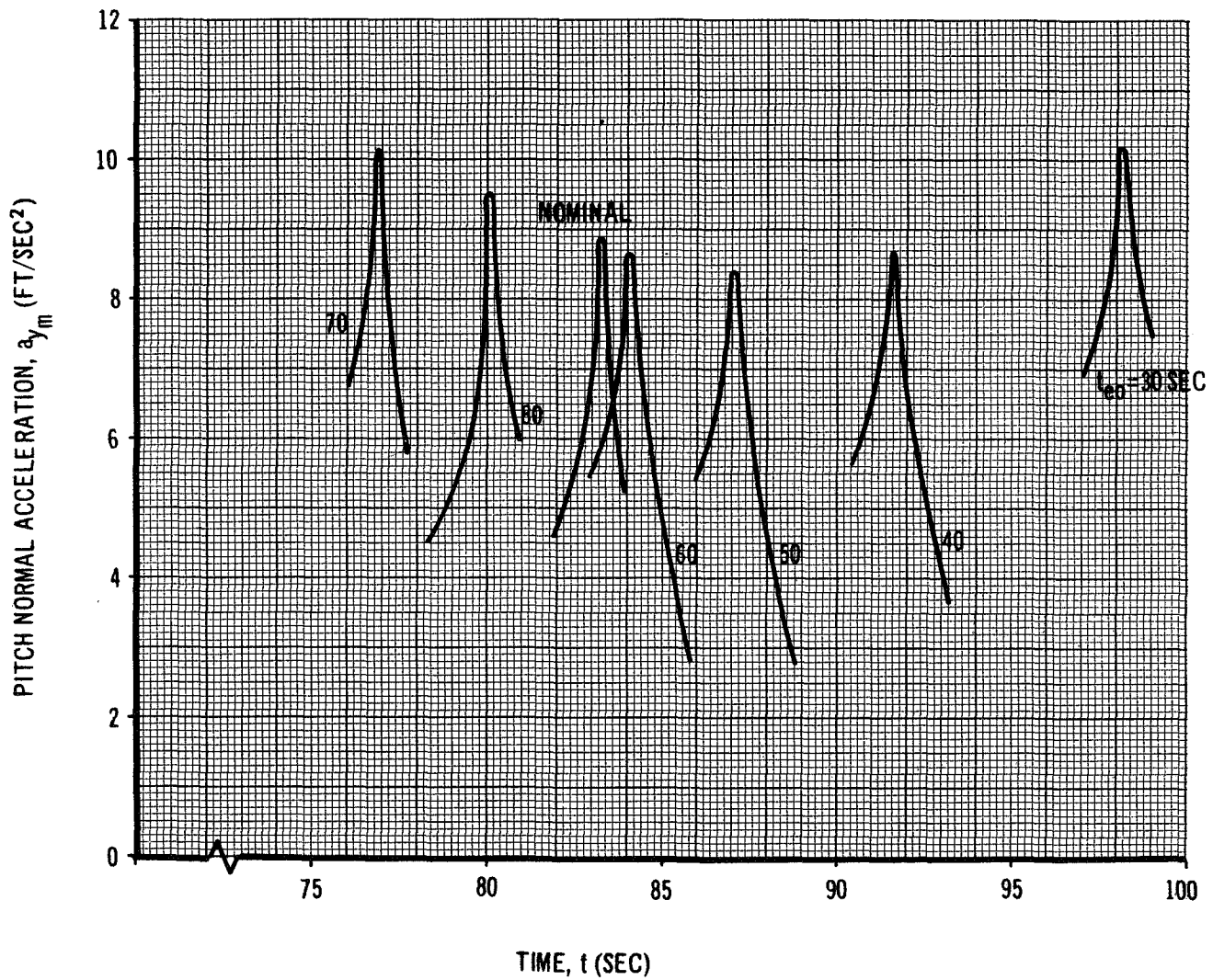

FIGURE 48

PITCH ANGULAR ACCELERATION RESPONSE
TO A HEAD WIND GUST
NUMBER 3 ENGINE FAILURE AT 30, 40, 50, 60, 70,
AND 80 SECONDS

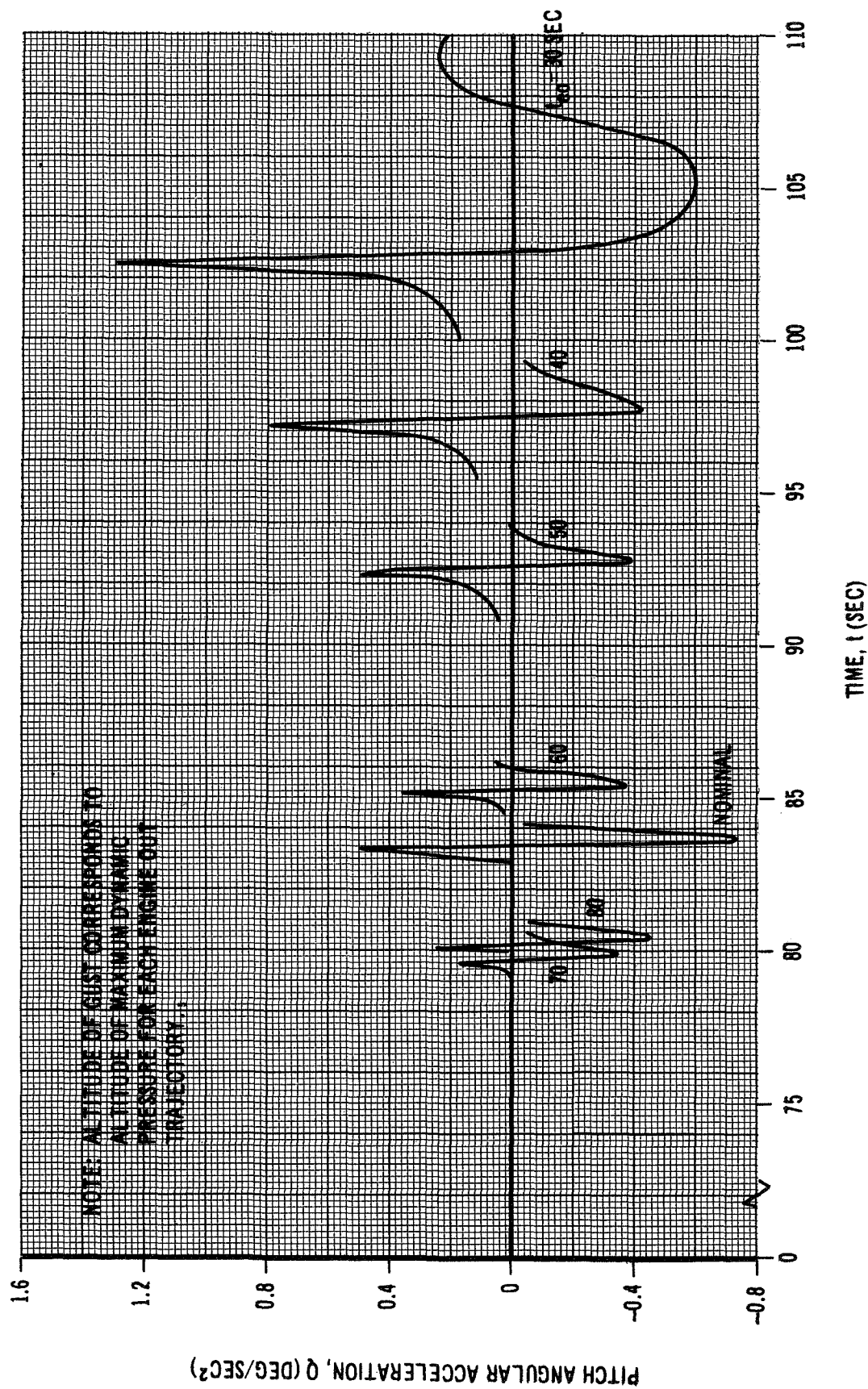FIGURE 49

AVERAGE PITCH ENGINE DEFLECTION ANGLE
RESPONSE TO A HEAD WIND GUST
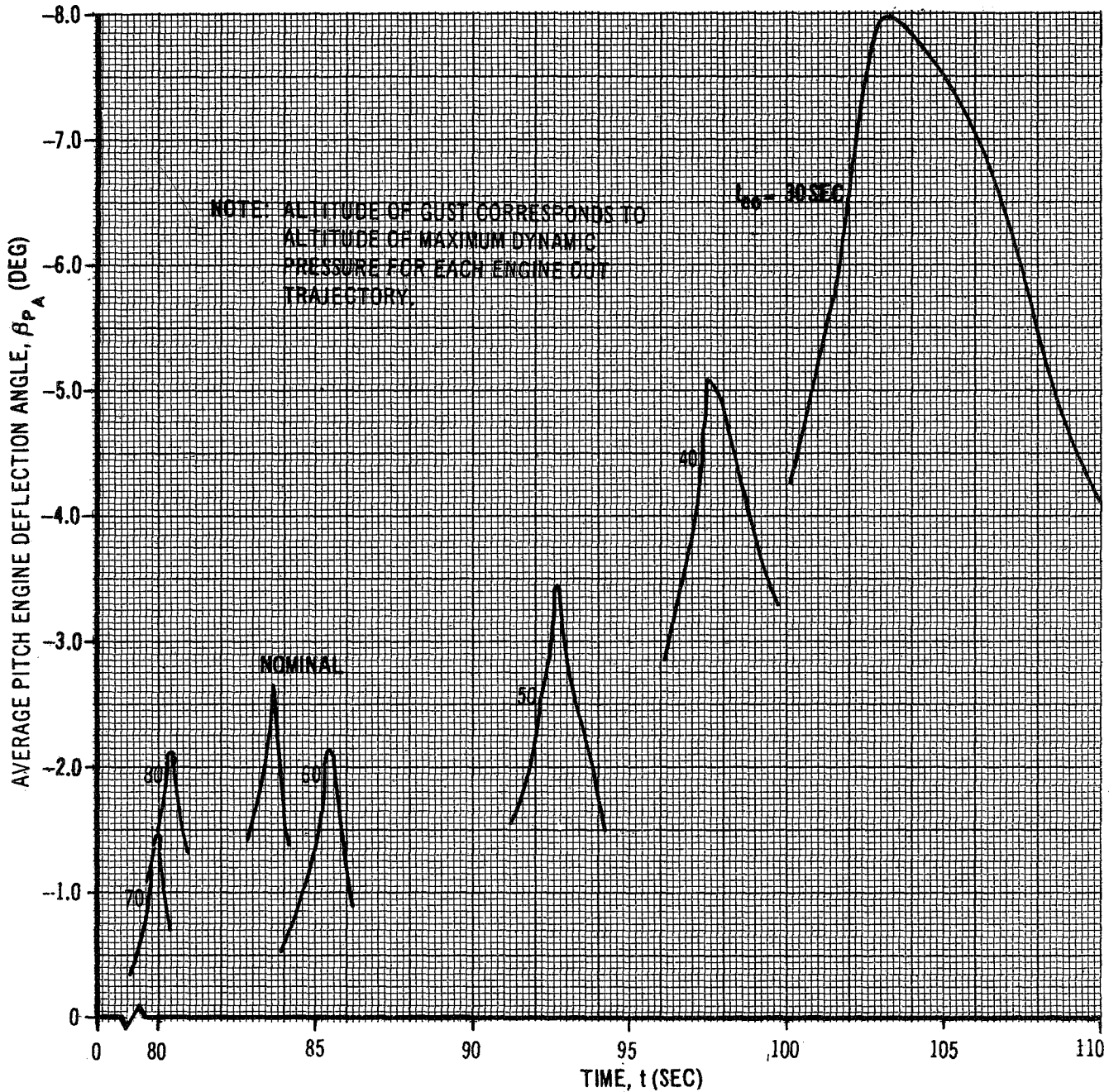### NUMBER 3 ENGINE FAILURE AT 30, 40, 50, 60, 70, AND 80 SECONDS

NOTE: ALTITUDE OF GUST CORRESPONDS TO
ALTITUDE OF MAXIMUM DYNAMIC
PRESSURE FOR EACH ENGINE OUT
TRAJECTORY.

FIGURE 50

63

ANGLE OF ATTACK RESPONSE TO A RIGHT
SIDE WIND GUST

NUMBER 3 ENGINE FAILURE AT 30, 40, 50, 60, 70,
AND 80 SECONDS

NOTE: ALTITUDE OF GUST CORRESPONDS TO
ALTITUDE OF MAXIMUM DYNAMIC
PRESSURE FOR EACH ENGINE OUT
TRAJECTORY.

TIME, t (SEC)

YAW ANGLE OF ATTACK, α_Y (DEG)
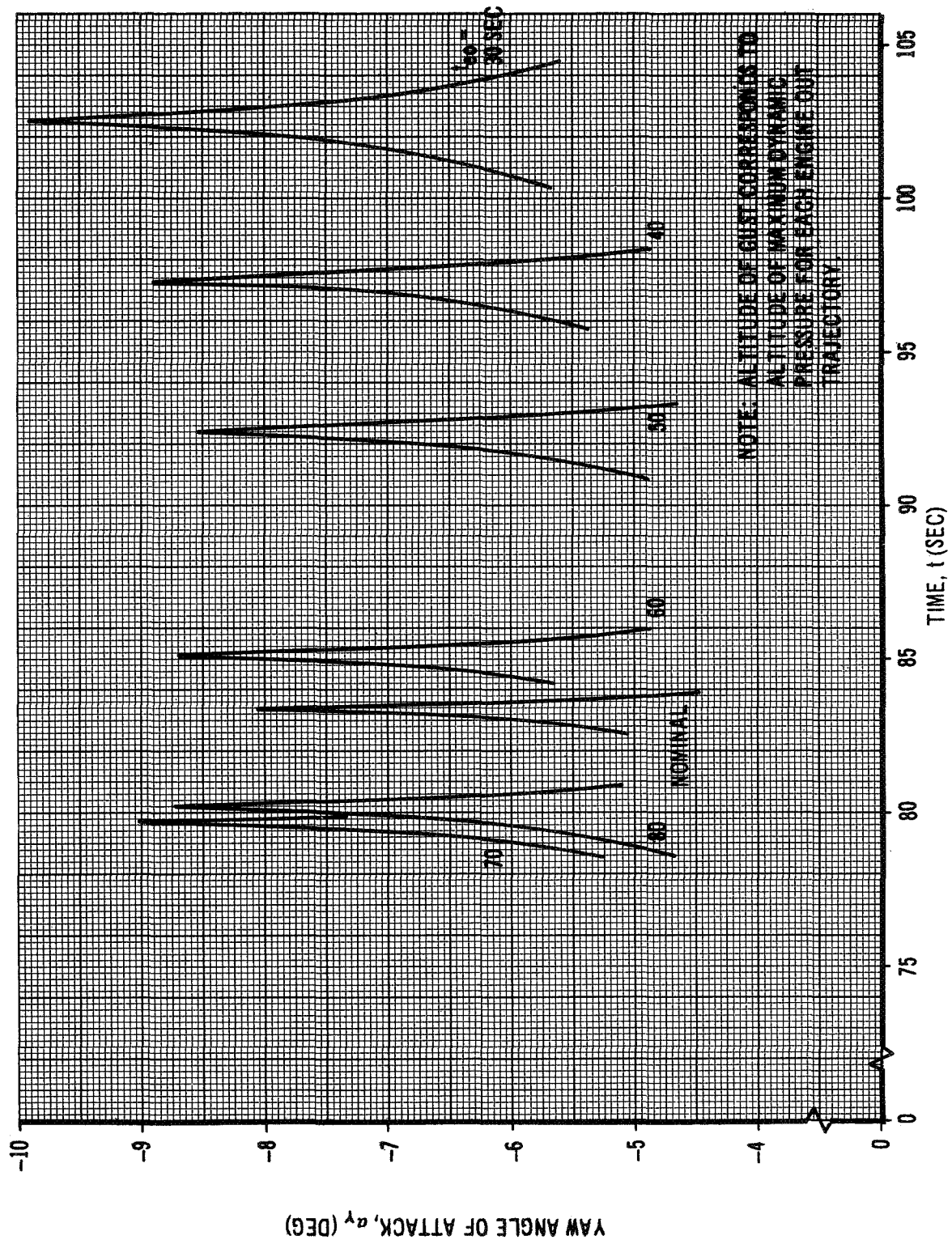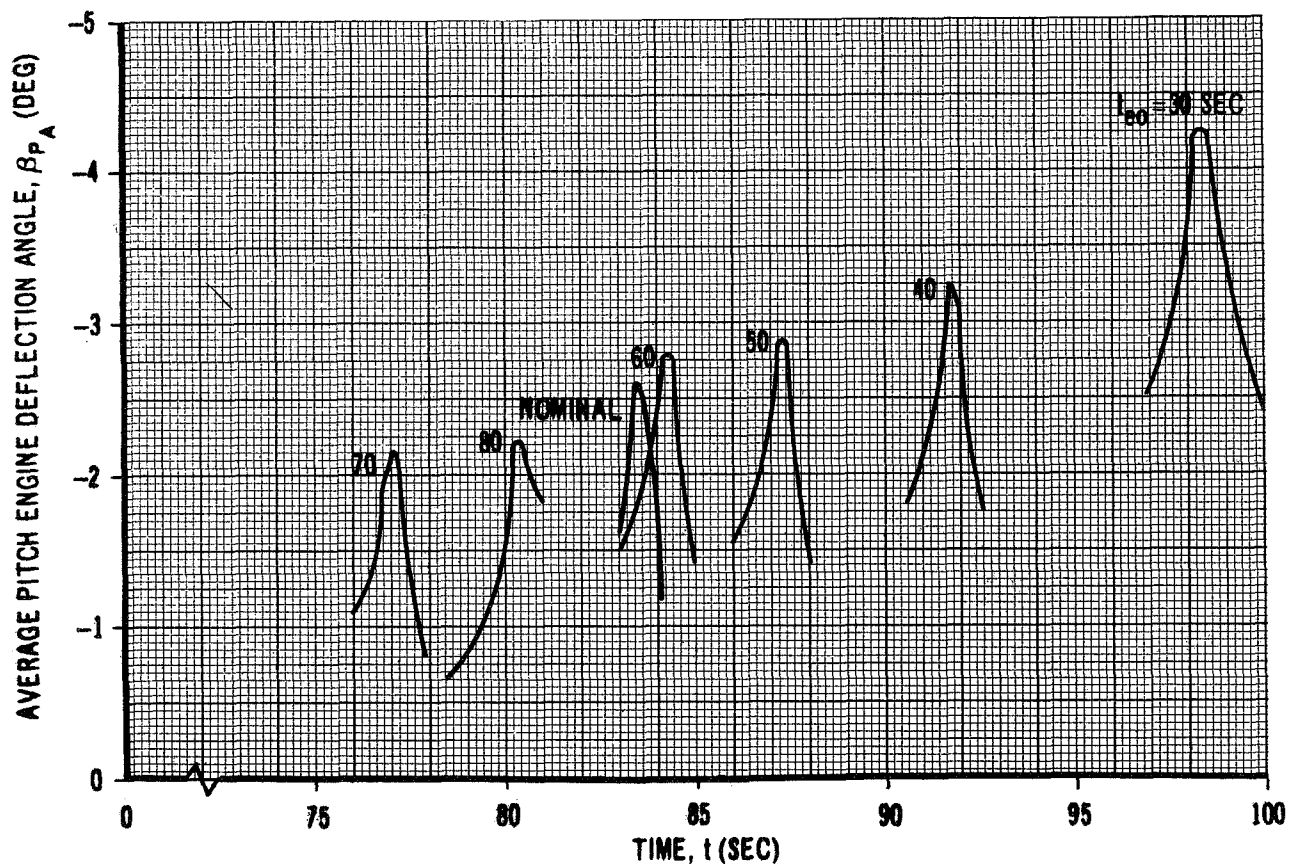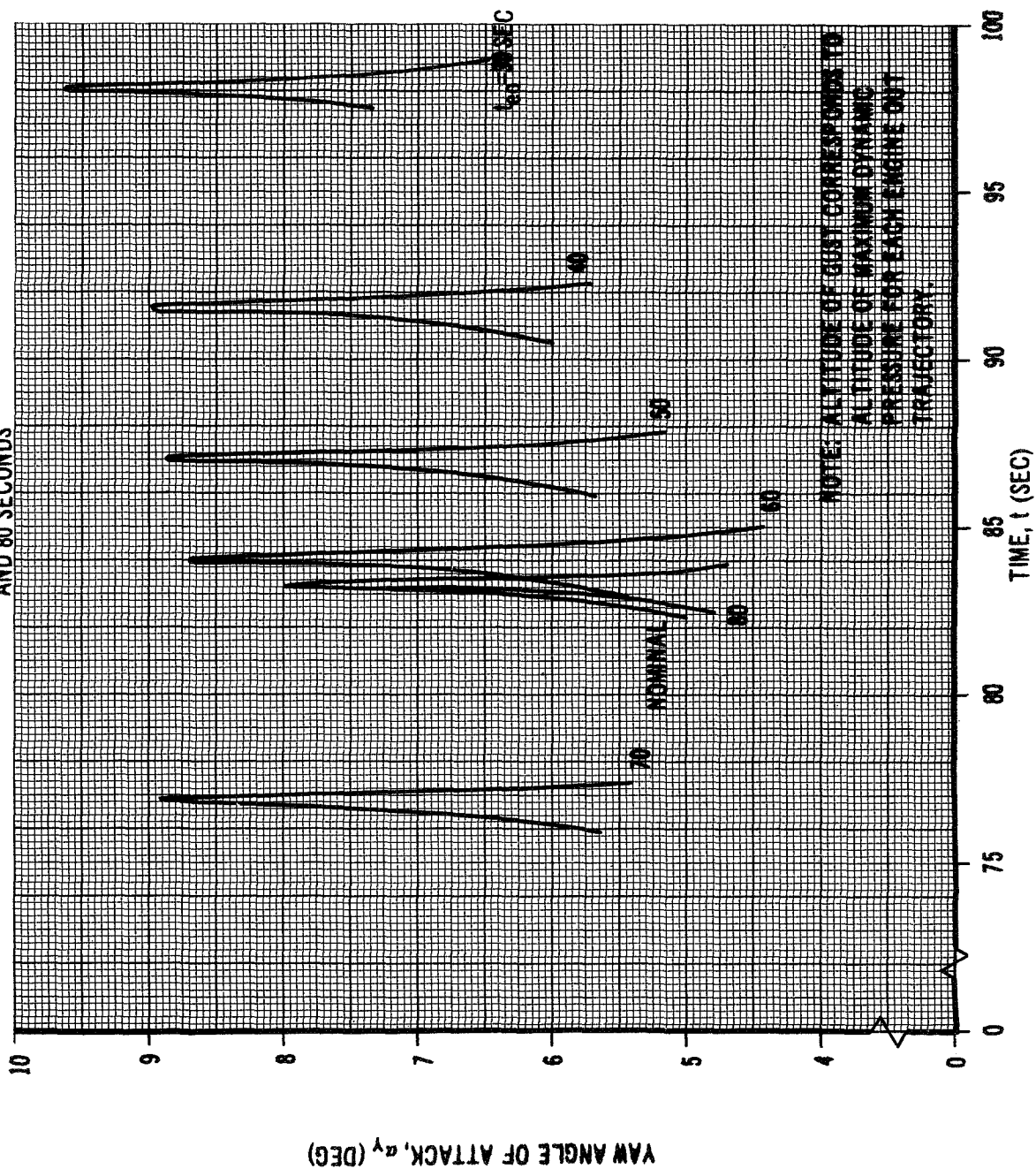
DYNAMIC PRESSURE RESPONSE TO A RIGHT
SIDE WIND GUST

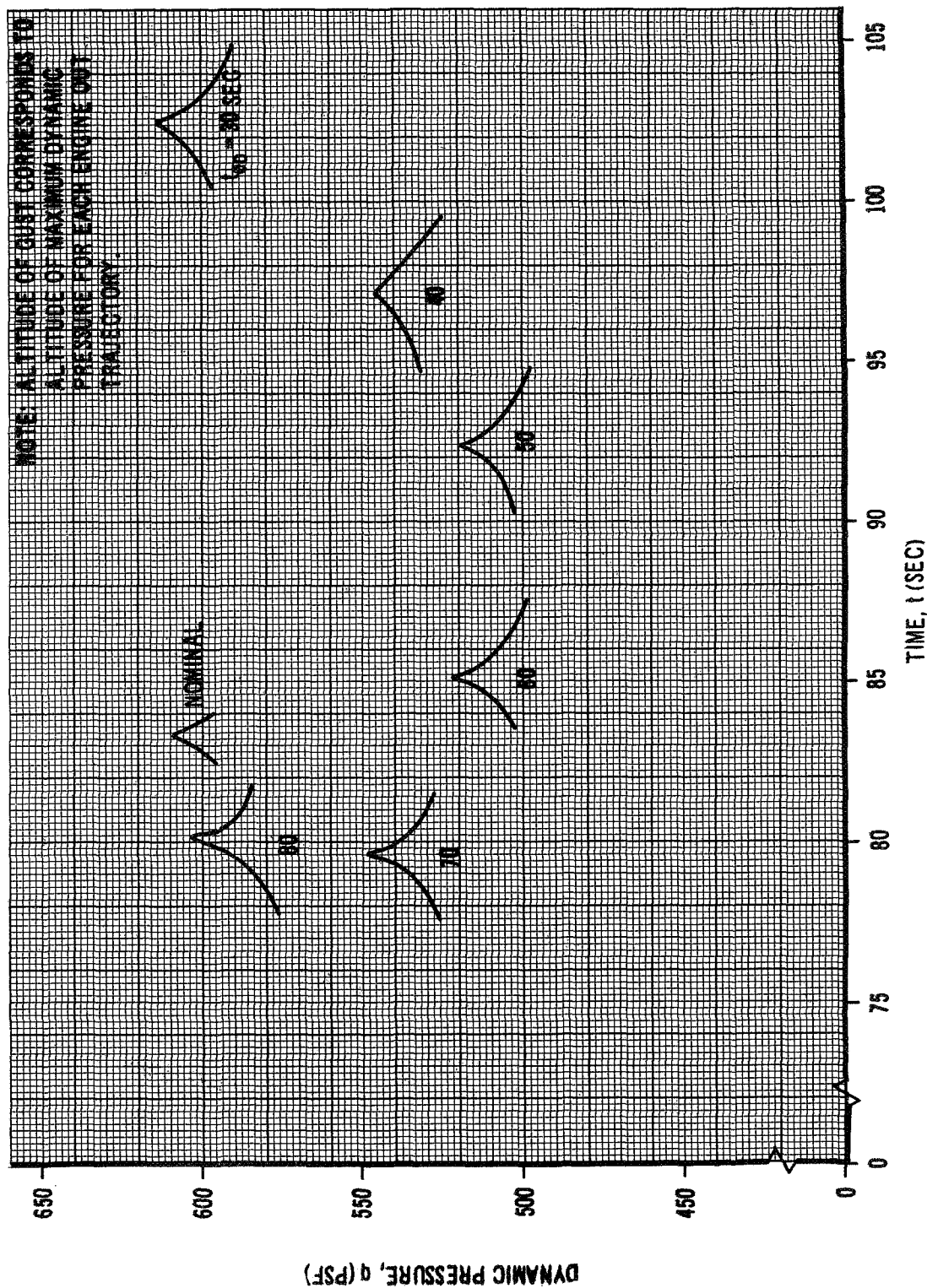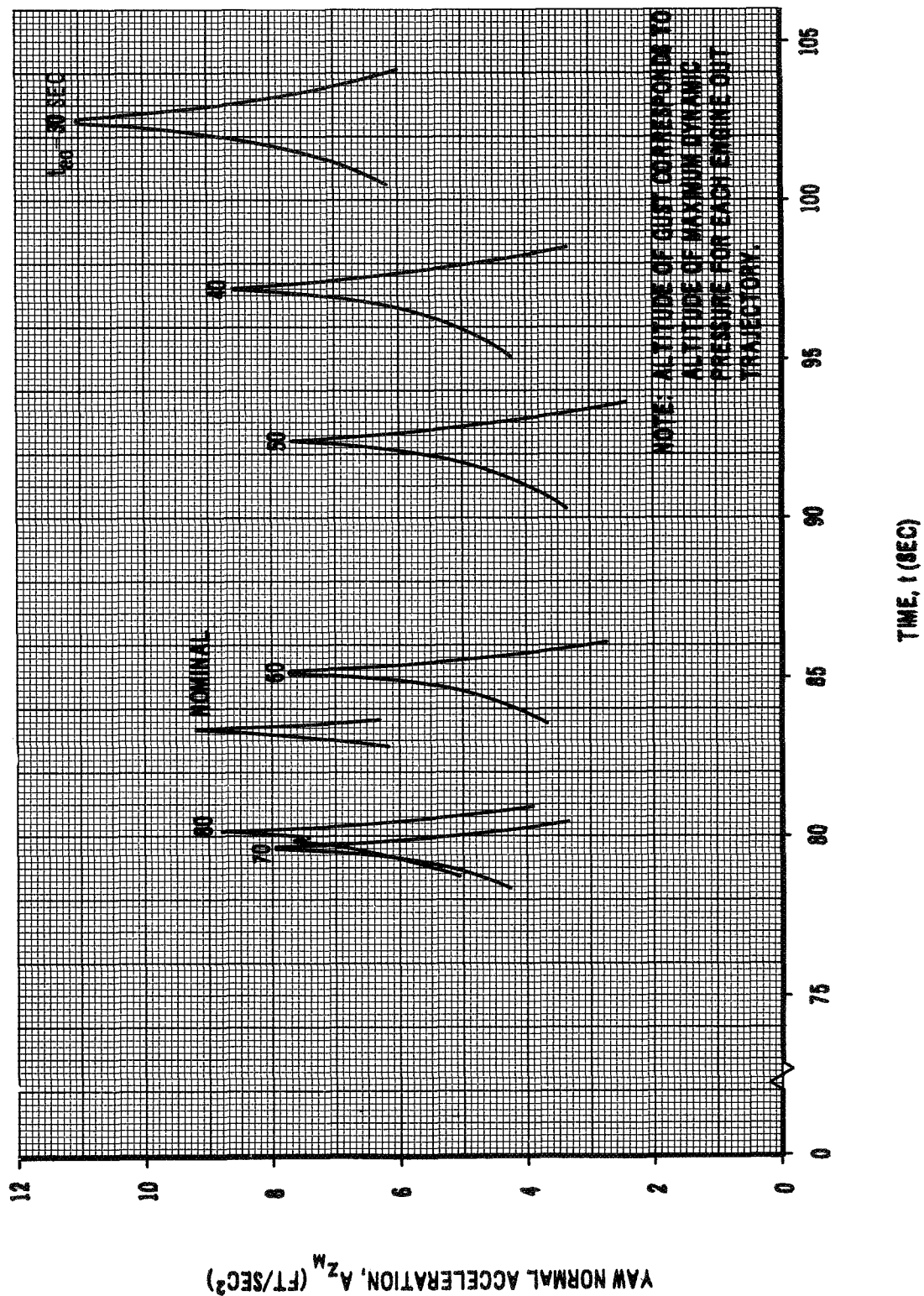NUMBER 3 ENGINE FAILURE AT 30, 40, 50, 60, 70,
AND 80 SECONDS
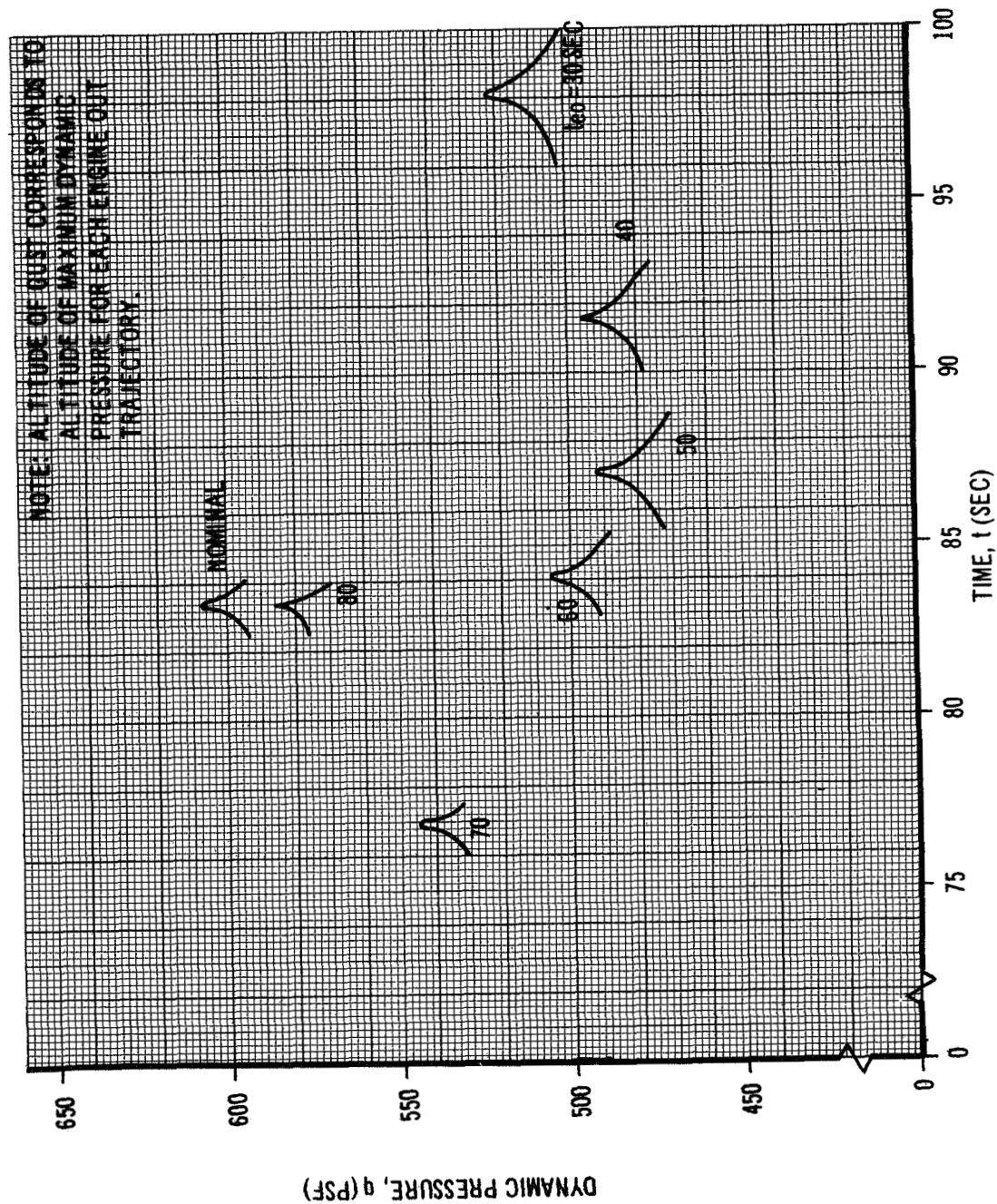
FIGURE 52

YAW NORMAL ACCELERATION RESPONSE TO A
RIGHT SIDE WIND GUST

NUMBER 3 ENGINE FAILURE AT 30, 40, 50, 60, 70,
AND 80 SECONDS

NOTE: ALTITUDE OF GUST CORRESPONDS TO
ALTITUDE OF MAXIMUM DYNAMIC
PRESSURE FOR EACH ENGINE OUT
TRAJECTORY.
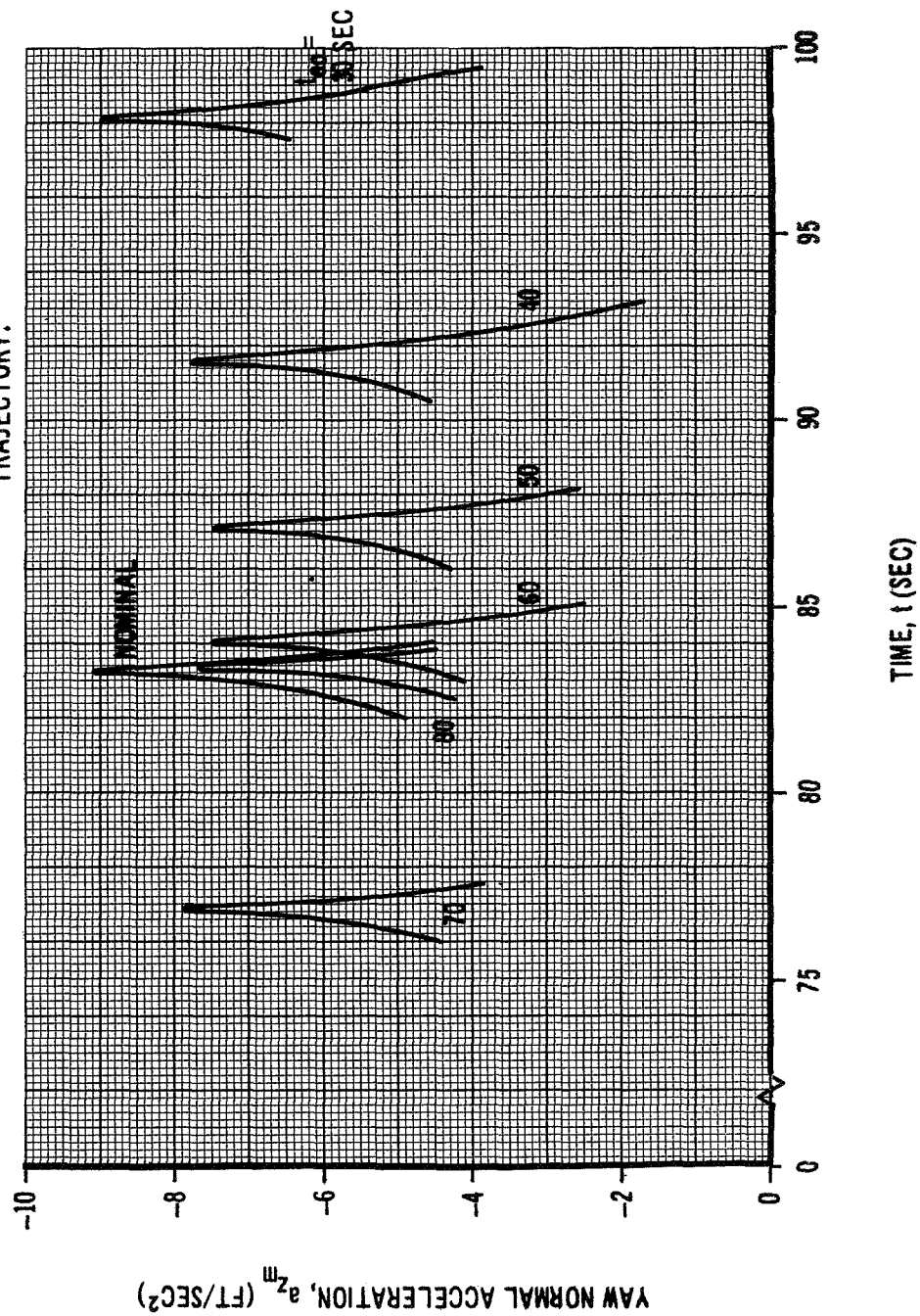
FIGURE 53
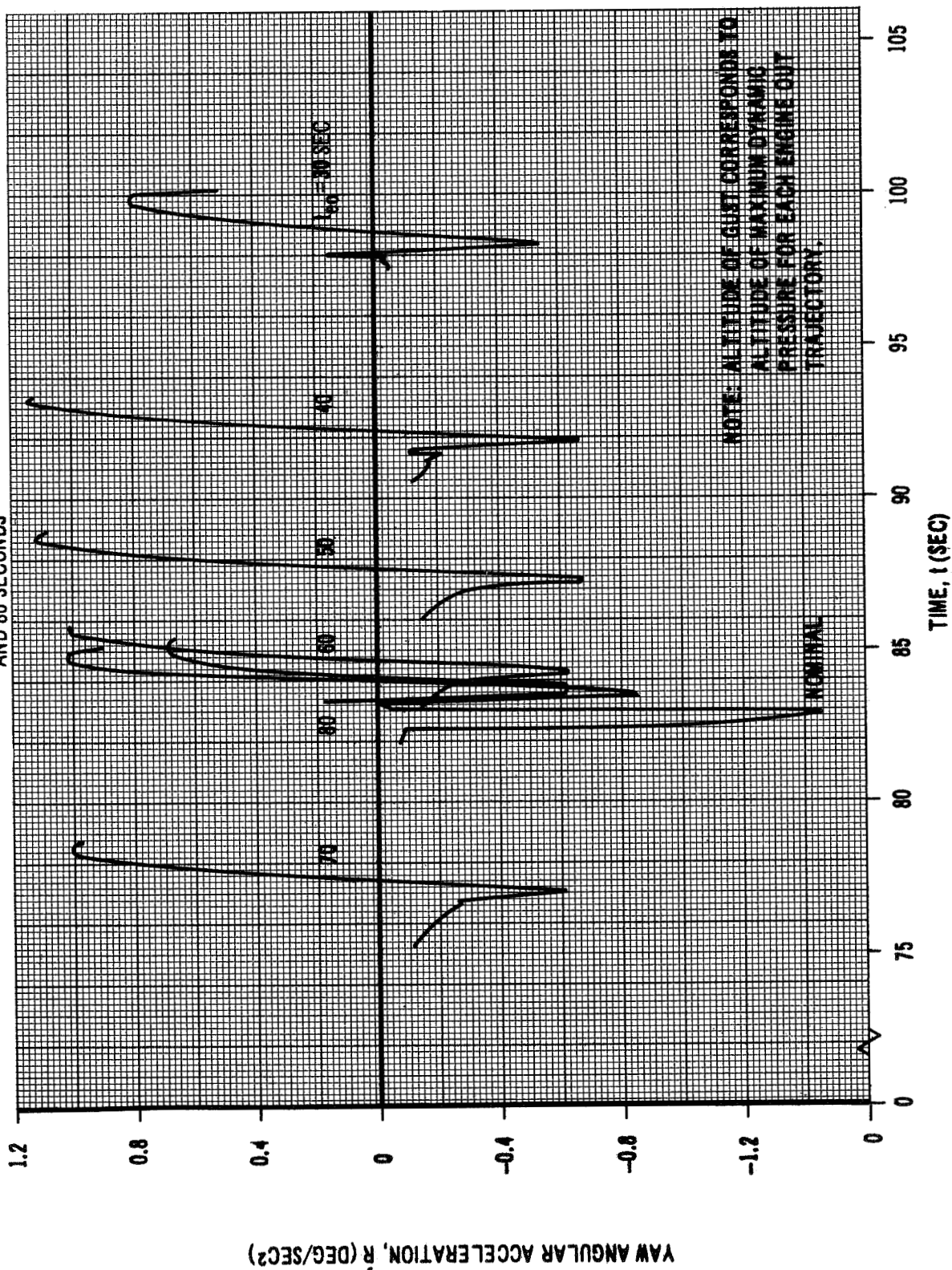
FIGURE 54

AVERAGE YAW ENGINE DEFLECTION ANGLE
RESPONSE TO A RIGHT SIDE WIND GUST
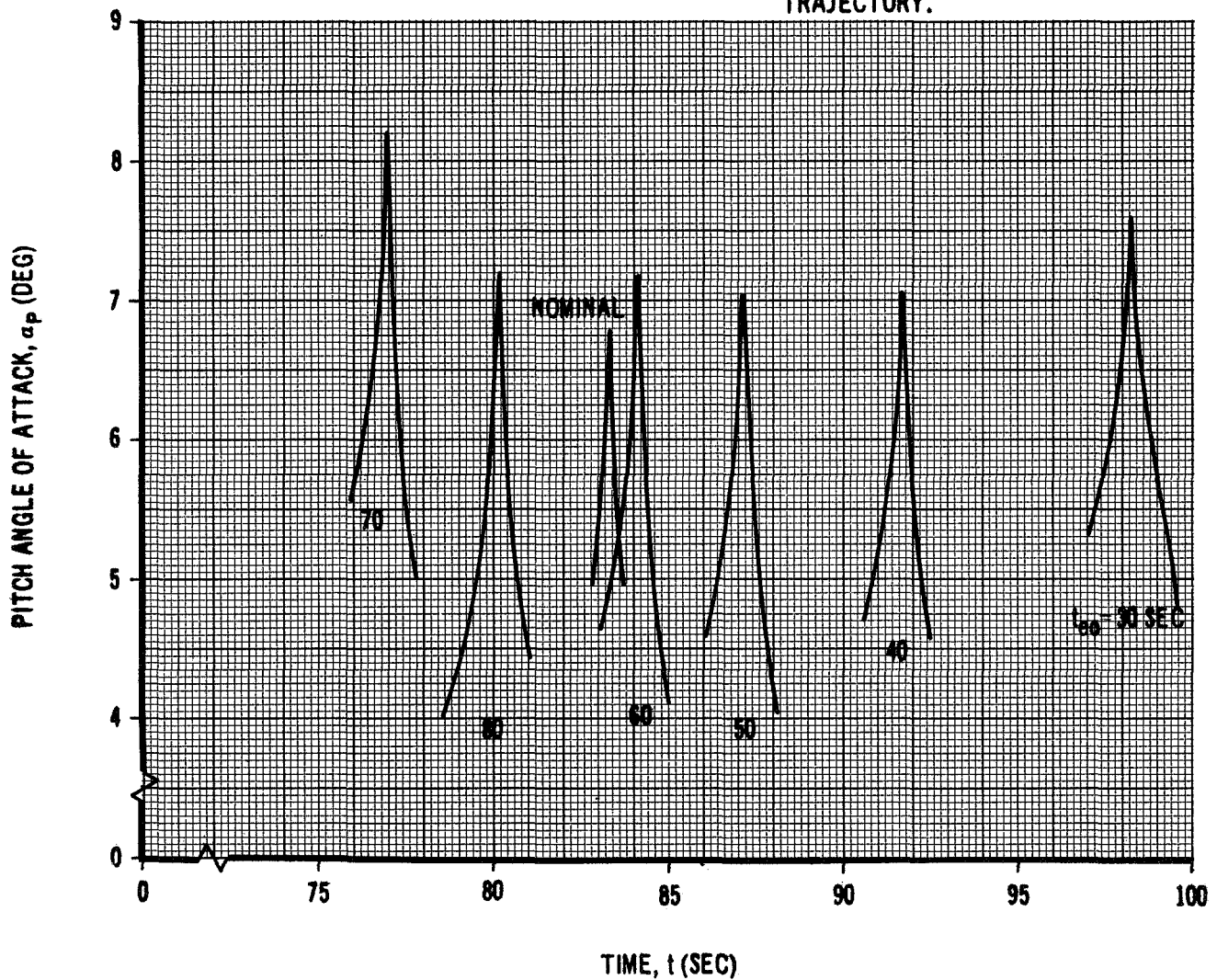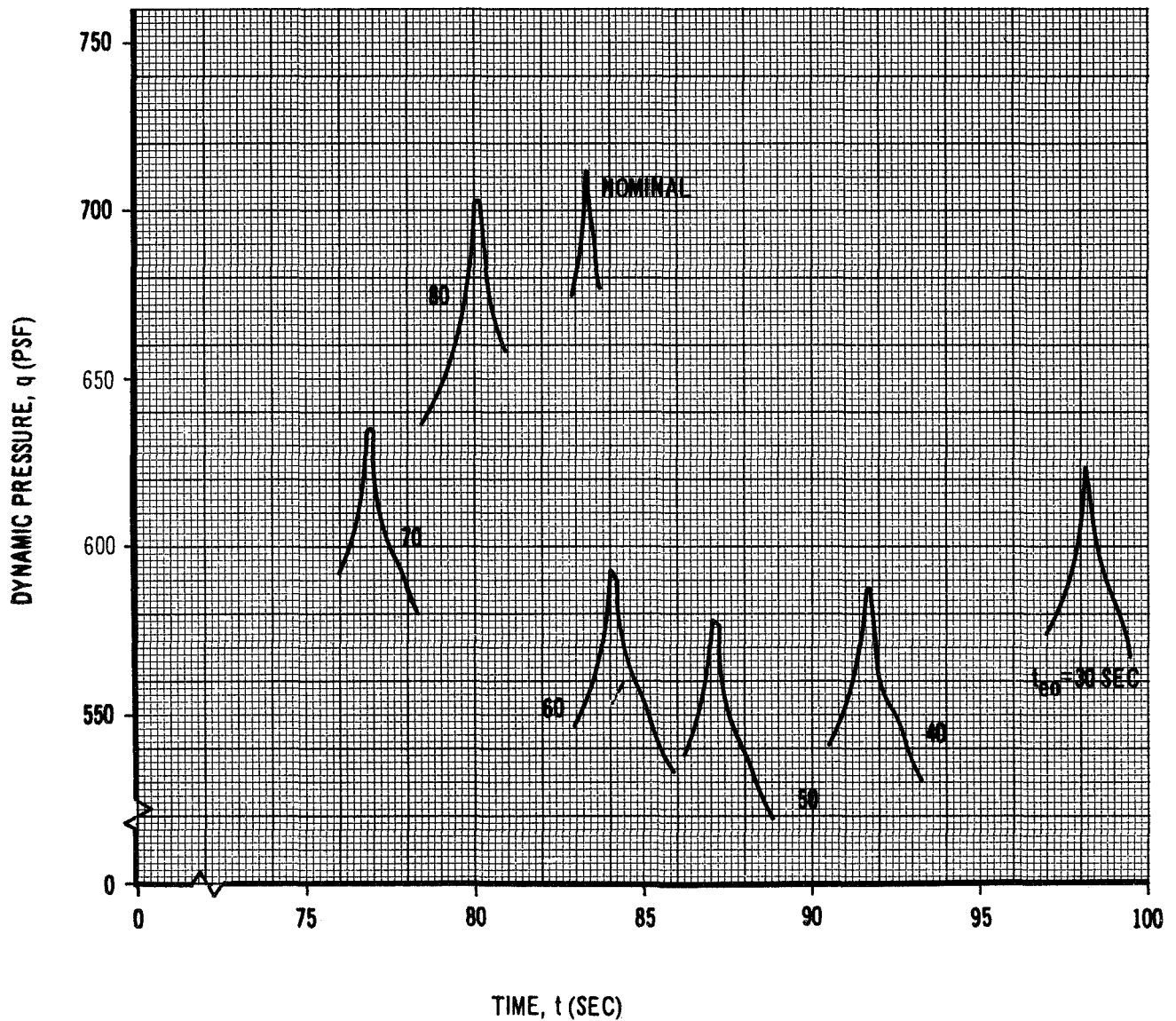NUMBER 3 ENGINE FAILURE AT 30, 40, 50, 60, 70,
AND 80 SECONDS

NOTE: ALTITUDE OF GUST CORRESPONDS TO
ALTITUDE OF MAXIMUM DYNAMIC
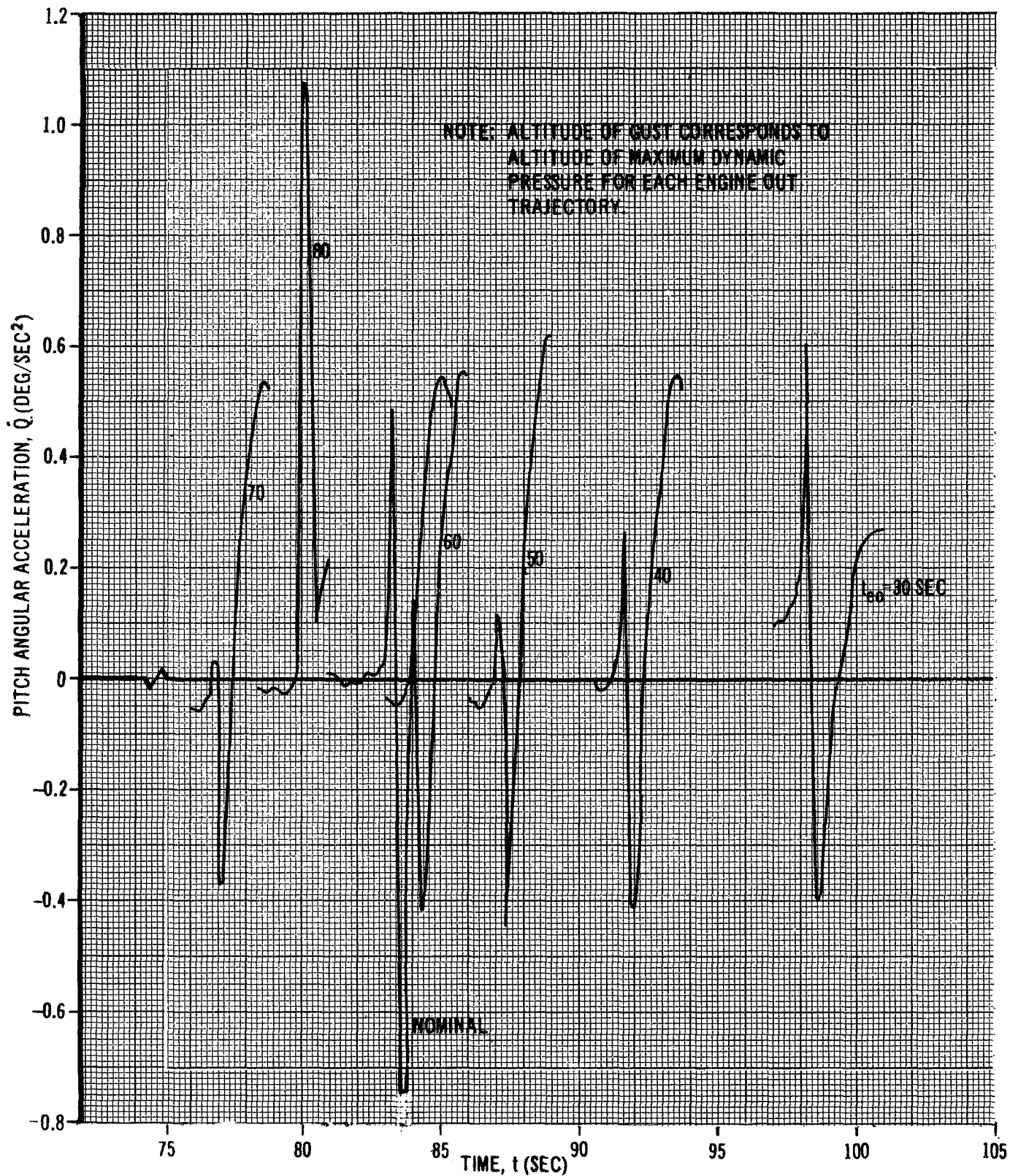PRESSURE FOR EACH ENGINE OUT
TRAJECTORY.
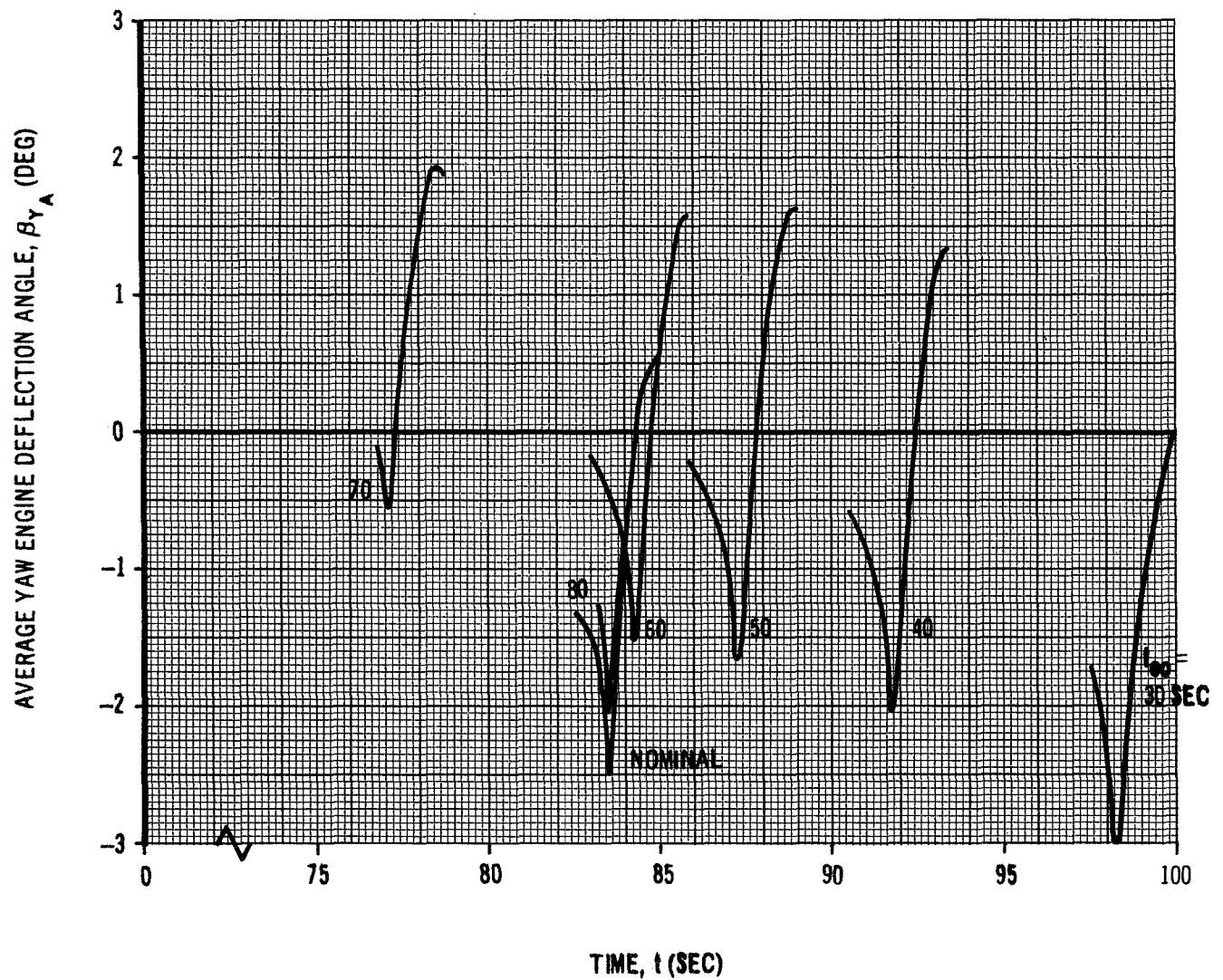
FIGURE 55

shown in figures 46 through 50, and 51 through 55. These figures present the vehicle dynamic response for each trajectory studied, which for each particular engine and time of failure represents the most critical control and aerodynamic loading conditions. The vehicle dynamic response for the most critical trajectories, which are defined by the worst case envelope presented in figure 35, was used in conjunction with the vehicle's physical characteristics to calculate the structural loading. The resulting loads will be discussed in section 5.4.

5.3 Dispersions

After establishing the more "critical" (defined as the maximum product of dynamic pressure and angle of attack presented in figure 35) engine-out cases, the effect of vehicle parameter dispersions on these critical cases was investigated.

5.3.1 Vehicle Parameter Variations

The following vehicle and autopilot parameters, selected as having the most significance with respect to the vehicle performance, were varied in the dispersion analysis:

a. Total Thrust (ΔT)

   Change, in percent, of the total vehicle thrust.

b. Thrust Unbalance (T_u)

   A positive unbalance will produce nose up or nose left vehicle motion.

c. Angle of Attack Gain (Δb_o)

   A positive variation tends to reduce aerodynamic loads.

d. Attitude Gain (Δa_o)

   A positive variation tends to increase the aerodynamic loads (opposes angle of attack gain).

e. Center of Pressure (Δcp)

   Positive variation is a cp shift toward the nose.

f. Center of Gravity (Δcg)

   Positive variation is a cg shift toward the nose.

The assumed three sigma variations (ΔD_i) of the above parameters are shown in table VI. These vehicle parameter dispersions were resolved into three sigma trajectory dispersions (ΔP_i) which were then used to

TABLE VI

SATURN IB PARAMETER DISTURBANCES

$(3\sigma$ VARIANCE LEVEL)

α_{RSS} CONDITIONS	FLIGHT TIME (SEC)				
	40	50	60	70	80
ΔCG (IN)	13.8	12.6	11.8	11.4	8.66
ΔCP (IN)	83.5	75.2	70.1	67.7	51.6
Δa_o (%)	7.01	6.34	5.91	5.71	4.35
Δb_o (%)	7.01	6.34	5.91	5.71	4.35
Tu (%)	1.52	1.38	1.28	1.24	0.94
ΔT (%)	0.71	0.71	0.71	0.71	0.71

determine the loads dispersions for each of the most critical engine-out trajectories.

5.3.2 Trajectory Parameter Variations

Variations in the maximum angle of attack and the dynamic pressure, normal acceleration, and angular acceleration at the time of maximum angle of attack were determined as a function of dispersions in the previously described vehicle and autopilot parameters. These variables were chosen because of their important influence on vehicle structural loading. The dispersion analysis (also the loads analysis) was performed for each of the five trajectories (the most critical trajectory for engine failure times of 40, 50, 60, 70 and 80 seconds as indicated in figure 35) listed below:

a. Engine number 1 failure at 40 seconds with head winds

b. Engine number 1 failure at 50 seconds with head winds

c. Engine number 1 failure at 60 seconds with head winds

d. Engine number 3 failure at 70 seconds with head winds

e. Engine number 1 failure at 80 seconds with left side winds.

The engine number 1 failure at 30 seconds with head wind trajectory is not listed because the unfavorable dispersions, such as a forward shift in the center of pressure, an aft shift in the cg, etc., resulted in vehicle tumbling due to the excessive aerodynamic moment. The relationships between the vehicle three sigma performance dispersions (∂P_i) and the parameter dispersions (∂D_j) were found by simulating two positive dispersions and two negative dispersions for each parameter investigated. The variation in angle of attack, dynamic pressure, normal acceleration, and angular acceleration as a function of the above vehicle parameter dispersions are shown in figures 56 through 71. These relationships were linearized about the nominal value in order to obtain an approximation for the partial derivative $\partial P_i / \partial D_j$. The three sigma parameter dispersions, ΔD_j, were then used to calculate the three sigma performance dispersion, ΔP_i, as,

$$\Delta P_i = \frac{\partial P_i}{\partial D_j} \Delta D_j$$

For each of the investigated trajectory parameters, these three sigma variations, P_i, were then root-sum-squared, such that,

$$P_i = \left[\sum \left[\frac{P_i}{D_j} (D_j) \right]^2 \right]^{1/2}$$

CHANGE IN MAXIMUM ANGLE OF ATTACK DUE TO DISPERSIONS IN CENTER OF GRAVITY, AND CENTER OF PRESSURE

NOTES: 1. NO. 1 ENGINE FAILURE
2. HEAD WINDS
3. PITCH ANGLE OF ATTACK

NOTES: 1. NO. 3 ENGINE FAILURE
2. HEAD WINDS
3. PITCH ANGLE OF ATTACK

LEGEND – ΔCG ———
ΔCP — —

NOTES: 1. NO. 1 ENGINE FAILURE
2. LEFT SIDE WINDS
3. YAW ANGLE OF ATTACK

ANGLE OF ATTACK, α (DEG)

CHANGE IN CENTER OF GRAVITY, ΔCG
AND CENTER OF PRESSURE, ΔCP (IN.)
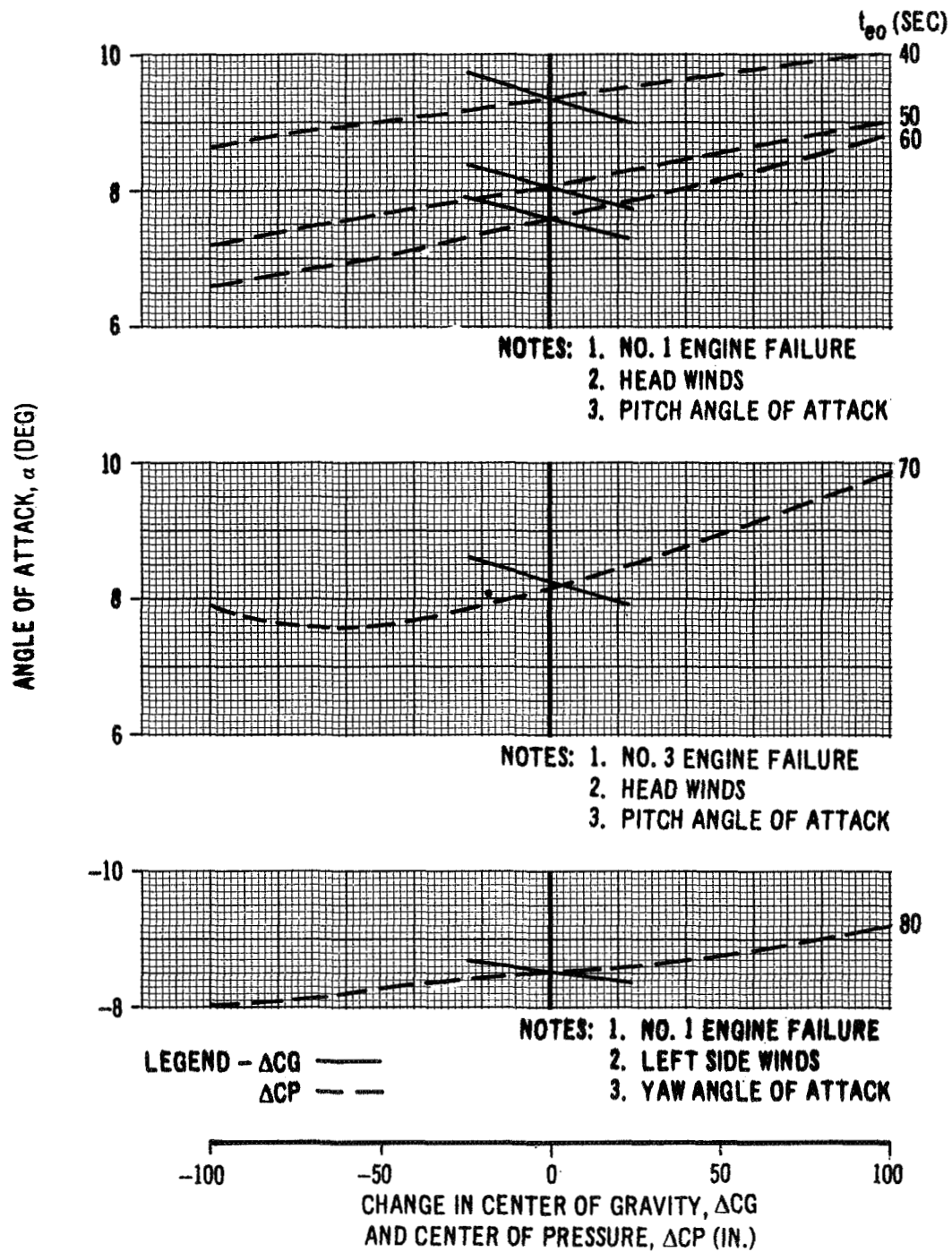
FIGURE 56

CHANGE IN DYNAMIC PRESSURE AT MAXIMUM ANGLE OF
ATTACK DUE TO DISPERSIONS IN CENTER OF
GRAVITY, AND CENTER OF PRESSURE
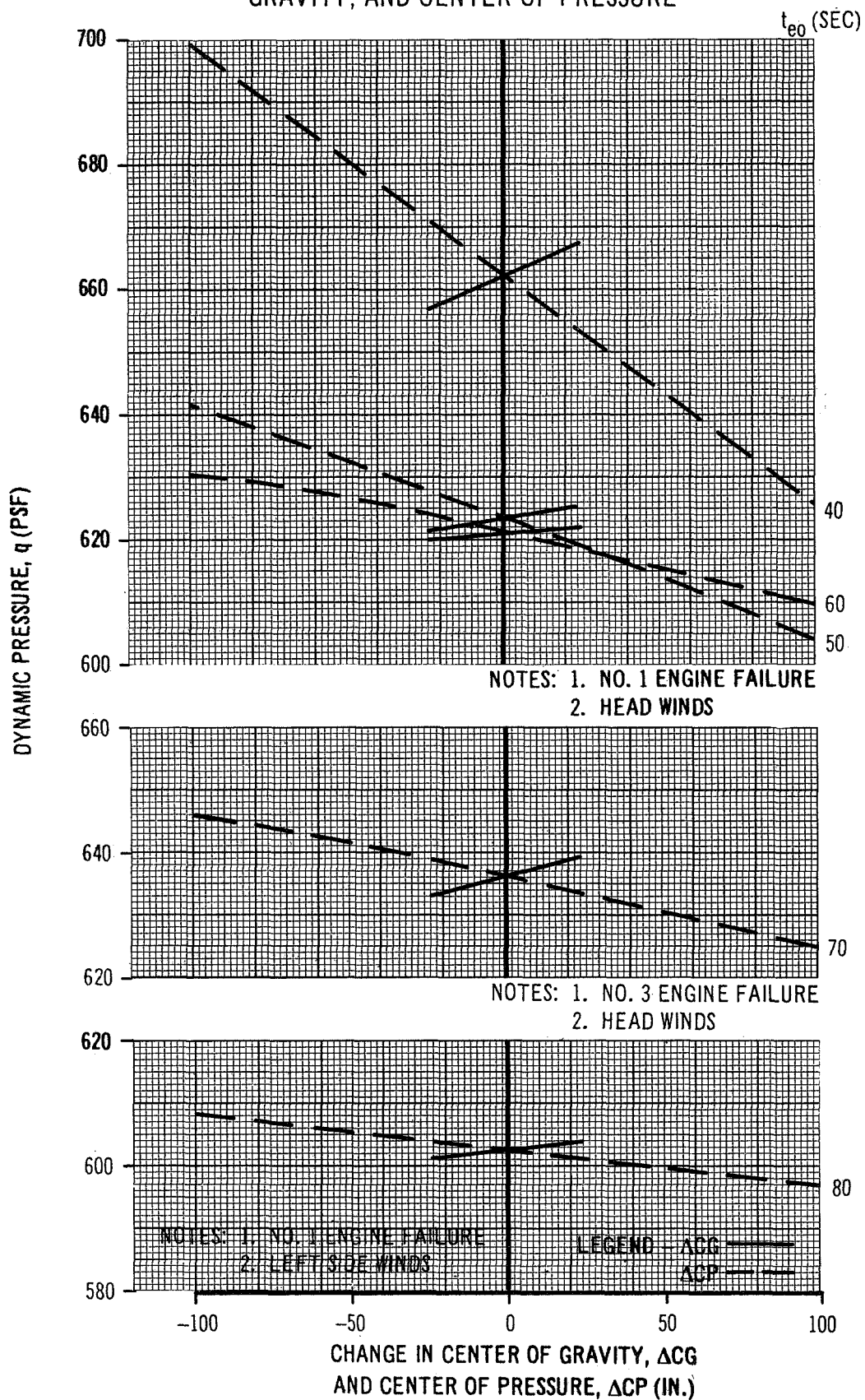
FIGURE 57

CHANGE IN NORMAL ACCELERATION AT MAXIMUM ANGLE OF ATTACK
DUE TO DISPERSIONS IN CENTER OF GRAVITY, AND CENTER
OF PRESSURE

NOTES: 1. NO. 1 ENGINE FAILURE
2. HEAD WINDS
3. PITCH NORMAL ACCELERATION

NOTES: 1. NO. 3 ENGINE FAILURE
2. HEAD WINDS
3. PITCH NORMAL ACCELERATION

LEGEND: ΔCG ———
ΔCP — —

NOTES: 1. NO. 1 ENGINE FAILURE
2. LEFT SIDE WINDS
3. YAW NORMAL ACCELERATION

CHANGE IN CENTER OF GRAVITY, ΔCG, AND CENTER OF PRESSURE, ΔCP (IN.)
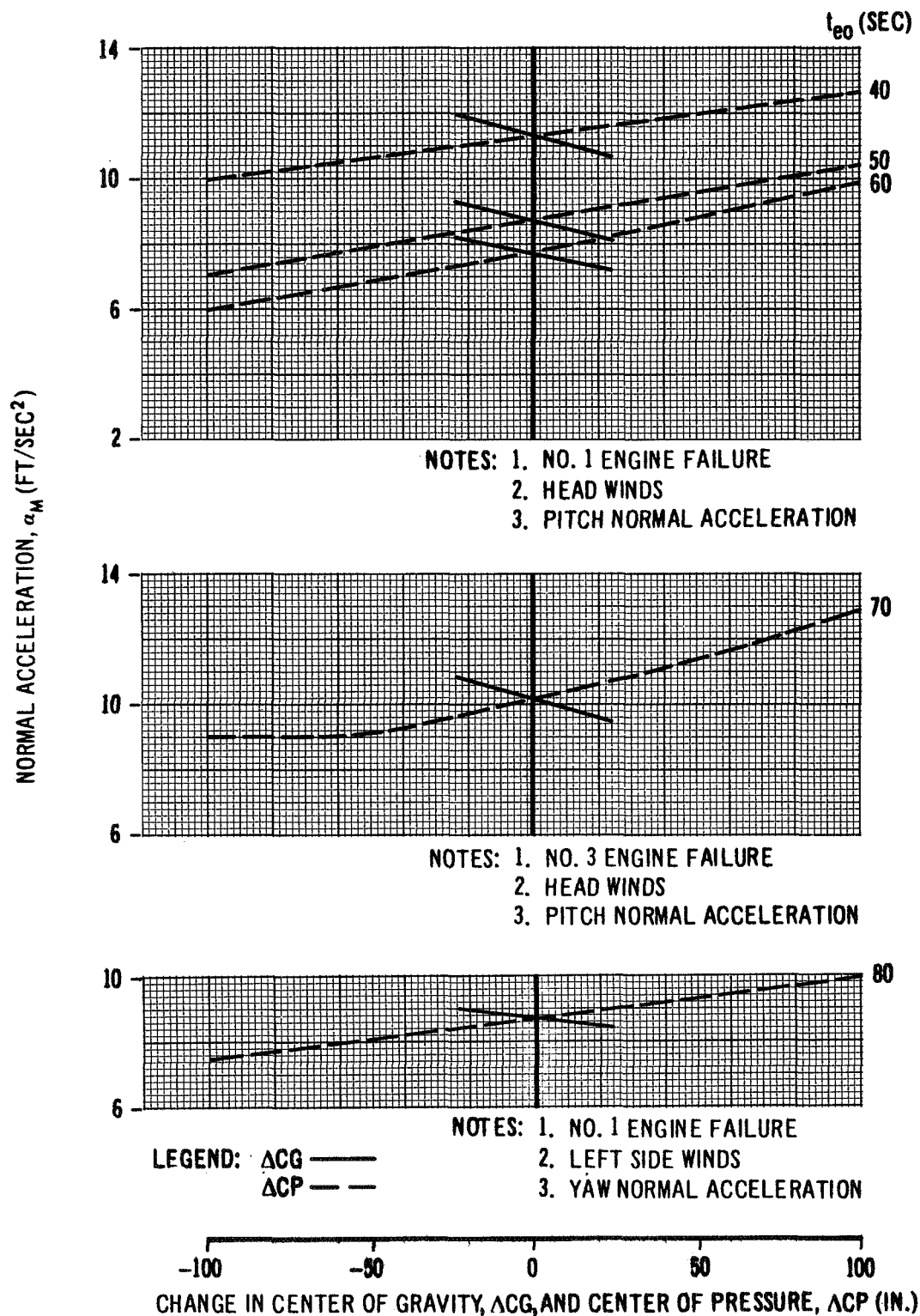
FIGURE 58

CHANGE IN ANGULAR ACCELERATION AT MAXIMUM ANGLE OF ATTACK DUE TO CENTER OF GRAVITY AND CENTER OF PRESSURE DISPERSIONS

NOTES: 1. NO. 1 ENGINE FAILURE
2. HEAD WINDS
3. PITCH ANGULAR ACCELERATION

NOTES: 1. NO. 3 ENGINE FAILURE
2. HEAD WINDS
3. PITCH ANGULAR ACCELERATION

LEGEND:
ΔCG ——
ΔCP — —

NOTES: 1. NO. 1 ENGINE FAILURE
2. LEFT SIDE WINDS
3. YAW ANGULAR ACCELERATION

CHANGE IN CENTER OF GRAVITY, ΔCG, AND
CENTER OF PRESSURE, ΔCP,(IN)

FIGURE 59

75

CHANGE IN MAXIMUM ANGLE OF ATTACK DUE TO DISPERSIONS
IN ANGLE OF ATTACK GAIN (b_0) AND ATTITUDE GAIN (a_0)

t_{eo} (SEC)

NOTES: 1. NO. 1 ENGINE FAILURE
2. HEAD WINDS
3. PITCH ANGLE OF ATTACK

ANGLE OF ATTACK, α (DEG)

NOTES: 1. NO. 3 ENGINE FAILURE
2. HEAD WINDS
3. PITCH ANGLE OF ATTACK

LEGEND – a_0 ———
b_0 – – –

NOTES: 1. NO. 1 ENGINE FAILURE
2. LEFT SIDE WINDS
3. YAW ANGLE OF ATTACK

CHANGE IN GAIN, a_0 OR b_0 (%)

FIGURE 60

CHANGE IN DYNAMIC PRESSURE AT MAXIMUM ANGLE OF
ATTACK DUE TO DISPERSIONS IN ANGLE OF ATTACK
GAIN (b_0) AND ATTITUDE GAIN (a_0)

FIGURE 61

CHANGE IN NORMAL ACCELERATION AT MAXIMUM ANGLE OF
ATTACK DUE TO DISPERSIONS IN ANGLE OF ATTACK GAIN
(b_0) AND ATTITUDE GAIN (a_0)
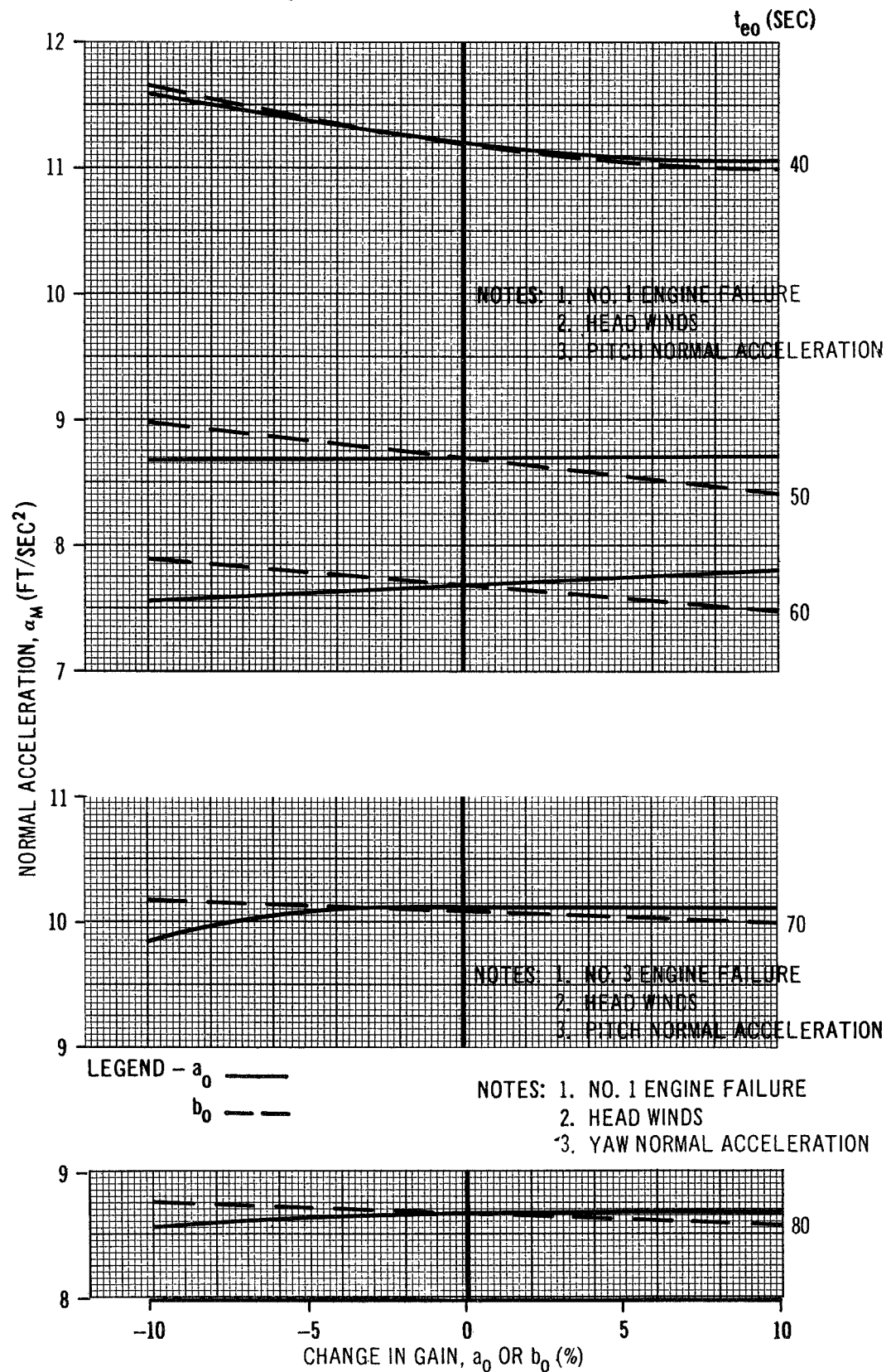
FIGURE 62

CHANGE IN ANGULAR ACCELERATION AT
MAXIMUM ANGLE OF ATTACK DUE TO
DISPERSIONS IN ANGLE OF ATTACK
GAIN (b_0) AND ATTITUDE
GAIN (a_0)
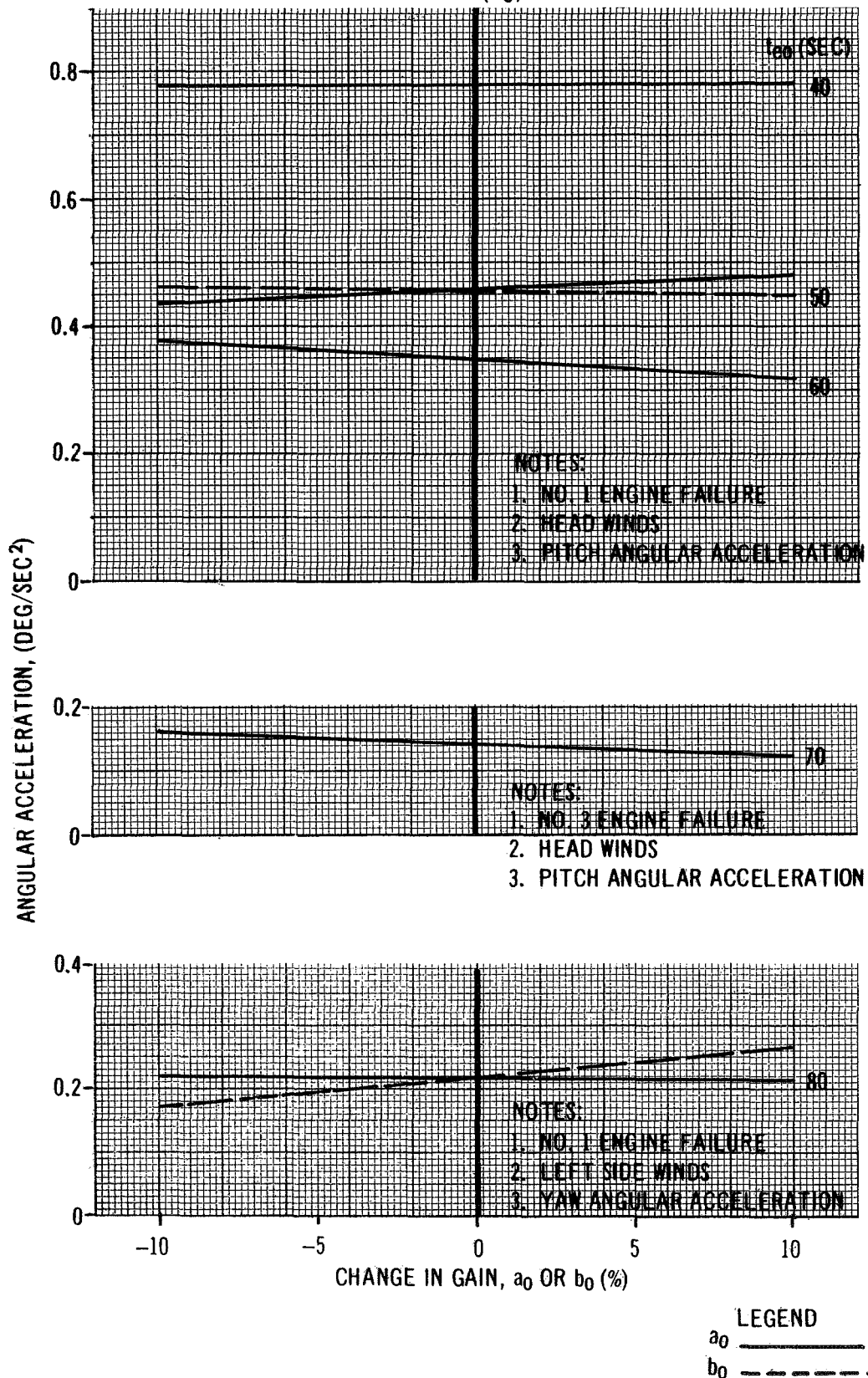
FIGURE 63

CHANGE IN MAXIMUM ANGLE OF ATTACK DUE TO DISPERSIONS
IN TOTAL VEHICLE THRUST

t_{eo} (SEC)

NOTES: 1. NO. 1 ENGINE FAILURE
           2. HEAD WINDS
           3. PITCH ANGLE OF ATTACK

NOTES: 1. NO. 3 ENGINE FAILURE
           2. HEAD WINDS
           3. PITCH ANGLE OF ATTACK

NOTES: 1. NO. 1 ENGINE FAILURE
           2. LEFT SIDE WINDS
           3. YAW ANGLE OF ATTACK

ANGLE OF ATTACK, α (DEG)

CHANGE IN TOTAL THRUST, ΔT (%)
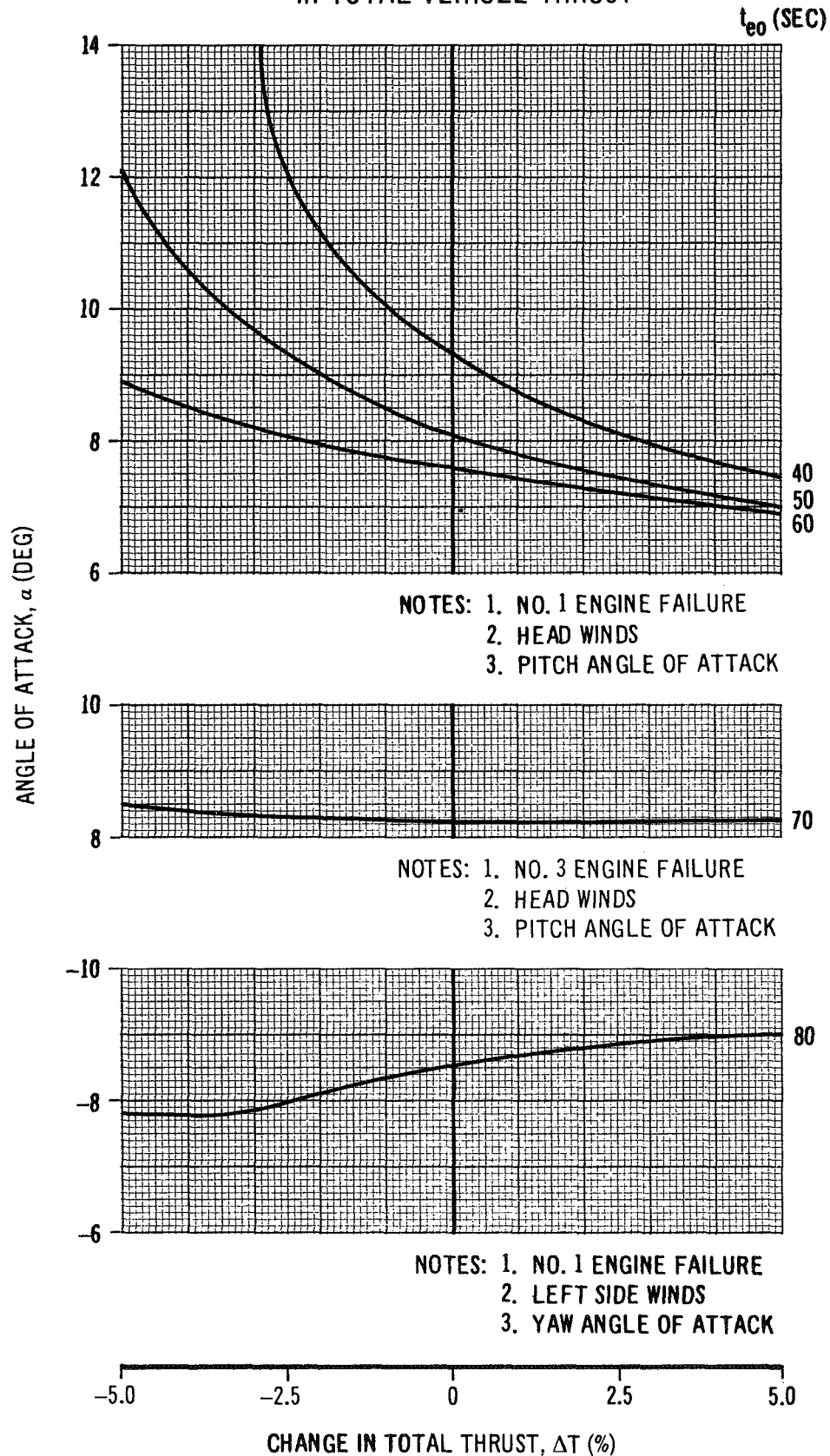
FIGURE 64

CHANGE IN DYNAMIC PRESSURE AT MAXIMUM ANGLE-
OF-ATTACK DUE TO CHANGES IN TOTAL
VEHICLE THRUST

FIGURE 65

CHANGE IN NORMAL ACCELERATION AT MAXIMUM ANGLE-OF-ATTACK DUE TO DISPERSIONS IN TOTAL VEHICLE THRUST
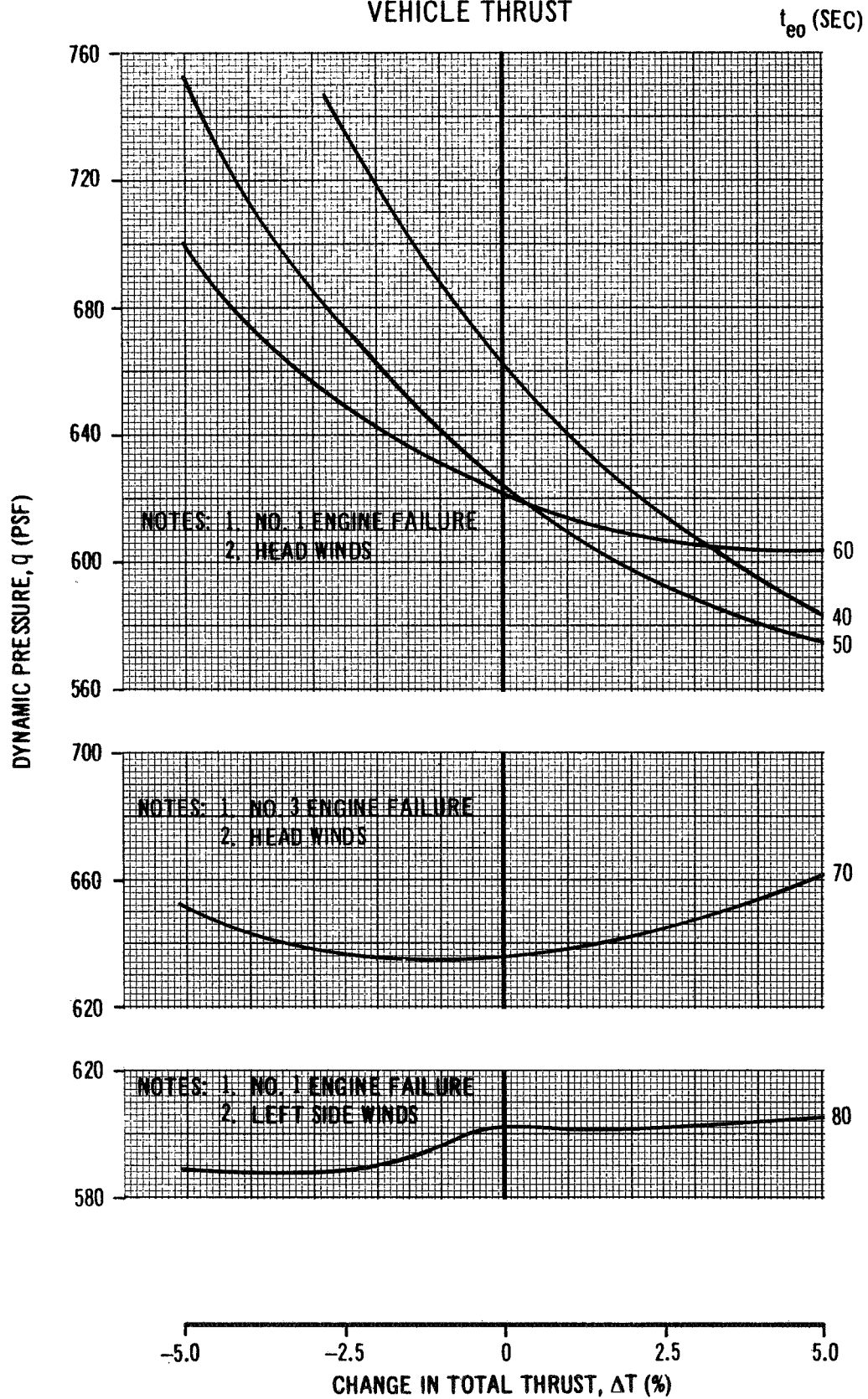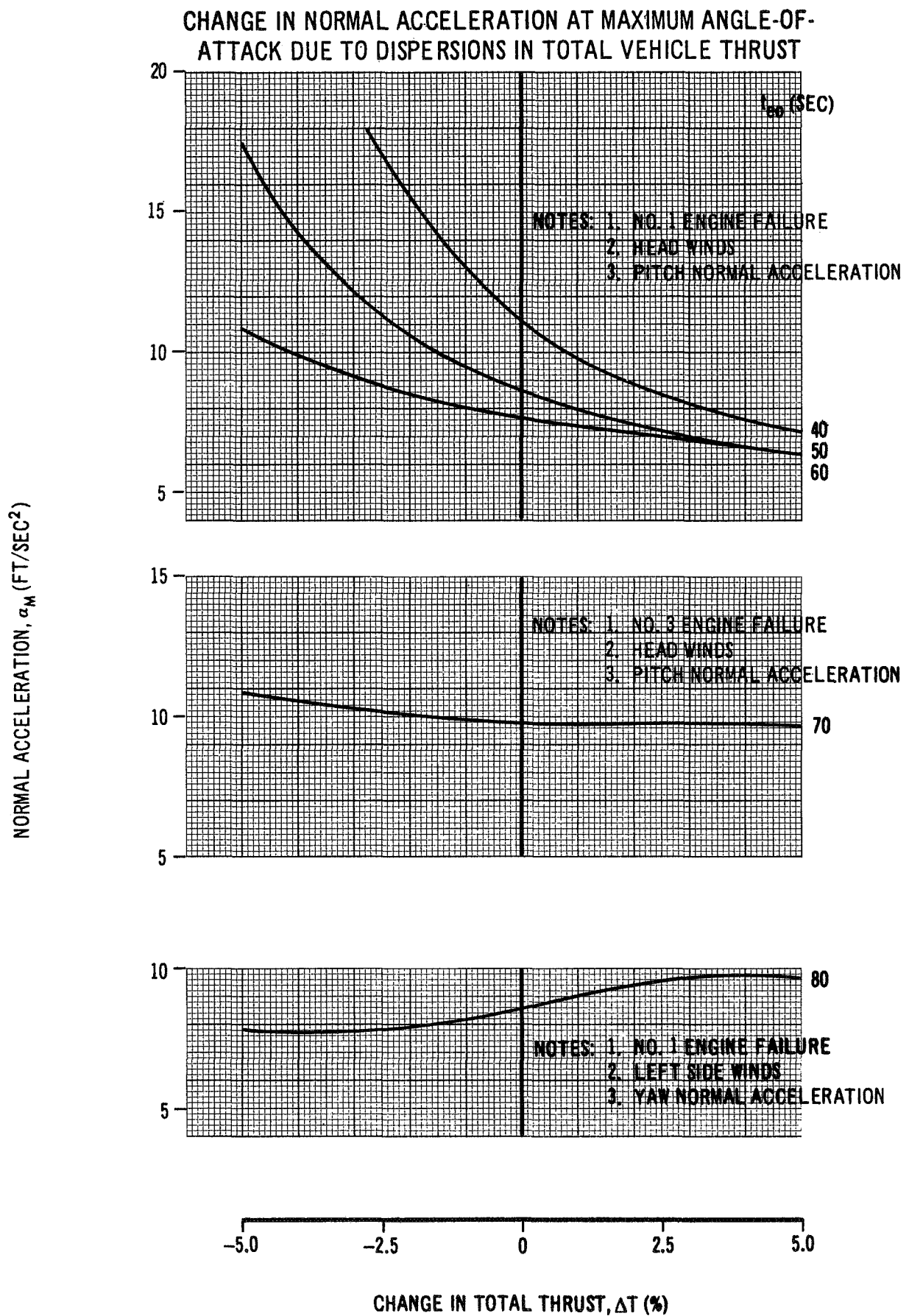
FIGURE 66

CHANGE IN ANGULAR ACCELERATION AT
MAXIMUM ANGLE OF ATTACK DUE TO
DISPERSIONS IN TOTAL
VEHICLE THRUST
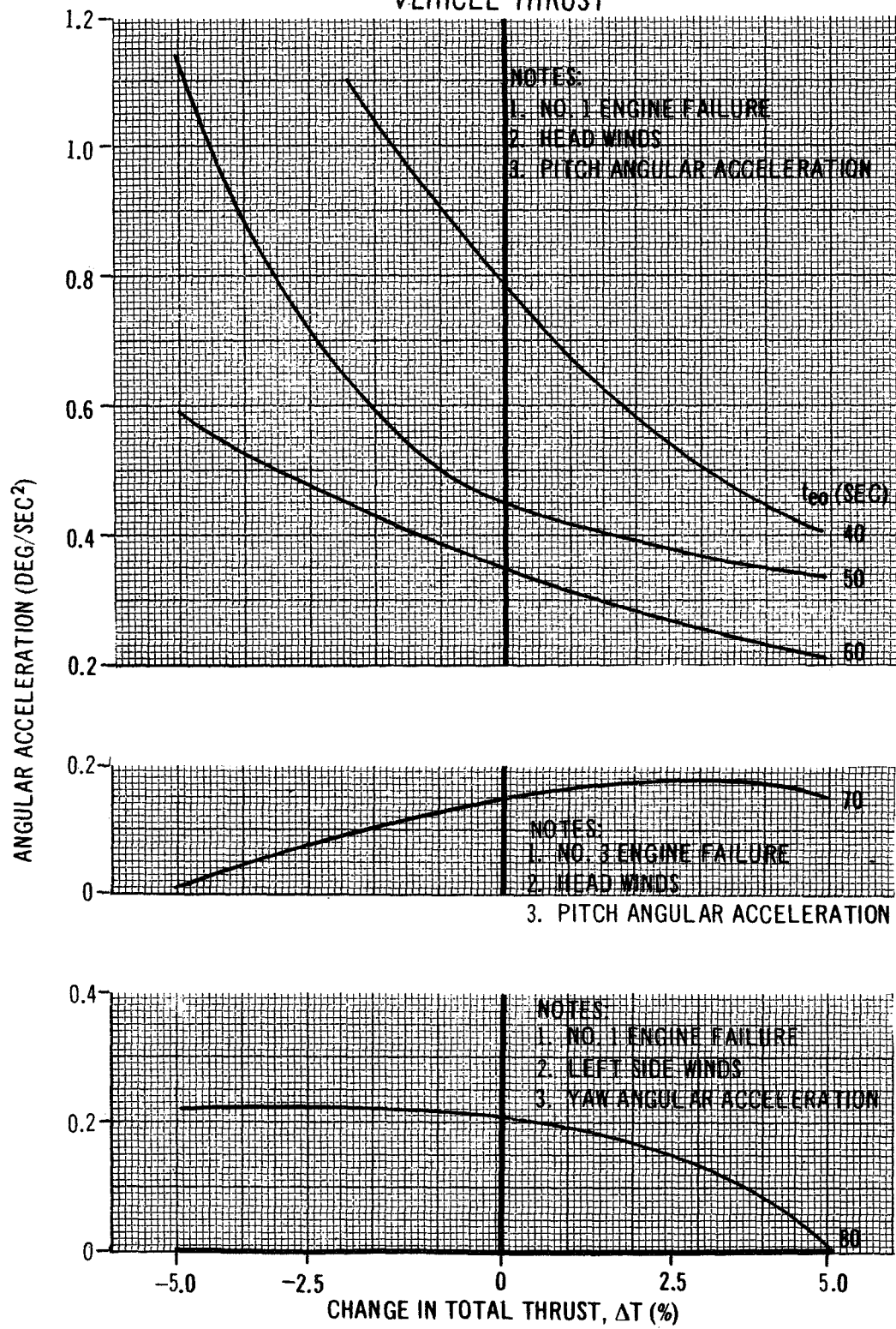
FIGURE 67

CHANGE IN MAXIMUM ANGLE OF ATTACK DUE TO DISPERSIONS
IN INDIVIDUAL CONTROL ENGINE THRUST
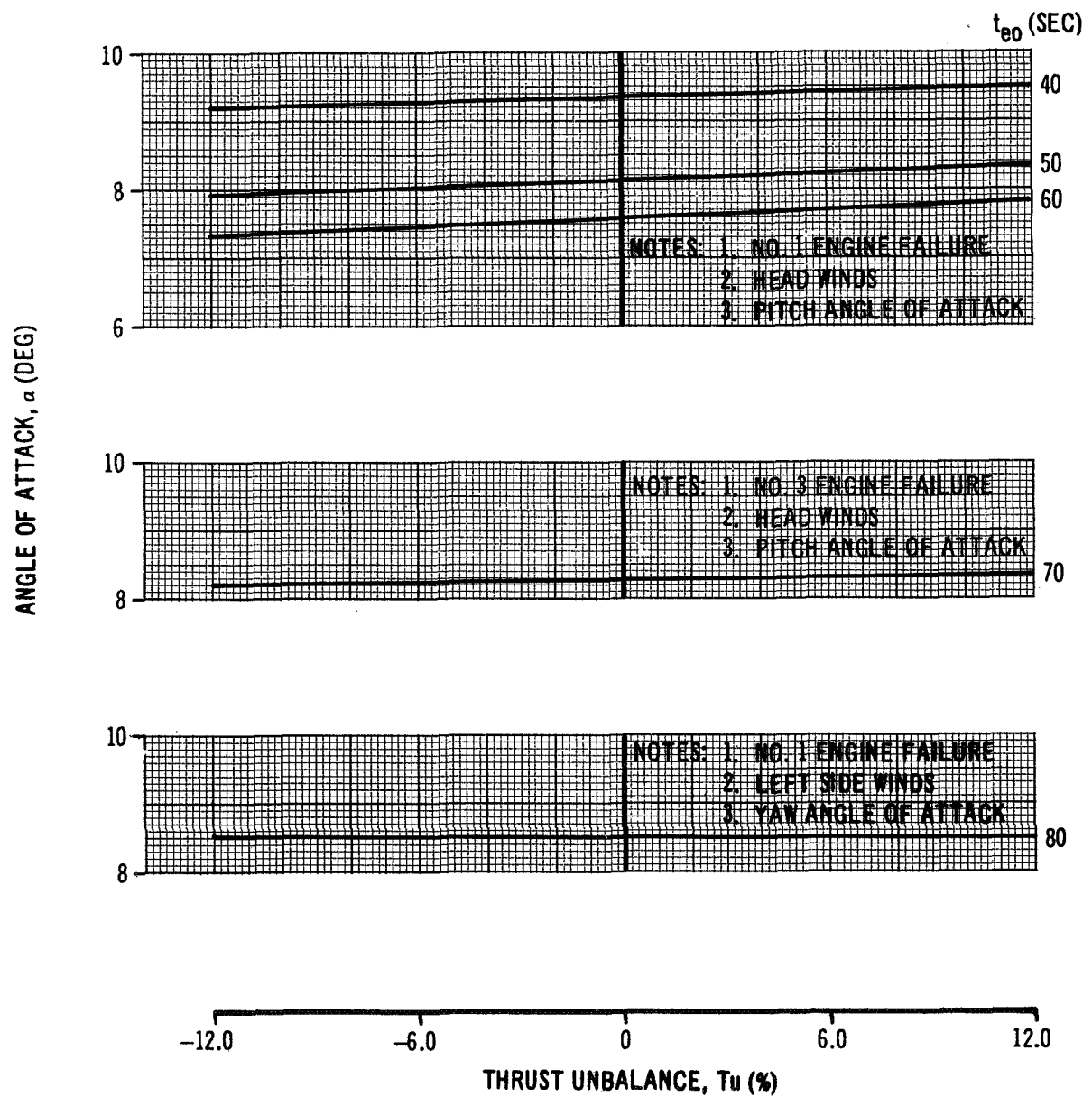
FIGURE 68

CHANGE IN DYNAMIC PRESSURE AT MAXIMUM ANGLE
OF ATTACK DUE TO DISPERSIONS IN INDIVIDUAL
CONTROL ENGINE THRUST
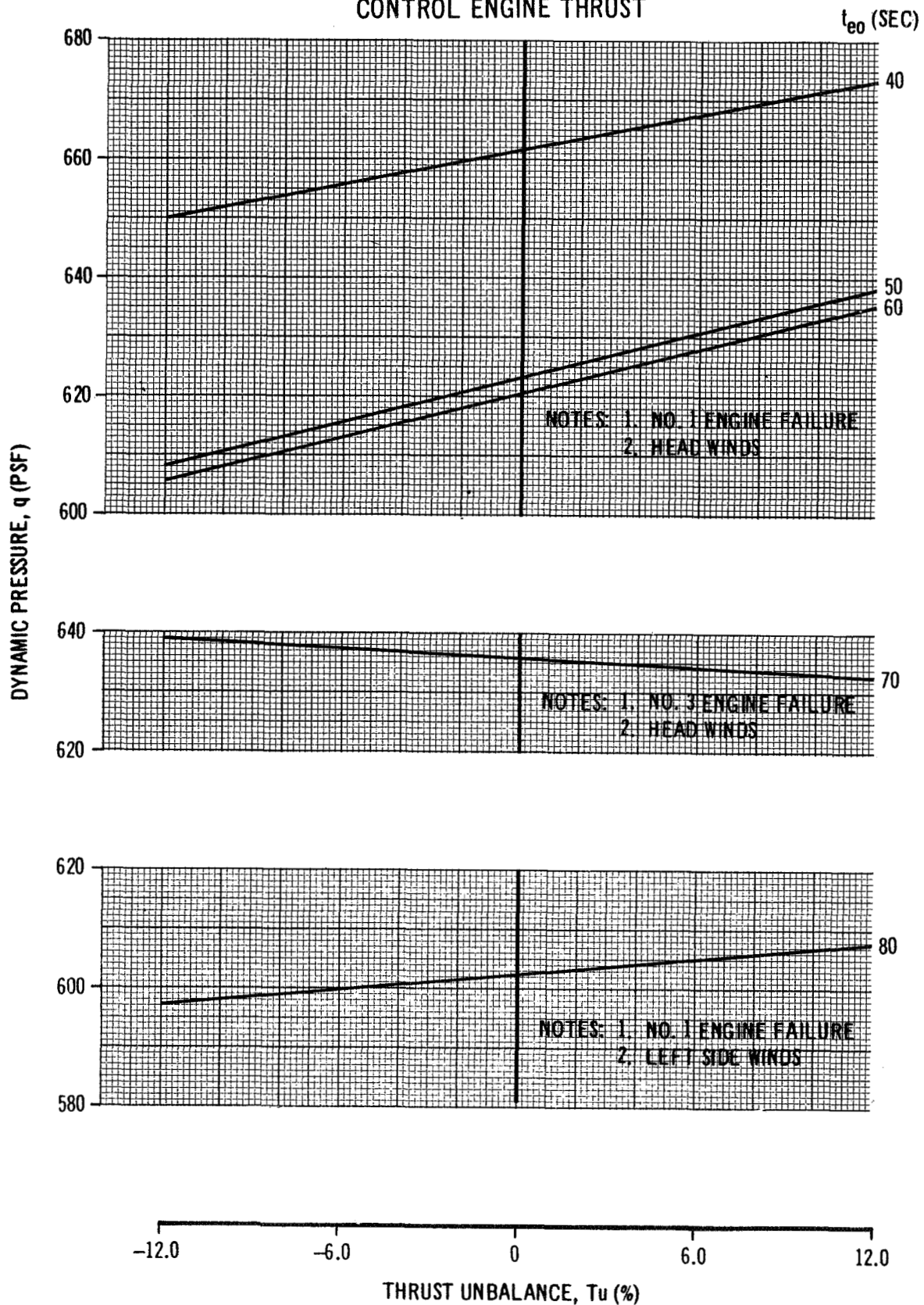
FIGURE 69

CHANGE IN NORMAL ACCELERATION AT MAXIMUM ANGLE OF ATTACK DUE TO DISPERSIONS IN INDIVIDUAL CONTROL ENGINE THRUST

NOTES: 1. NO. 1 ENGINE FAILURE
2. HEAD WINDS
3. PITCH NORMAL ACCELERATION

NOTES: 1. NO. 3 ENGINE FAILURE
2. HEAD WINDS
3. PITCH NORMAL ACCELERATION

NOTES: 1. NO. 1 ENGINE FAILURE
2. LEFT SIDE WINDS
3. YAW NORMAL ACCELERATION

THRUST UNBALANCE, Tu (%)
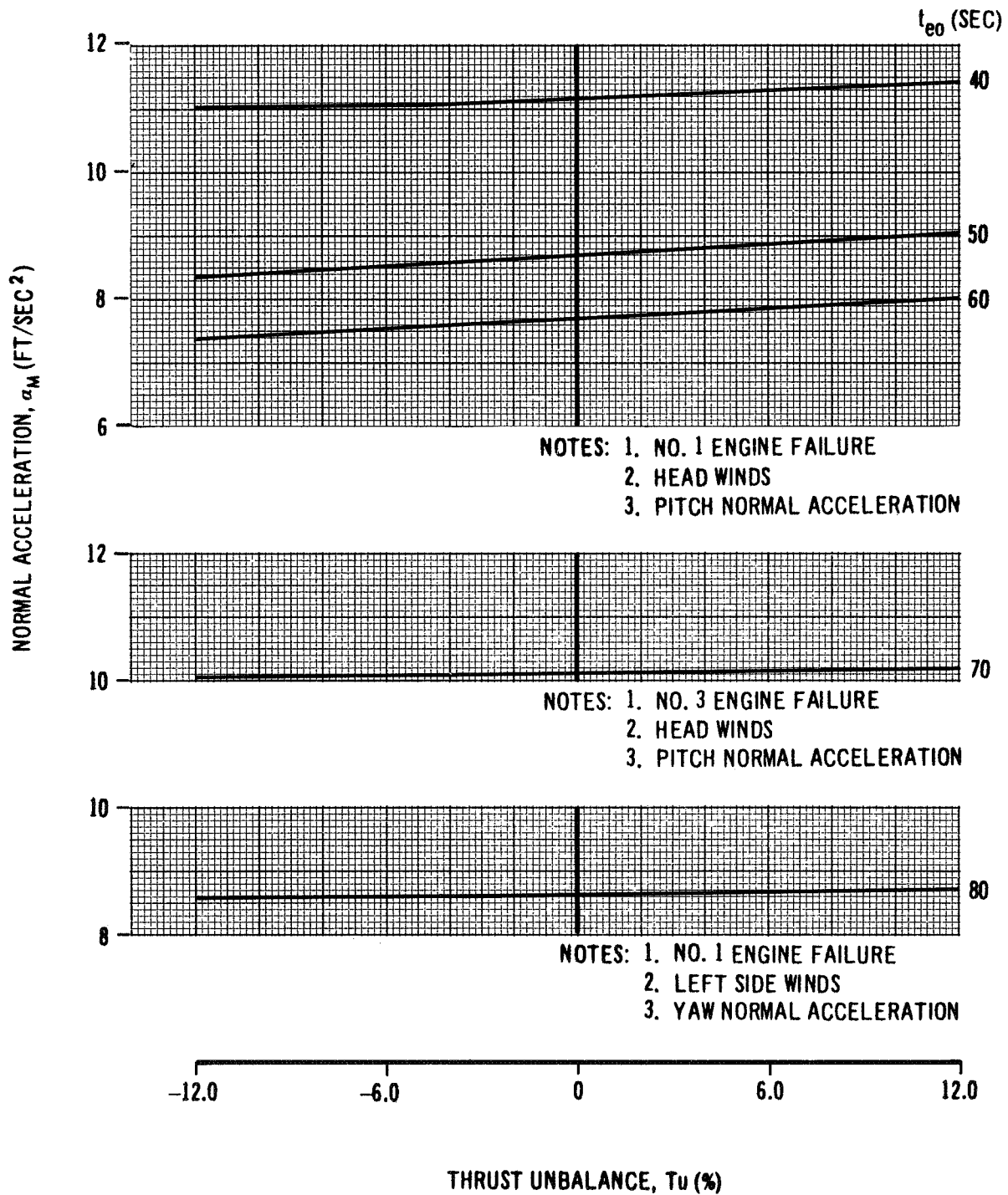
FIGURE 70

CHANGE IN ANGULAR ACCELERATION AT
MAXIMUM ANGLE OF ATTACK DUE TO
DISPERSIONS IN INDIVIDUAL
CONTROL ENGINE THRUST

NOTES: 1. NO. 1 ENGINE FAILURE
       2. HEAD WINDS
       3. PITCH ANGULAR ACCELERATION

NOTES: 1. NO. 3 ENGINE FAILURE
       2. HEAD WINDS
       3. PITCH ANGULAR ACCELERATION

NOTES: 1. NO. 1 ENGINE FAILURE
       2. LEFT SIDE WINDS
       3. YAW ANGULAR ACCELERATION

THRUST UNBALANCE, T_u (%)

ANGULAR ACCELERATION (DEG/SEC^2)

t_{eo} (SEC)

FIGURE 71

The values of the P_i's resolved by this procedure represented the variances about the nominal trajectory parameters. These variances were later employed in the loads dispersion analysis.

5.4 Load Analysis

Limit loads on the S-IVB stage during first stage flight of the Saturn IB vehicle have been calculated at the time of maximum product of dynamic pressure and angle of attack $(q\alpha)$ for both the standard 8-engine trajectory and the five most critical engine-out trajectories. The results of these calculations are presented in figures 72 and 73.

In these figures, equivalent compressive load, $N_c'(lb/in)$, for two S-IVB stage stations is plotted against time of engine failure. The parameter N_c' is defined as the maximum load at a cross-section due to combined axial loading and bending, or

$$N'_c = \frac{p}{2\pi r} + \frac{m}{\pi r^2}$$

The stations selected for the presentation of results are the S-IVB/instrument unit interface (Station 1662.859) and the S-IVB/S-I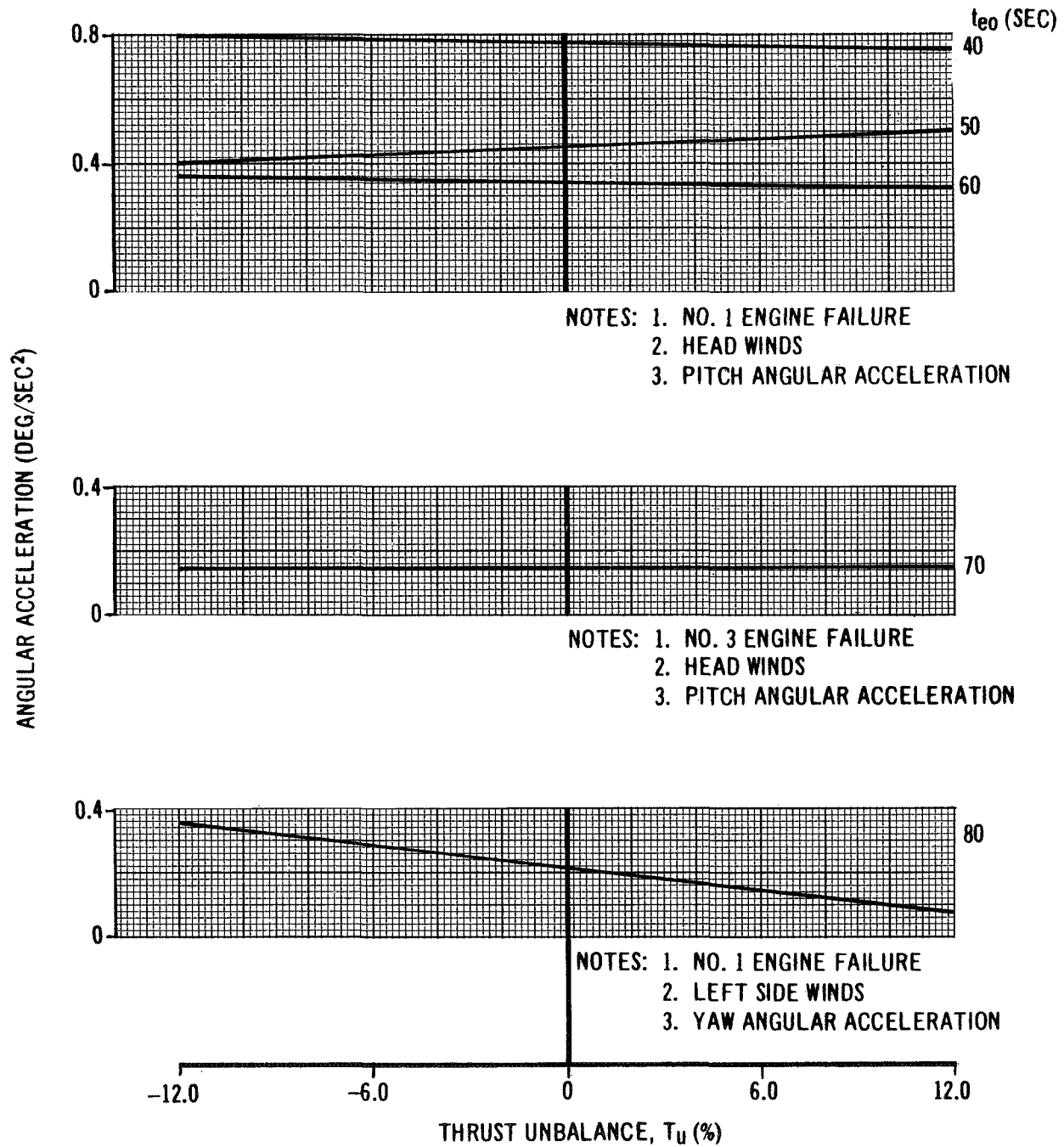B interface (Station 962.304). These stations are currently the most critical, or minimum margin of safety, stations on the stage.

Figure 72 shows a comparison of N'_c at the maximum $q\alpha$ point for a standard 8-engine trajectory with N'_c for the maximum $q\alpha$ points of each of the engine failure trajectories. To indicate the spread in loads calculated for similar trajectory conditions by MSFC (reference 5) and DAC, the other constant slope line has been entered on the graph. When N'_c for a particular time of engine failure lies above either of the constant-slope lines, the S-IVB stage possibly may experience permanent deformation or structural instability. Values of N'_c at Station 1662.859 for three sigma high and low dispersions about the nominal conditions (as discussed in Section 5.3.2) at maximum $q\alpha$ for each time of engine failure considered, are also presented. No attempt has been made to construct a curve through these points since they are somewhat erratic. However, it should be noted that the effect of these dispersions on loads does not appear to be pronounced for engine out times prior to 60 seconds.

The foregoing discussion applies also to figure 73 with respect to Station 962.304.

Because of varying strength capabilities along the vehicle for the same load condition, it is hazardous to attempt to infer an exact time of engine failure from each figure that would be a noncritical one from a structural standpoint. It can be safely inferred that the earlier the time of engine failure the more likely the possibility of permanent deformation or structural instability.

SATURN IB/S-IVB STAGE
EQUIVALENT COMPRESSIVE LOAD VS
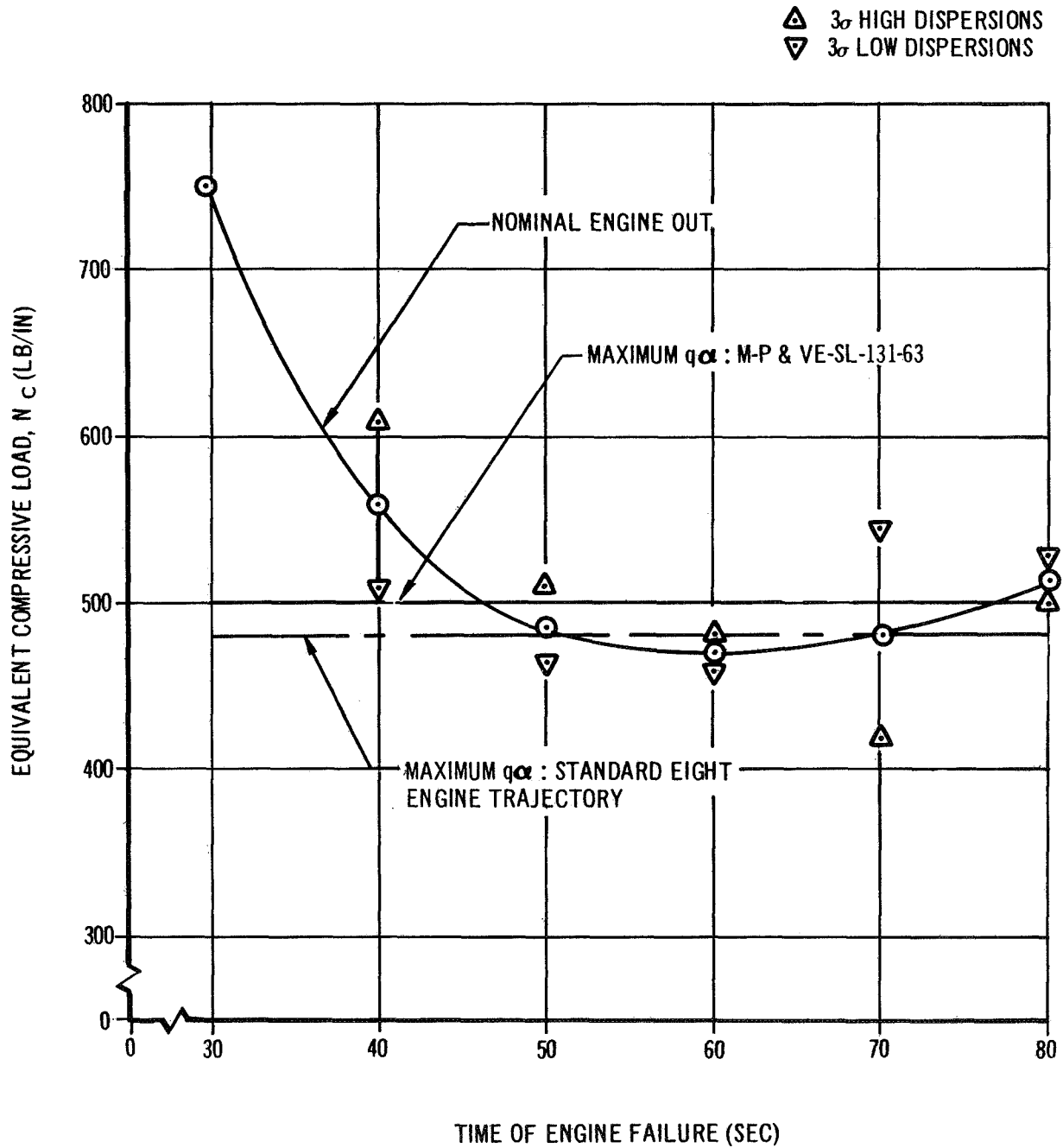TIME OF ENGINE FAILURE
STATION 1662.859

FIGURE 72

SATURN IB/S-IVB STAGE
EQUIVALENT COMPRESSIVE LOAD VS
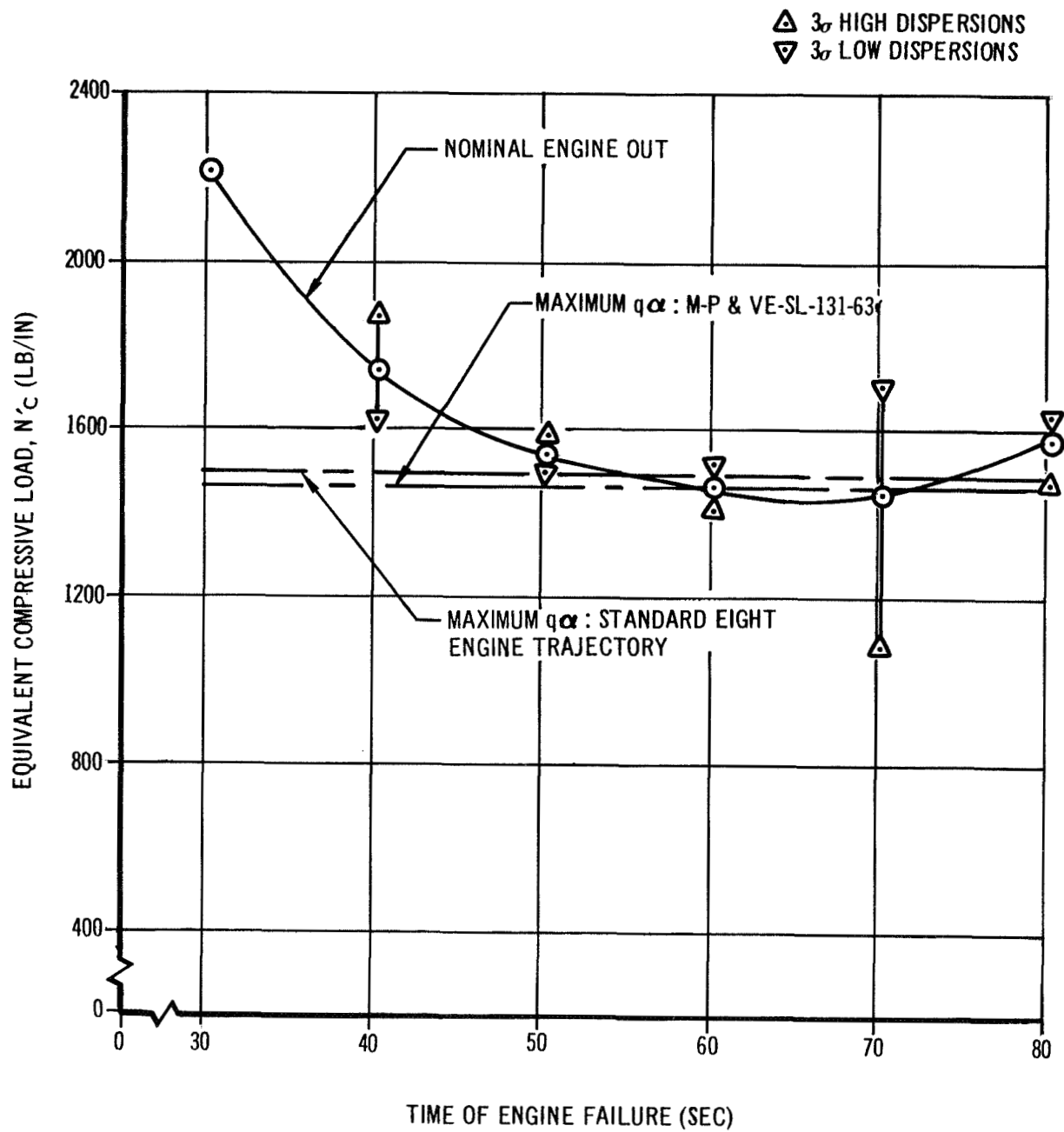TIME OF ENGINE FAILURE
STATION 962.304

FIGURE 73

6.0 CONCLUSIONS

An analysis has been made to determine the effects of the failure of the most "critical" boost stage (H-1) engine upon vehicle controllability and mission completion.

The vehicle was said to be controllable if stability was maintained and its structural limitations were not exceeded. The analysis results indicate the controllability is critical for engine failure prior to the maximum dynamic pressure altitude region or prior to about 83 seconds of flight time. This general conclusion is based on the results of a loads and dispersion analysis performed for the five most critical engine-out trajectories which included the most severe wind disturbances. The bar graph presented in figure 74 summarizes the effects of each criterion used to evaluate the vehicle performance. These criteria include the ability to maintain control, to maintain structural loads at a safe level and to achieve the desired orbit.
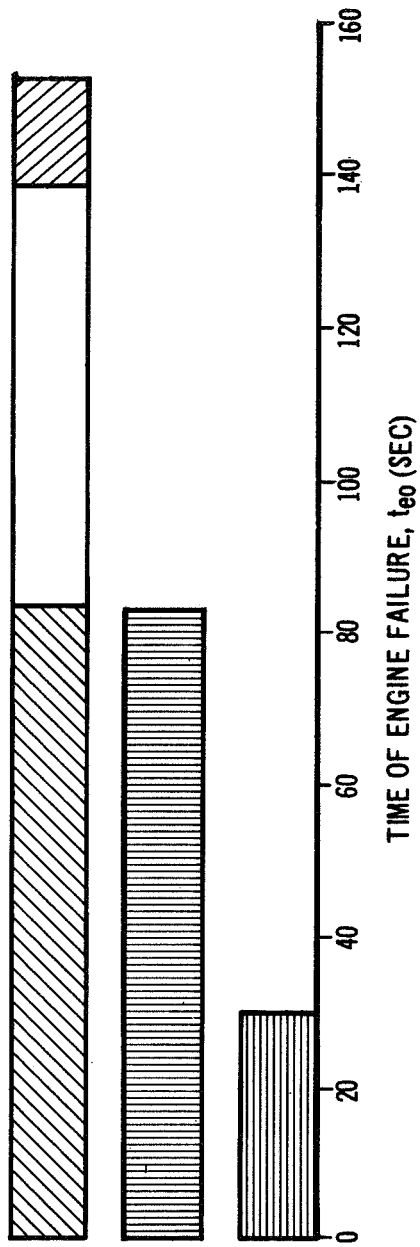
If structural loading is not considered, vehicle control is maintained for all engine failures after 30 seconds of flight assuming dispersions less than or equal to the assumed three sigma dispersion listed in table VI. Prior to 30 seconds engine number 1 failures resulted in tumbling in the maximum dynamic pressure altitude region. This tumbling occurs for engine 1 failures prior to 20 seconds without wind disturbances and dispersions. Combinations of wind disturbances and unfavorable dispersions increase the time that an engine number 1 failure will result in loss of control to 30 seconds of flight time.

The results of the loads analysis indicated that the loads as presented in reference 5 will be exceeded at Station 962.304 for each of the five trajectories selected for the analysis. When the effects of dispersion are not considered, there is a time interval from 59 to 72 seconds, during which an engine failure will not result in excessive loads. However, the effects of dispersions indicate that load limits could be exceeded during this period.

The orbit capability analysis was performed without the effects of wind disturbances and dispersions in vehicle parameters. The results indicate that for an engine failure prior to approximately 139 seconds of flight time orbit injection can not be achieved, though use of flight performance reserve propellants in the S-IVB stage can better this situation somewhat.

When an engine failure occurs at a flight time where the loss of controllability is not predicted and no suitable orbit conditions can be achieved, there are no pressing demands for immediate abort. That is, there is a choice of the abort procedure. For the case where loss of controllability is predicted the earlier the engine failure occurs the greater is the time before which abort is mandatory, since actual structural failure doesn't occur until the vehicle is in the maximum dynamic pressure region of the trajectory.

MISSION CAPABILITY OUTLINE

TIME OF ENGINE FAILURE, t_{eo} (SEC)

*INCLUDES EFFECTS OF DISPERSIONS AND WINDS
**NO DISPERSIONS OR WINDS INCLUDED

LEGEND:

TUMBLING OCCURS*

SAFE STRUCTURAL LOAD LIMIT EXCEEDED.*

ORBIT INJECTION NOT POSSIBLE, MISSION ABORT MANDATORY PRIOR TO REGION OF MAXIMUM DYNAMIC PRESSURE**

ORBIT INJECTION NOT POSSIBLE, MISSION ABORT MANDATORY PRIOR TO ORBIT INJECTION**

POSSIBILITY OF SECONDARY MISSION SUCCESS**

FIGURE 74

There are several areas of possible interest which were not included in this study. There are also items which were touched upon but deserve more extensive analysis. These include topics such as survey of less critical engines, aerodynamic heating, time of abort with regard to vehicle controllability and the chance of debris striking inhabited areas, time of abort with regard to re-entry module recovery, alternate optimum attitude command history, compromise attitude command history, optimization of gain program for loads, extended research on possible alternate mission objectives, and a thorough examination of probabilities of FPR propellants availability.

REFERENCES

1. Schulze, W. A., M-P&VE-E, "Preliminary Mass Characteristics of the Saturn IB Vehicle," (C), memorandum No. M-P&VE-ES-110-63, dated June 25, 1963

2. Weight and Performance Review Board, M-P&VE-V, "Saturn I, IB, and V Launch Specifications, Weights and Compatible Trajectories," (C), memorandum No. M-P&VE-V-33, dated May 13, 1963

3. Aerodynamic Design Section, M-AERO-AA, "Preliminary Aerodynamic Characteristics of a Saturn IB Apollo Two-Stage Orbital Configuration," (U), memorandum No. M-AERO-A-90-63, dated August 28, 1963

4. Daniels, Glenn E., "Natural Environment (Climatic) Criteria Guidelines for Use in MSFC Launch Vehicle Development," (U), memorandum No. MTP-AERO-63-8, dated 1963 Revision

5. Kroll, G. A., M-P&VE-S, "Preliminary Structural Loads for Saturn IB Vehicle, 32,500 Pound Payload," (C), memorandum No. M-P&VE-SL-131-63, dated July 16, 1963.